Modes of electrical systems and grids with renewable energy sources

Book · November 2019

CITATIONS
2

READS
68

4 authors, including:

Vladislav Kuchanskyy
The Institute of Electrodynamics of the National Academy of Sciences of Ukraine
77 PUBLICATIONS **180** CITATIONS
SEE PROFILE

Olena Rubanenko
Vinnytsia National Technical University
72 PUBLICATIONS **122** CITATIONS
SEE PROFILE

Iryna Hunko
Vinnitsia National Technical University
24 PUBLICATIONS **56** CITATIONS
SEE PROFILE

V. Kuchanskyi, A. Nesterko,

O. Rubanenko, I. Hunko

Modes of electrical systems and grids with renewable energy sources

Contents

INTRODUCTION

The main task of electric power networks is providing effectively the needs of consumers in energy of the appropriate quality at minimum costs and sufficient level of reliability. This causes a constant increase in the size of the grids and the complexity of the structure. In its turn these conditions lead to a combination complex problem of the transformation, stabilization of parameters and transport of electricity. At the same time, with the development of new technological processes, the share of asymmetric, nonlinear and dynamic consumers of electricity is continuously increasing. In practice, all this leads to the fact that in electrical networks such factors of electricity distortion of quality as deviation, oscillation, asymmetry and non-linearity of voltage have become permanent disturbances. They significantly reduce the efficiency of both: the power supply system's themselves and consumers which are power supplied from them.

In general, the principles of construction, development of modern and promising electricity networks, methods and means of controlling their regimes should be consistent with the level and pace of the overall progress of technology. But, as you know, the development of technical systems in the direction of complication requires the further realizing and development of appropriate methods and tools for their modeling. Thus, the deviation of the electrical energy parameters from the nominal values leads to, on the one hand, increasing the losses of voltage and power in the networks, reducing their transmitting capacitance, and on the other hand - to the disfunction of normal operation and reducing the technical term of the electrical equipment, thereby reducing the quantity and quality of produced products.

Therefore, the development of mathematical models of electric networks modes in the presence of distortion sources, as well as improvement of methods for analyzing processes of abnormal regime is consequential and important problem.

In particular, in order to solve this scientific and technical problem, in work simulation of quasi-stationary modes of electric networks in the presence of

distorting sources was performed. It is shown that the reliability of the operation of electric networks increases if, in the case of incomplete mode, it is possible to leave in work unfaulted phase in operation. However, this asymmetric abnormal mode is accompanied by significant deviations of parameters, and therefore requires careful modeling and analysis. Accordingly, there were improved methods and mathematical models for studying such a regime, which increased the adequacy of the modeling and the validity of the recommended measures to prevent abnormal overvoltages, depreciation of electricity quality and regulation of frequency.

In the work special attention is paid to abnormal modes of electric networks, which are accompanied by abnormal resonance overvoltages (ARO). The criteria for the occurrence of such overvoltages are determined, the flow of transient processes and resonance phenomena are investigated, and the means of preventing them are proposed. The developed models and methods were used to prepare and put into operation the recommendations for the management of abnormal modes in electrical networks of different levels of hierarchy and functional purpose.

The analysis of the mutual influence of the main criteria of the efficiency of electricity supply - quality and losses of electric energy on its transport is carried out. Since normal regime is determined not only by the degree of reliability and failure of power supply, but also by fulfillment of requirements for power supply of consumers with electric energy of the appropriate quality with the losses. The value of electric power losses, as an optimality criterion, depends to a large extent on changes in the mode parameters; therefore, the simulation of power losses on the basis of system analysis was performed. In addition, it has been shown that the electrical quality is uncertain, which is solved in the standards by means of a deterministic approach.

With this approach, it is possible to make only a definite conclusion about the conformity or non-compliance of the indicators of quality of electric energy with the established norms, but it is impossible to determine the degree of this conformity. This significantly reduces the informativeness of the assessment of the

quality of electrical energy, does not allow fully tracking the dynamics of changes in indicators and preventing their further deterioration. Therefore, modern methods were used in the work to assess the quality of electrical energy, which is a generalization of deterministic and probabilistic.

The optimization tasks that are considered in the work are multicriteria, and between the different criteria there is a mutual dependence with a number of restrictions. The general approach to the solution of the problem of multicriteria optimization was to find the area of compromise, in which the decrease in the value of one criterion is accompanied by the growth of the other and vice versa. This applies especially of problems related with frequency.

Theoretical and practical significance are concluded the methods of optimization of quasi-stationary abnormal regimes in power supply systems. It is shown that the real electric network is heterogeneous in its structure, and the regime in an electrical network with a high degree of distortion sources is abnormal and is accompanied losses. This heterogeneity is an internal factor of the electrical network, therefore its compensation is recommended to be performed by the introduction of additional suppression measure. The measures presented in the work can be realized in practice in order to optimize the modes of electric networks, and the proposed method, in contrast to the existing ones, enables the use of real voltage of power sources of the network, as well as the choice of the law of regulation.

Taking into account all of the above, we can conclude that the high relevance of scientific and technical problems, the solution of which is dedicated to the work. Studies are performed at the appropriate scientific level, have a great theoretical and practical value, so we believe that research work is performed in accordance with the technical requirements and in full.

1. CLASSIFICATION OF SOURCES OF DISTORTION IN BULK ELECTRIC POWER NETWORKS

1.1 Abnormal resonance overvoltages in bulk electrical power systems with sources of distortion

In the design and construction of the bulk elements of the electrical network for the base accept a normal mode, in which the technical and economic indicators of its work are optimal in terms of reliability, quality and efficiency of electricity supply. But the electric network is a dynamic system, which changes in time (changes in circuits and loads), and in space (the appearance of new elements in the process of development or reconstruction). As a result of continuous changes in the network, the established mode will always be different from the design, so pre-made decisions should be subjected to constant correction to preserve the desired values of the optimality criteria.

The first extra high voltage (EHV) transmission line 750 kV was put into service in Ukraine in 1980th. Nowadays the transmission lines 750 kV are the main system-forming lines in the United Electric Grid of Ukraine and provide electricity from powerful power units and also the necessary exchange between separate power systems. In addition, their development and efficient operation are an important prerequisite for the integration of the United Energy System of Ukraine into the European Network of Transmission System Operators for Electricity (ENTSO-E) in the future [6,8,10-15]. That is why damage such lines or equipment, which ensures their connection to the grid, is a severe system failure, can cause the collapse of the combined system into separate parts in which there will be a shortage or excess of generating capacities and, accordingly, cause disconnection of consumers in scarce regions and blocking of power stations in excess regions. Of course, such an abnormal mode of the bulk network will be significantly different from the optimal [2,8,10,14]. Thus, the prevention of the failure of the EHV transmission lines - an important scientific and practical task in terms of providing reliability of electricity supply and the provision of satisfactory indicators of quality and efficiency of operation of main electrical networks.

In the monograph, one of the main sources of nonsinusoidal distortion EHV lines is considered the nonlinearity of the volt-ampere characteristic when the unloaded autotransformer is switched on. Such a regime causes the conditions for the appearance of overvoltages of even harmonic. It should be noted that the process of occurrence of overvoltages on the even harmonic is not generally known and the value of the characteristics of this kind of overvoltages depends on many factors of the abnormal regime. It should be noted that nowadays in the world the measures that are used for ensuring the required reliability of the transmission line EHV is building additional lines [18,19]. It is clear that this requires additional capital expenditures. But it is possible to increase the reliability of electricity supply by carrying out repair work under voltage, as well as by using incomplete phase modes of the overhead line [10,13,14]. At the same time in the case of application incomplete phase modes, the losses from lack of electricity are reduced, the stability of the power systems and the optimal flow distribution regime are maintained, the possibility of timely elimination of defects during the preventive repair of the lines and switches are appeared.

One of the main reasons for failure of equipment in the bulk electrical network are overvoltages - an increase in the value of the operating voltage above the maximum permissible value, in accordance with the technical regulations [7, 8, 10-13]. This is due to the fact that a relatively small isolation reserve is provided for the constituent elements of bulk electrical networks due to the high cost for this voltage class.

Durable internal overvoltages arise due to resonance at coincidence of the values of the parameters of the circle elements [3-12, 14]. This type of overvoltage occurs due to the properties of the network can be eliminated by changing the relationship between the parameters of the network and its mode [14-18]. Unlike switching overvoltages that last for hundreds of seconds, abnormal occur unpredictably, and can last for a long time above seconds, until the action of protection against voltage increase, voltage regulators or personnel interference does not affect the change of circuit or mode.

Abnormal resonance overvoltages are not taken into account when selecting isolation or parameters of traditional measures for suppression overvoltages, since these protective measures are designed to limit switching overvoltages, rather than to extinguish a long process. Therefore, the probability of the occurrence and development of systemic accidents at ARO is quite significant. For this reason, the work is devoted to the study of internal durable ARO. The abnormal overvoltages in main electrical networks can exist on the basic harmonic during incomplete modes of overhead lines and shunting reactors and overvoltage with automatic self-excitation of higher harmonic components [1,3-6,20,23]. But it should be noted that under the real conditions of existing power systems one or another type of abnormal overvoltage may not exist at all or the amplitudes of these overvoltages are so small that their research does not constitute a practical interest.

The use of the term of abnormal overvoltage is not accidental [8,10-12,23], because when working out literary sources [1,3-5,7,9,11,20,21] and studies of experimental results [18, 19], it was concluded that this kind of overvoltage is fundamentally different from traditional ones. The difference and the special characteristics of overvoltages is that they are caused by an abnormal regime, primarily due to the effect of the source of distortion [3-5,20,21].

On (Fig. 1.1), the division of this type of internal overvoltage into two main categories, depending on the resonance at a certain frequency, is shown on the basic harmonic and higher harmonic components. Such a division is driven by the fact that the modes of bulk electric networks caused by the switching of unloaded power autotransformers in saturation mode and network modes in which the source of distortion does not contain nonlinear elements. That is, was done another division by the linearity sources of distortion - nonlinear or linear and the resonance in which circle - linear or nonlinear.

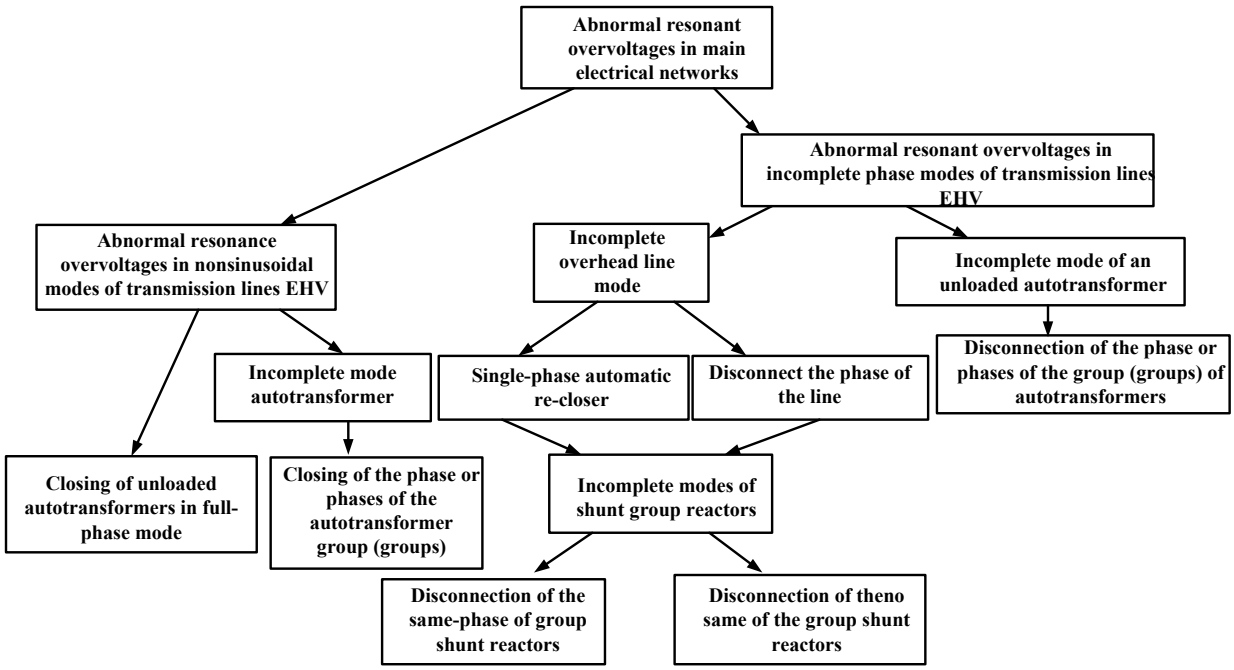

Fig. 1.1 Classification of ARO

The following types of ARO are considered in the paper according to the developed classification given on (Fig. 1.1). The first type of ARO is caused by the source of higher harmonic components. The most typical case for main electrical networks is the connection of the transmission lines EHV to the unloaded group of autotransformers. An increase in voltage occurs on higher harmonic components: overvoltages arise at even harmonics in a linear circle to which the source of distortion is connected (a magnetic shunt of autotransformer operating in unloaded mode). The second type of abnormal overvoltages occurs in the asymmetric mode. A typical situation is the disconnection of the phase of the EHV transmission line with the possible disconnection of one of the groups of shunt reactors. Overvoltages can occur with a combination of asymmetric and nonsinusoidal modes. In the work of this type includes the switching of transmission lines EHV to an incomplete autotransformer group.

Durable ARO are one of the most difficult to analyze types of internal overvoltages [1-10, 14]. The research problem is due to the fact that there are many elements in the main electrical network, the processes in which it is difficult to accurately and adequately simulate. These elements, in particular, include inductors with steel cores and conductors of EHV with corona discharge, as well as

secondary arc of alternating current during single phase automatic re-closer, since these processes are non-linear [2,5,7,8,,20,21]. That is, the volt-ampere elements are described by non-linear equations. This is an important circumstance because of the presence of such elements that it is impossible to obtain accurate results about the existence of overvoltage in one mode or another.

It should be noted, that permissible short-term voltage rises in the frequency of 50 Hz in service conditions should not exceed the values relative to the highest operating voltage divided in [6] for electrical equipment of alternating current for voltage 750 kV are indicated in the table 1.1. The value of normal operation voltage for electrical equipment is 643 kilovolt.

Table 1.1

Permissible in the operation of short-time voltage rises in frequency of 50 Hz

Type of electrical equipment	Permissible increase of voltage value with duration			
	20 minutes	20 seconds	1 seconds	0.1 seconds
Power transformers (autotransformers)	1.1	1.25	1.67	1.76
Shunt reactors, apparatuses, capacitive voltage transformers, current transformers, coupling capacitors, bus supports	1.1	1.3	1.88	1.98
Arresters	1.15	1.35	1.4	-

As is well known, the nonsinusoidal voltage and current causes the aging of electrical machines, transformers and cables due to heating, as well as the occurrence and last of ionization processes in isolation, especially at high frequencies of an alternating electric field. For electrical machines, transformers and cables, the most significant is the thermal aging of insulation, and the effect of higher harmonic components caused by significant distortions of the shape of the

curves of voltage and current at the excitation of the autotransformer, on the ionization processes in the insulation, enhance the aging effect. Thus ARO due to saturation of the autotransformer magnetic shunt have a double negative effect on the isolation of the equipment, for example, from ARO in asymmetrical modes.

1.2 Abnormal resonance overvoltages at nonsinusoidal distortions

The question of the emergence of the second harmonic of the extra high voltage transmissions line (EHV TL) 750 kV is one of the most difficult in modern theoretical electrical engineering. Despite of the fairly large number of publications on this topic, the causes and conditions for the appearance of this harmonic are still not completely clear. Moreover, the published works of different authors contradict each other in some questions [1,3,9,20,21].

Now there are two main reasons for the occurrence of durable resonant second-harmonic overvoltages in EHV TL. The first is the non-sinusoidal nature of the flux linkage of the nonlinear inductance when it is connected to the source. If there is an aperiodic component in the flux linkage, higher harmonics components will appear in the current [3,9]. The voltage drops from these components on the circuit elements cause the appearance of corresponding harmonics in the autotransformer (AT) and line. Overvoltages at transient resonance are not limited to corona wires and can exist for a long time with a slow decrease in the aperiodic component of the flux linkage [4].

The second possible reason for the appearance of a long second harmonic is a periodic change in the inductance of the AT magnetizing shunt. In this case, the oscillogram seems to be completely unclear: the second harmonic, initially small, begins to develop after quite a long time (0.1-0.5 seconds) Fig.1.2 a certain switching, for example, when the line is switched on to an unloaded AT. Moreover, it increases, reaching significant values after 0.8-1.2 seconds.

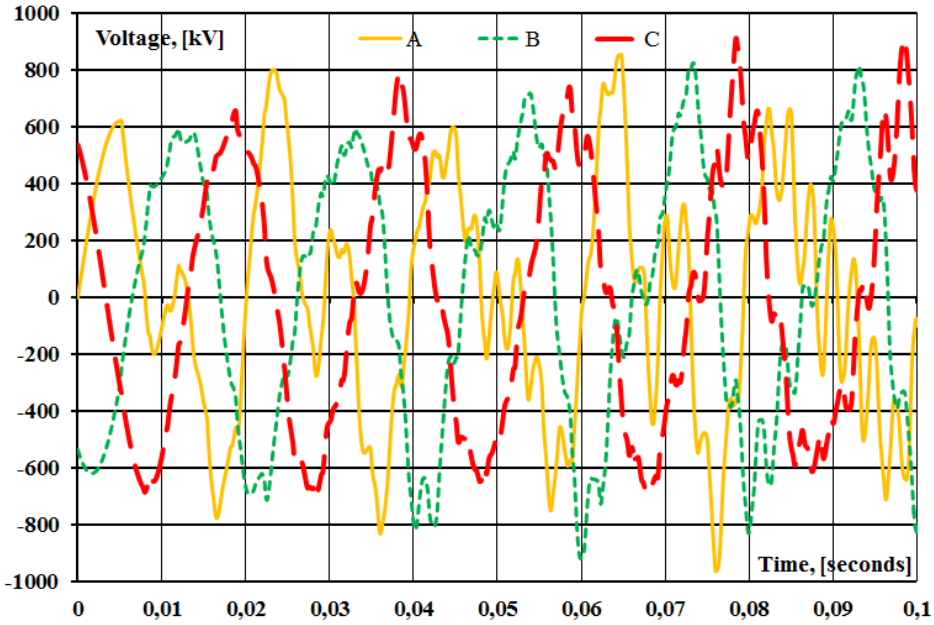

Fig. 1.2 Abnormal resonance overvoltages on second harmonic component

The mechanism of this phenomenon, called self-excitation of the second harmonic, has not been studied enough so far, although many theoretical papers have been published [2,8]. Unfortunately, not one of these well-known works deals with the study of the physical nature of the phenomena taking place, while clarifying this essence is the only way to develop an engineering approach to the phenomenon and methods for its suppression.

It should be noted that this type of resonant overvoltage was observed on two EHV power lines: the Khmelnitsky nuclear power plant - the substation Rzeszow (Poland) and the South Ukrainian nuclear power station - Isakcha (Romania). The problem of operating an extra-high voltage power line in non-sinusoidal modes with the possible occurrence of resonant overvoltage does not allow to operate the Uraine-European Union energy bridge during switching of unloaded autotransformers. These lines are characterized by lengths that require the installation of three shunt reactors and, as studies have shown [1,5,7] directed at these lines resonant overvoltages at the second harmonic are observed. The studies cited in the article are dictated by the need to ensure reliable and efficient operation of the Ukraine-European Union energy bridge with bulk EHV TL.

1.2.1 Processes at commutations of an autotransformer

The physical nature of the appearance of resonance overvoltages on second harmonic is due to the periodic change in the inductance of the AT magnetic shunt when passing through it alternating current [5,9]. As a result of the capacitive effect, the voltage on the AT increases caused by the saturation of its magnetic circuit. This in turn causes deep modulation of the magnetic shunt of the AT that will vary with a double frequency in relation to the applied voltage, since the degree of magnetization does not depend on the direction of the current. The appearance in the spectrum of the second harmonic component and is a sufficient condition for the emergence of resonance overvoltages on the ultraharmonics of pairwise multiplicity.

During switching in the magnetic circuit of the AT there is a free decaying aperiodic component of the flux, which leads to the appearance in the magnetization current of harmonic components. The latter, in turn, cause on the elements of the electric circuit a voltage drop equivalent to the a corresponding frequency in the range of longitudinal electromotive force.

The problem of studying resonant overvoltages that occur when an unloaded autotransformer is turned on is that: today there is no exact answer to the question about the cause of this type of overvoltage. Since the beginning of the 1960s [9], as soon as they began to construct and operate EHV TL, studies were carried out to identify the determining factors for the occurrence of resonant overvoltages on higher harmonic components.

In the case of connecting an unloaded autotransformer, autoparametric resonance and oscillations occurring in the system due to periodic changes in those system parameters that determine the amount of stored energy will occur. In this case, parametric oscillations in the oscillating circuit are excited due to the periodic change in the nonlinear inductance of the magnetic circuit.

The main drawback of the first studies is the presence of a too fundamental theoretical explonation of the occurrence nature of resonant oscillations in circuits

with nonlinear inductance. A significant bias has been made towards the physical nature and classification of resonance phenomena in electrical networks and systems. All of the above refers to the steady-state regimes of circuits with nonlinear inductances. As for the transient processes, they are practically not studied at all. It is not known what initial conditions lead to the occurrence of a harmonic, and which are not.

The magnetization of AT due to its energization is considered the most unfavorable case, causing inrush currents of magnetization of the greatest amplitude. When an AT is disconnected, the magnetization voltage is zero and the magnetization current decreases to zero, while the magnetic induction varies according to the magnetization characteristic of the core. This causes the presence of remanent flux in the core.

When, after some time the autotransformer is re-energized, the magnetic flux begins to change according to the sinusoidal law, but with a shift to the value of remanent flux. The residual flux can be 80–90% of the nominal flux, and thus the point can move beyond the magnetization curve knee point of the magnetization characteristic Fig.1.3, which, in turn, causes a large amplitude and distortion of the current waveform.

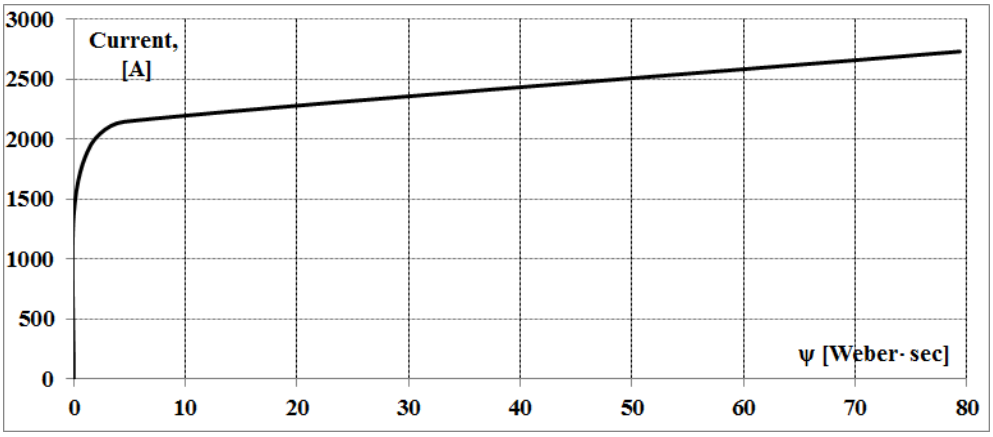

Fig. 1.3 Magnetization curve of the autotransformer 333000/ 750/330

This eventually led to a DC component in the AC circuit, but not from a DC source, but from the fact that the core is saturated at the peaks of the AC sinusoid

and the inductance stops hindering the flow of current - the current peaks grow to infinity.

As you can see Fig.1.4, due to the saturation of the magnetic system, the inrush current when switched on AT reaches very large values that can exceed even the rated current. When power AT is turned on, there is a surge inrush of magnetization current, which has a decaying character Fig.1.4.

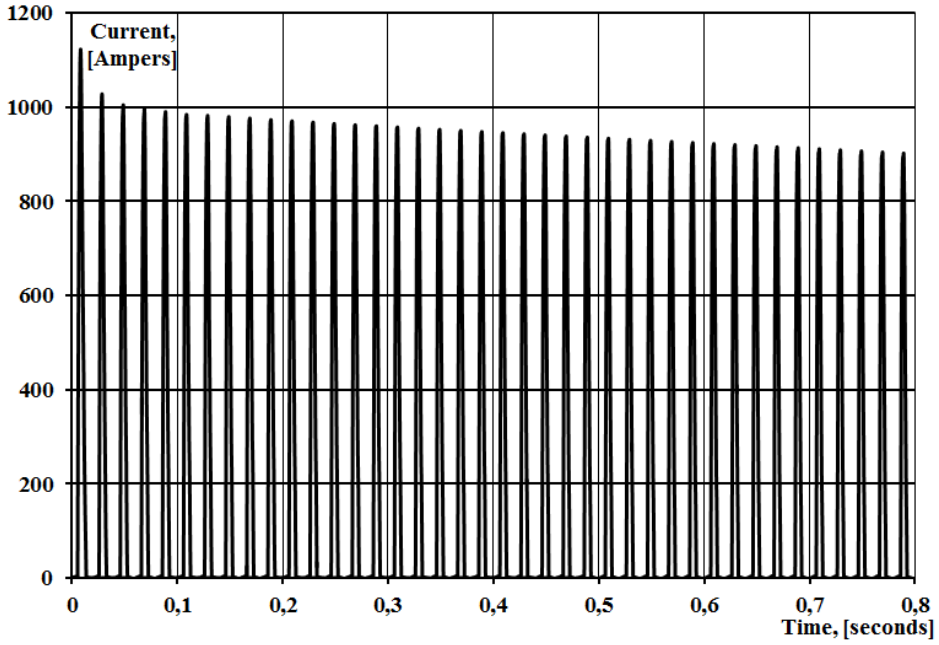

Fig 1.4 Inrush currents of autotransformer

The change in current in time is characterized by the following features:

- the current curve is asymmetrical, until the current I reaches a steady-state value;

- the curve can be decomposed into aperiodic and sinusoidal current component of different harmonics. The aperiodic component has a very large specific value in the rated current;

- the time of attenuation of currents is determined by the time constants of the AT and the network, and can reach 2-3 seconds. The more powerful the AT, the longer the attenuation lasts;

- the initial inrush current can reach 5-10 times the transformer rated current. Power AT has a multiplicity less than low-power ones.

1.2.2 The influence of remanent flux on appearance of resonance overvoltages

The Fig. 1.4 shows the characteristic form of magnetization current surges. This waveform displays the presence of a long-decaying aperiodic component that can be characterized by the content of different harmonics and large current amplitude at the initial moment of time (up to 30 times the value of the AT rated current). The curve decays significantly in tenths of a second, but the total attenuation can happen after a few seconds. Under certain circumstances, the magnetized inrush current decays only several minutes after the AT is energized.

When a autotransformer is switched on for an alternating voltage, the magnetic core can go into a saturation state, in which a small increment of the magnetic flux through it causes a sharp increase in current through the AT winding [3,4,8,9]. At the same time, the resulting magnetic flux Φ_{rez} Wb through the magnetic core at the moment of switching on plays the determining value for the current value:

$$\Phi_{res} = \Phi_{st} + \Phi_{tran} \pm \Phi_{rem} \qquad (1.1)$$

where Φ_{st} - steady state magnetic flux, Wb;

Φ_{tran} - magnetic flux of transient process, Wb;

Φ_{rem} - remanent flux, Wb.

When excitation is removed from the AT, some of the magnetic domains retain a degree of orientation relative to the magnetic field that was applied to the core. This phenomenon is known as residual or remanent magnetism. Remanent flux Φ_{rem} that value of flux which would remain in the core few minutes after the interruption of an exciting current of sufficient magnitude to induce the saturation flux. When excitation is removed from the AT, some of the magnetic domains retain a degree of orientation relative to the magnetic field that was applied to the core. This phenomenon is known as residual magnetism.

The most effective and most justified among the methods for reducing the inrush current of AT is to reducing the resulting magnetic flux by the beginning of the transient process in the "AT primary winding - line" circuit.

The use of a device for removing the residual magnetization of the Φ_{rem} AT magnetic circuit is preliminary before switching the AT into a random phase, it allows to obtain the value $\Phi_{rem} = 0$, then the resulting magnetic flux of the through the magnetic conductor at the moment of switching on:

$$\Phi_{rez} = \Phi_{st} + \Phi_{tran} \tag{1.2}$$

Switching on the AT according to the method of reducing the starting current of the AT at the time when the alternating voltage of the network is in the phase of 90°, after preliminary implementation of the method of removing the residual magnetization of the AT magnetic circuit, allows to get the values $\Phi_{rem} = 0$, then the resulting magnetic flux through the magnetic core at the moment inclusions:

$$\Phi_{res} = \Phi_{tran} \tag{1.3}$$

Abnormalities of nonsinusoidal modes are characterized by the appearance of higher harmonics of current and voltage [1,11,14]. The distortion of the shape of the curve of the voltage and currents in this case is due to the nonlinearity of the magnetization shunts. In recent years, great attention in the study of modes of electric networks has been given to fluctuations in circles with steel. The reason for this is the appearance of complex phenomena on the transmission lines of the EHV, such as resonances at frequencies different from the main [1,8].

The resonance phenomenon in circuit with steel, which are united under the general name of ferroresonance processes, have been known for almost a hundred years, but only with the development of modern theory of nonlinear oscillations using the latest methods implemented on modern computers, these phenomena have received a sufficiently complete theoretical justification The theory of nonlinear oscillations revealed a number of features that fundamentally distinguish nonlinear oscillatory systems from linear ones. Such features are a leap-like change

in the nature of oscillations when changing system parameters (trigger effect), the appearance of oscillations and resonance at frequencies different from the frequency of the electromotive ferce of the circle - subharmonic, ultragarmonic, and resonances on the main freaquency [9].

Among the methods of research, the most widely used modernized methods of small parameter, complex amplitudes and methods of analysis of the theory of stability of periodic oscillations and other classical methods of analysis. And in order to investigate in detail the behavior of the autoparametric behavior of elements of a nonlinear circle, it is necessary to apply the theory of nonlinear dynamics and deterministic chaos. In general, these studies constitute a separate problem of modern electrical engineering. In this paper we consider resonance phenomena in a linear electric circuit, and nonlinear inductance is only a source of distortion, not an integral part of a circle.

In this monography, the attention is paid to the occurrence of overvoltages on even harmonic components caused by the connection of unloaded autotransformers in complete phase mode and incomplete mode of operation (Fig. 1.5). In literary sources [1,5,8-10], the causes of overvoltages are considered either briefly and confusingly, or engineering methods for calculating self-excitation regions of harmonics of even multiplicity are presented, from which the physics of the process of occurrence of overvoltages is unclear. This means that the mechanism and physical nature of the phenomenon of abnormal overvoltage is not clearly described, since there is no information about the full development of the process from the beginning to the end, and the source of the even harmonics is considered only to change the inductance of the magnet of the autotransformer. In general, the presence of a significant amount of contradictory information does not allow analyzing in detail the phenomena that occur when the low-loaded or unloaded autotransformer is turned on.

As already noted above, in order to solve the problem of harmonic overvoltages, it is necessary first of all to adequately reproduce the nonlinear nature of the magnetization shunt. In practice, it is difficult to do so, when solving

this problem, it is necessary to make certain compromises. Implementing the exact method is problematic, not only because of the great accounting difficulties. The accuracy of the source data and its completeness is no less important, since it is obvious that the accuracy of the analysis cannot exceed the accuracy of the output data. In addition, for the research it is necessary to have data from the manufacturer of autotransformers on the curve of magnetization.

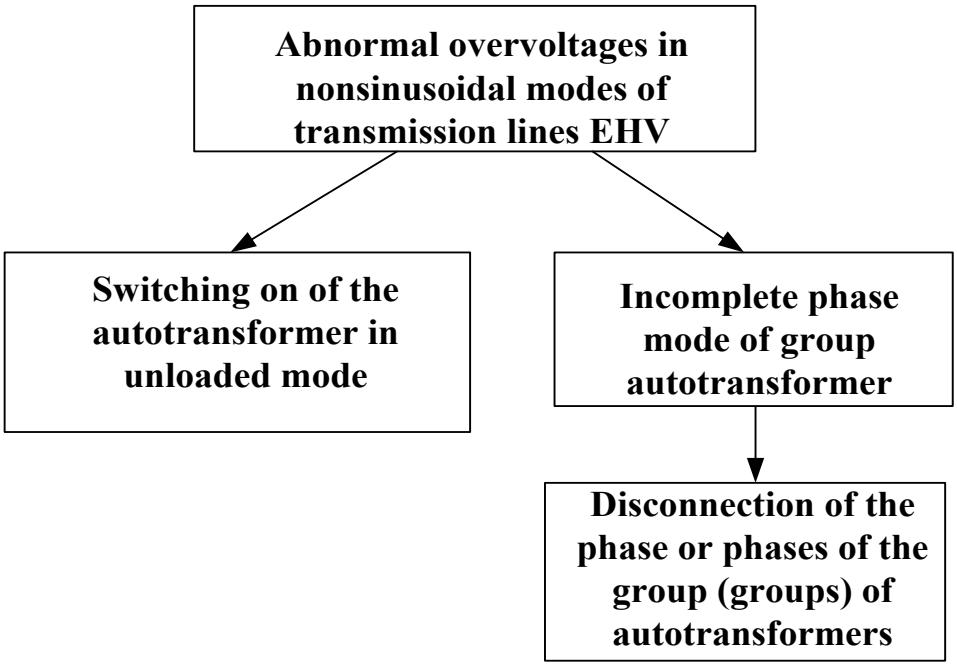

Fig. 1.5 Classification of ARO in nonsinusoidal modes

The physical nature of the emergence of even harmonics on the transmission line of the EHV with an attached autotransformer is due to the periodic change in the inductance of the magnetic shunt when passing through it alternating current. This inductance varies with a double frequency in relation to the applied voltage. Provided that the proper frequency of the equivalent circuit is equal to 100 Hz, there may be an overvoltage on the second harmonic. For this it is necessary that the input impedance was capacitive and was approximately equal to the average value of the inductive resistance of the magnetic shunt of the autotransformer at this frequency.

The maximum overvoltage depends on many parameters, the most important of which are: the operating voltage of the transmission lines EHV; transmission line length; number of groups of shunt reactors and degree of compensation of charge capacity; the ratio of the positive sequence reactive resistance of the line and the zero sequence of the line; the value of the preinsertion active resistance to the switch and the duration of their connection; the moments of switching on individual poles.

It should be noted that although the occurrence of this type of overvoltage outlined quite long ago, but nowadays, the process of their origin and development is insufficient. It remained unclear even the reason for their appearance. Some authors believed that the source of distortion is a constant component of the flow coupling AT, other scientists determined the reason for changing the parameters of the magnet shunt [11, 20].

Basically, harmonic overvoltages (Fig. 1.6) arise during the first stages of the restoration of electricity supply, when the whole system is weakly damaged. When switcing on the autotransformer, operating in idle mode, the magnetic shunt is saturated. This, in turn, results in the melting of magnetizing currents with a substantial content of the harmonics, including the second harmonic component, and thus the current source generating harmonic components appears to be connected to the transmission lines of the EHV. As a rule, the values of harmonic resonance overvoltages have a large multiplicity and are durable, so they can activate relay protection devices which led to disconnection of EHV line with all negative consequenses [20,21] or damage equipment isolation.

Thus, when the initial excitation of the autotransformer occurs, its magnetic core enters the state of saturation, in which magnetizing currents are generated causing an increase in the voltage of the harmonic components. To investigate the possibility of abnormal overvoltage it is expedient to use mathematical modeling [11-15]. However, studies conducted using the toolkit does not take into account the correlation between the factors affecting the characteristics of overvoltages. In addition, the use of simulation only makes it impossible to fully reproduce the

probabilistic nature of overvoltage due to the lack of development of appropriate procedures in mathematical maintenance. In the work to solve these problems in order to study ARO, it is proposed to use an artificial neural network and software complexes, the creation of which is necessary for the preparation of the functioning of the artificial neural network. It is precisely this combination of modern analysis tools that has provided an opportunity to ensure that the results of research with the necessary accuracy in the current state of the complexity of the electric networks of the EHV are obtained.

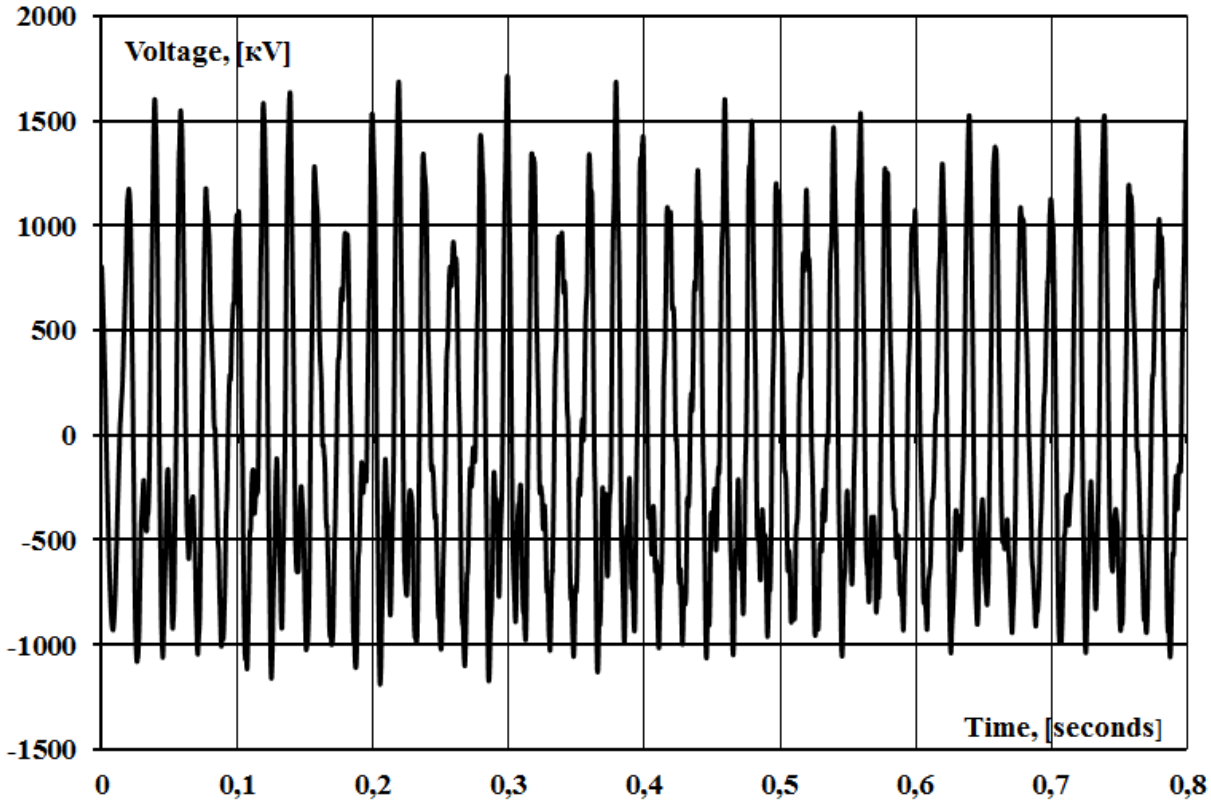

Fig. 1.6 ARO in nonsinusoidal modes

Accordance with requirements which are shown on table 1 we can conclude that, ARO in nonsinusoidal source of distortion are very dangerous for insulation of power equipment. In such abnormal mode occur significant and slow decaying ARO on even harmonics. Analysis of Figure 1.6 shows that overvoltages under the influence of higher even harmonic attain large values, develop rapidly and durable exist. A distinctive feature of this type of overvoltage is the rapid self-excitation of pair harmonics and a significant distortion of the shape of the voltage sinusoid.

In this mode, it is clearly traced the influence of the fields of higher harmonics on the ionization processes in isolation only aggravate due to the fact that the forms of the curves of voltage and current are significantly spoiled when excited autotransformer. Thus, the overvoltages arising from the saturation of the magnetic shunt of the autotransformer have a double effect on the isolation of the equipment. On the one hand, there is abnormal increase of voltage and on the other hand, there is an action of the nonsinusoidality.

1.3 A physical reason of resonant overvoltages in bulk electrical power systems

1.3.1 A physical reason of resonant overvoltages on higher harmonic components

The physical nature of the overvoltage of even harmonics on power lines connected with AT can be explained in any other way than periodical changing of magnetic shunt inductance during flowing alternate current through it. This inductance changes with double frequency relative to the applied voltage. If natural frequency of equivalent linear circuit will be approximately equal to 100 herz, the possible conditions of existence resonance overvoltages are performed. Also it is necessary that impedance has capacitive character and is approximately equal to the average inductive reactance of magnetic shunt autotransformer at this frequency. The process of appearance resonance overvoltage during connection no-loaded autotransformer is shown on Fig. 1.7.

Generally the necessary conditions of resonant overvoltage at higher harmonic components are:

a) the natural frequency of the resonant linear circuit should be close to the harmonics frequency and its resistance should have a capacitive nature;

b) the harmonic amplitude which occurs should be large enough;

c) active power losses in circuit at the frequency of harmonics must be small.

The resonance circuit is formed by connecting the phase of overhead line and unloaded autotransformer is shown on Fig. 1.8. It adopted the following notation elements on equivalent circuit:

L_S - the equivalent inductance of the power system;

L_L - inductance of transmission line;

L_{SHR} - inductance of groups shunt reactors;

C_E - capacity between phase to earth;

C_M - capacity between the phases of transmission line;

l - length of the line;

ω - angular speed.

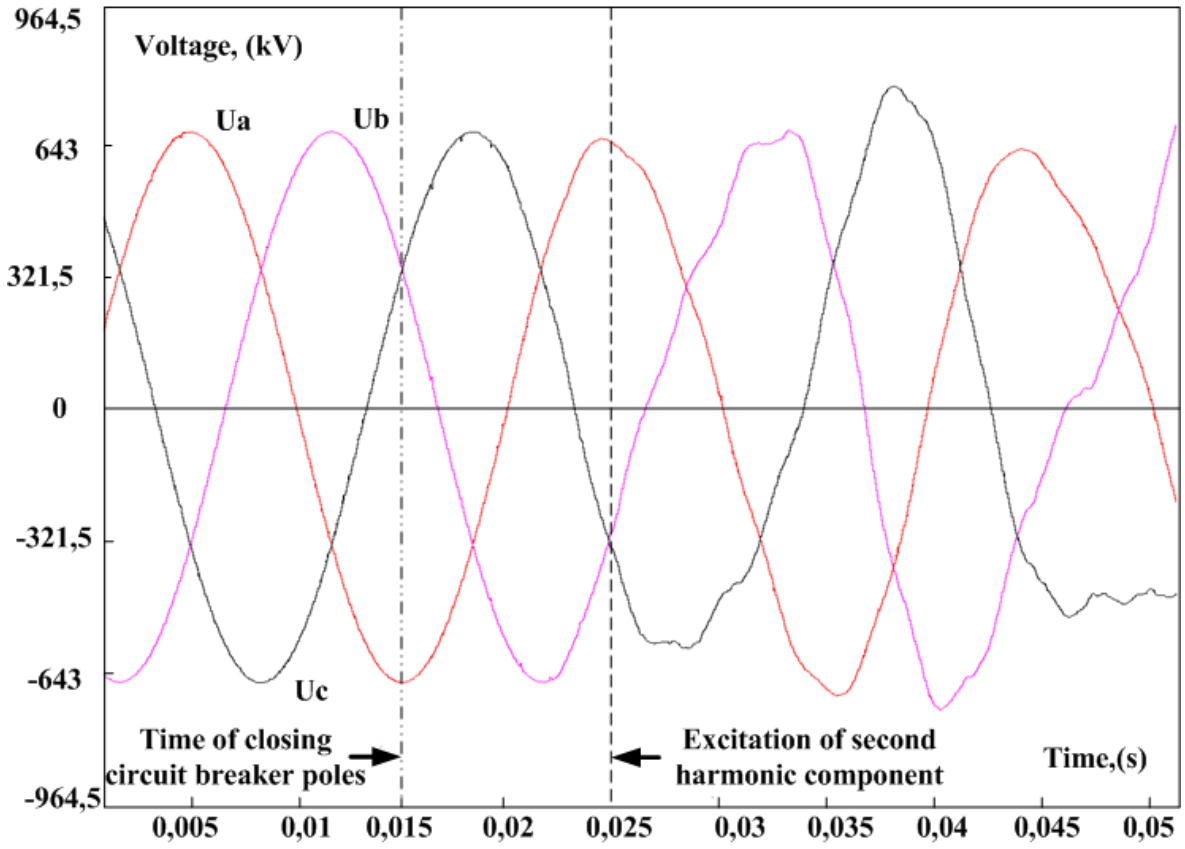

Fig.1.7 The appearance of overvoltages on higher harmonic components

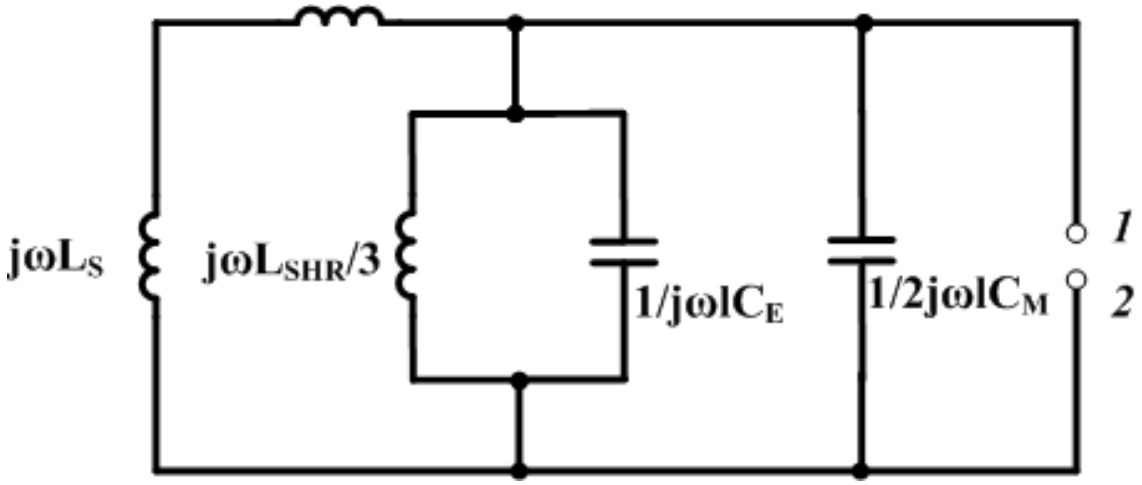

Fig.1.8 The resonance circuit of lineal part of overhead line

Input impedance X_{In} of resonant circuit between points 1 and 2 is described by the following analytical equation:

$$X_{In} = \frac{L_{SHR}\omega^2(\mathrm{L}_S + \mathrm{L}_L l)}{2C_M\omega^2 l\left[3(\mathrm{L}_S + \mathrm{L}_L l) + L_P(1 - C_E\omega^2\, l(\mathrm{L}_L l - \mathrm{L}_S\,\omega^2))\right] - 3} = \frac{P(\omega)}{Q(\omega)} \qquad (1.4)$$

As seen from the equation (1.4) in the resonant circuit is possible resonance of current $Q(\omega)=0$ that gives rise to overvoltages on the line:

$$2C_M\omega^2 l\left[3(\mathrm{L}_S + \mathrm{L}_L l) + L_P(1 - C_E\omega^2\, l(\mathrm{L}_L l - \mathrm{L}_S\,\omega^2))\right] \qquad (1.5)$$

From equation (1.5) obtained the polynomial of the third degree, which describes the resonance frequency of the line. In order to determine the resonance frequency the parameters of the line varied in long-range:

$$a_1 l - a_2 l^2 - a_3 l^3 - 3 = 0 \qquad (1.6)$$

$$a_1 = 0.084 \div 0.27$$

$$a_2 = 1.996 \cdot 10^{-4} \div 3.1 \cdot 10^{-4}$$

$$a_3 = 2.055 \cdot 10^{-7} \div 1.55 \cdot 10^{-6}$$

The resonance frequency (1.6) was obtained for two real overhead lines and the results of this computation are shown in table 1.2.

Table 1.2

Parameters of line and calculation results of resonance freaquency

Overhead line	Parameters of line			
	Resonance frequency, (Hz)	Length, (km)	Nominal voltage, kV	Numbers of groups shunt reactors, n
Khmelnytsky Nuclear Power Plant (Ukraine) – Rzeszow (Poland)	105	396	750	3
South-Ukrainian nuclear power plant (Ukraine) – Isaccea (Romania)	110	403		

To investigate the occurrence possibility of abnormal overvoltage is appropriate to use mathematical modeling Fig.1.9 [12]. Although there are works in which characteristics of the overvoltages are determined by the analytical methods of resonance circuits [12]. However, performed studies count out the correlation between the factors that influence the characteristics of the overvoltages. In addition, the use of simulation only makes it impossible to fully investigate the nature of this kind of overvoltages. Because of the abovementioned reasons, the simulation model was developed for extra high voltage system in modeling tools MATLAB / Simulink [12]. In this model, it is taken over that the shunt reactors are three. From practical experience it is known that overvoltages appear in lines that need to compensate reactive power with these numbers of groups shunt reactor.

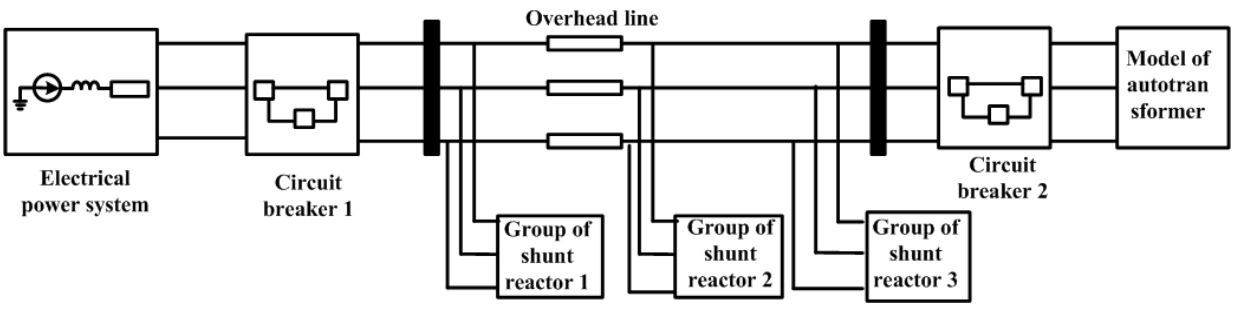

Fig. 1.9 The model of extra high voltage transmission line

As it is known from the course of electrical engineering, the sinusoidal voltage of the industrial frequency has a period equal to 0.02 seconds, which is equal to 360 electrical degrees. Therefore, in the case of resonance overvoltages simulation by model Fig.1.3, the results are presented in the form of voltage graphs dependencies on time, in which x- axis indicates the time which is measured in seconds. Such a representation of the results is dictated by the fact that the model which is presented on Fig. 1.3 models transient switching processes when an unloaded autotransformer is switched on. Therefore, the voltage sine and the dependence of the overvoltage value on switching angle for three lines with the same values of the parameters are plotted in Fig. 1.4. The lengths of the lines are 410, 435, 445 kilometers. The closing time of the switch poles for all three phases is changed in the following ranges:

$$\delta \in [0;360] \text{ electrical degrees and } t \in [0;0.02] \text{ seconds}$$

Using the model Fig. 1.9, the voltage dependences on angle connection have been received. As shown on Fig. 1.10. overvoltages have reached the maximum values in the areas of sine wave voltage extremes (0, 140) and (220; 270) electrical degree. These results correspond to results obtained in papers [8-10]. It should be noted that the arcing processes in the switch are not modeled instead of results shown in the existing researches [7-9].

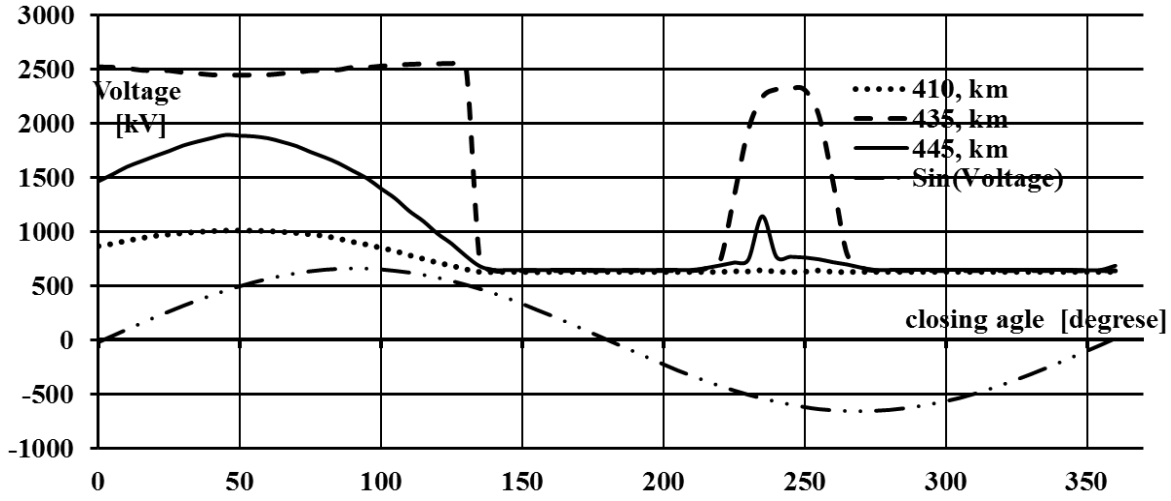

Fig. 1.10 Dependency graph of overvoltages on angle at connection autotransformer

The range of angle δ of switching at which the magnitudes of the overvoltages reach:

a) the maximum values of overvoltages correspond:

$$\delta \in [0{:}140] \text{ and } [210;270] \quad (1.7)$$

b) the minimum values of overvoltages correspond:

$$\delta \in [145;215] \text{ and } [275;355] \quad (1.8)$$

measures of supression resonance overvoltages on second harmonic

The article does not consider well-studied measures to suppress resonant overvoltages: controlled switching and pre-insertion resistances. These activities are included in the optional means of SF_6 switches.At the moment, it is of practical interest to use alternative measures based on studies of the effect of residual magnetization.

A method of reducing the inrush current of a AT and resonance overvoltages, including interruption at the time of reaching the maximum instantaneous voltage value in the phase of 90°. Such commutation is completely demagnetized prior to the closing of the switch contacts when the AT is connected to the network the residual magnetization of the magnetic circuit by applying a direct current to the primary winding.

The second method of suppression consists in demagnetizing the magnetic circuit from residual magnetization, which occurs as a result of a sudden discharge of the supply voltage and a break in the current when it passes through non-zero.Removal of residual magnetization is performed by passing a direct current of opposite polarities through one of the windings of each core of a AT magnetic circuit.

The process of demagnetization is carried out in several cycles. In the first cycle, the demagnetization current must be at least twice the no-load current of the autotransformer at rated voltage. In each subsequent cycle, the demagnetization current should be approximately 30% less than the current of the previous cycle. In

the last cycle, the demagnetization current should not be greater than the no-load current of the autotransformer at voltage.

Portable batteries, rectifying devices can be used as a source of direct current. For example, recommendations are given for suppressing resonant overvoltages, which resolve into to the following algorithm for connecting an unloaded AT:

- load connection from the AT windings;
- connection of the line to the AT.

Such a sequence of connecting an unloaded autotransformer, according to the author, allows suppression of resonant overvoltages. Thanks to the simulation, a series of calculations were made on the effect of the nature and values of the load on the autotransformer on the conditions for the occurrence of resonant overvoltages. Results of such algorithm you can see on Fig. 1.11.

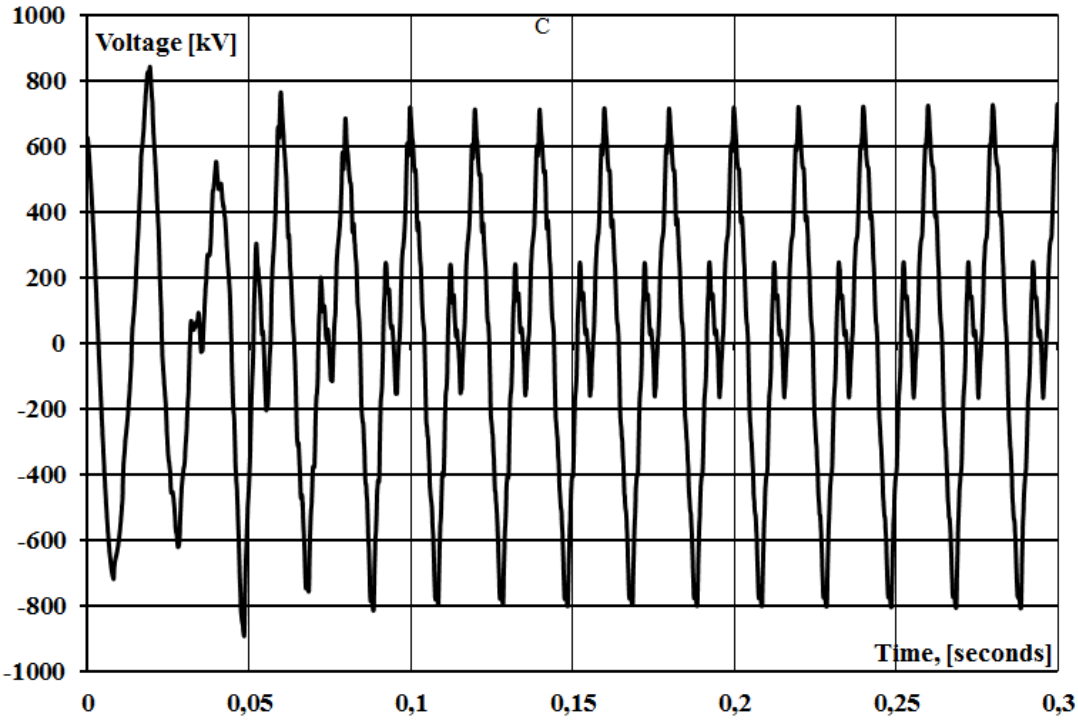

Fig. 1.11 Supression of resonance overvoltages in case of coincide moment of connection autotransformer and load

As you can see on Fig.1.12 the moment of connection autotransformer coincides with moment of connection of the load value 200 megawatt. So in this

case algorithm of connection supress resonance overvoltages but does not eliminate the second harmonic component.

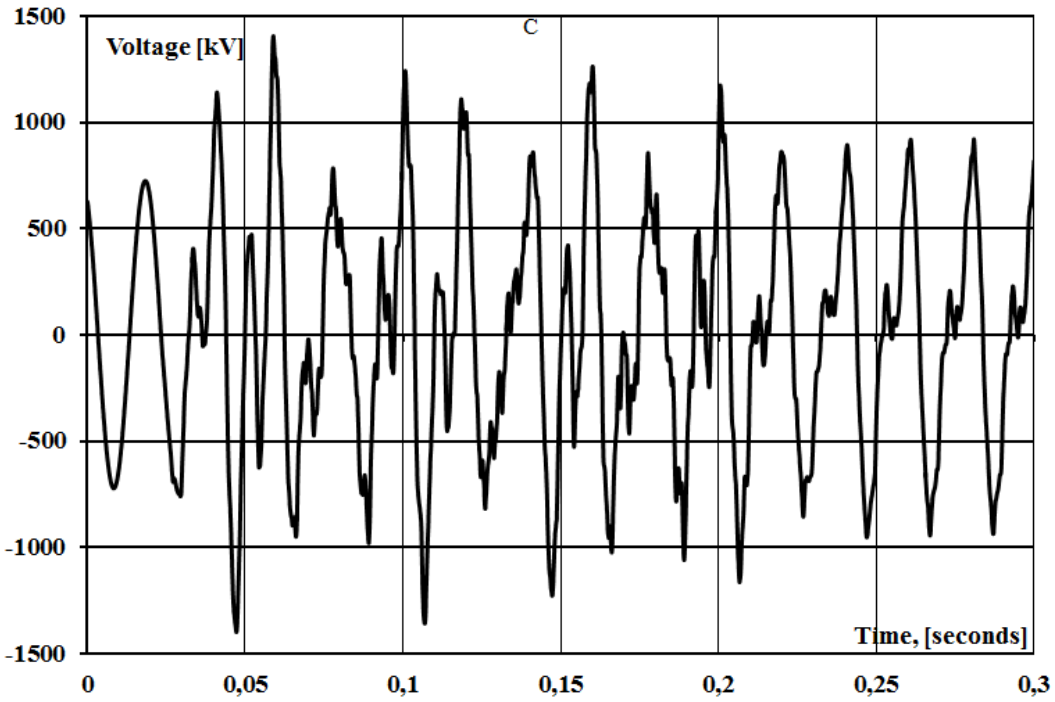

Fig 1.12 Supression of resonance overvoltages in case of noncoincidence moment of connection autotransformer and load

If the load is connected after connecting an unloaded autotransformer with an interval of 0.15 seconds, overvoltage will be observed at the second harmonic component, as can be seen from Fig. 1.12. Connecting an active load has a dissapative effect on resonant overvoltages.

1.3.2 Abnormal resonance overvoltages in the presence of asymmetric distortions.

Incomplete modes can occur spontaneously as emergency or planned modes especially as a measure that increases the reliability of the electrical system (Fig. 4). The latter category includes, for example, incomplete modes, which arise when applied on the lines of phase repair, as well as the disconnection of one or two phases of the line to melt the ice on overhead lines.

In main electrical networks, the flow of failures is almost entirely determined by accidents on the overhead line. In this case, as already noted, in

lines with a voltage of 750 kV the overwhelming part of the trips is caused by single-phase short circuits. Unstable single-phase short circuits occurring on the line are accompanied by minimal disturbances on adjacent systems if they are eliminated in a cycle of single phase automatic re-closer [10,15-19]. In this case, the damaged phase of the line is disconnected from the two sides by the switches, and then, after a certain time, the so-called powerless pause, is automatically re-closed. During an uninterrupted pause, the open arc of the alternating current in the overlap should be extinguished, namely, the overlapping surface must be deionized and almost completely restore its electrical strength. When exploiting EHV lines to 60-70% of single-phase short circuits are unstable, that is, they can be eliminated in a short-term cycle without interruption, with the subsequent restoration of the normal circuit.

Relevance of the use of long incomplete phase modes can be explained by a number of reasons. First, today in main power electrical system of Ukraine there is a rapid growth of electricity consumption with the simultaneous lagging of the construction of new transmission lines EHV. Secondly, there is a disproportion in the distribution of generating capacities on the territory of the country, as a result of which large volumes of power are transmitted over long distances. Thirdly, there appeared a large number of relatively low-power consumers who receive electrical energy by one-circuit EHV in the hundreds of kilometers long. It should be noted that with a large length of the line, the probability of both scheduled and sudden disconnections increases [13-15,23].

In itself, the disconnection of phases or phases of groups of shunt reactors in the normal mode of operation will not lead to an abnormal increase in voltage. The latter arise, as shown in the work, when the phase of the group of shunting reactors is switched off, which creates conditions for their resonance increase at the main frequency (Fig. 1.13).

It should be noted the possibility of occurrence of incomplete phase modes of overvoltage is not actually associated with the presence of asymmetry, but with nonsinusoidal distortions in the transmission lines EHV, which were considered in

the preceding paragraph. Thus the inclusion of an unloaded autotransformer at a certain length of the line leads to the appearance of ARO on pair harmonics. With incomplete phase activation of the autotransformer, the same processes take place as in the full-phase, but only at those phases that are activated. Specificity lies in the fact that the switching of the line occurs not on the three phases of the group of single-phase autotransformers, but on two. Such a mode in the bulk network is permissible from the point of view of asymmetry, because the value of the current in the reverse and zero sequence does not exceed the maximum permissible values. This is due to the fact that two or even three groups of single-phase autotransformers work on the terminal substation, so the disconnection of one phase does not lead to a significant deterioration of the regime.

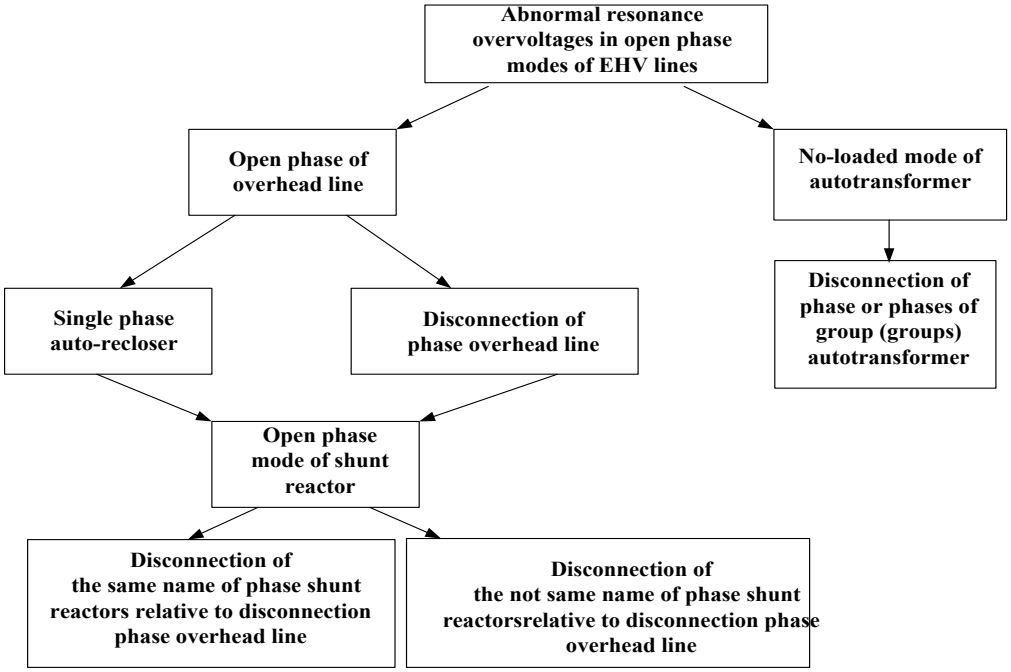

Fig. 1.13 Classification of ARO in assymetrical modes

When applying a single phase automatic re-closer, the switch-off phase of the transmission line leads to the of a transient process, after which the attenuation of a voltage in this phase is set at a level determined by the degree of compensation of distributed airline capacities by a group of shunt reactors [15,23]. This level may exceed the maximum permissible operating voltage. As the oscillograms of real processes in the operating networks have shown, often the transient process of

changing the voltage in the phase after its disconnection has the form of bits with the filling of the sinusoid of the industrial frequency. The values of the forced voltage depend on the parameters of a specific transmission line (length and design phase of the line, power supply system, availability, number and location of groups of shunting reactors). Single phase automatic re-closer may be accompanied by abnormal resonance overvoltages (Fig. 1.14). This type of overvoltage occurs due to the occurrence of resonant circuits with distributed line capacities and inductances of groups of shunt reactors. That is, at the actual lengths of the overhead line, the resonance properties of the line with the reactors appear not in the normal symmetric mode of operation, but in the asymmetric mode.

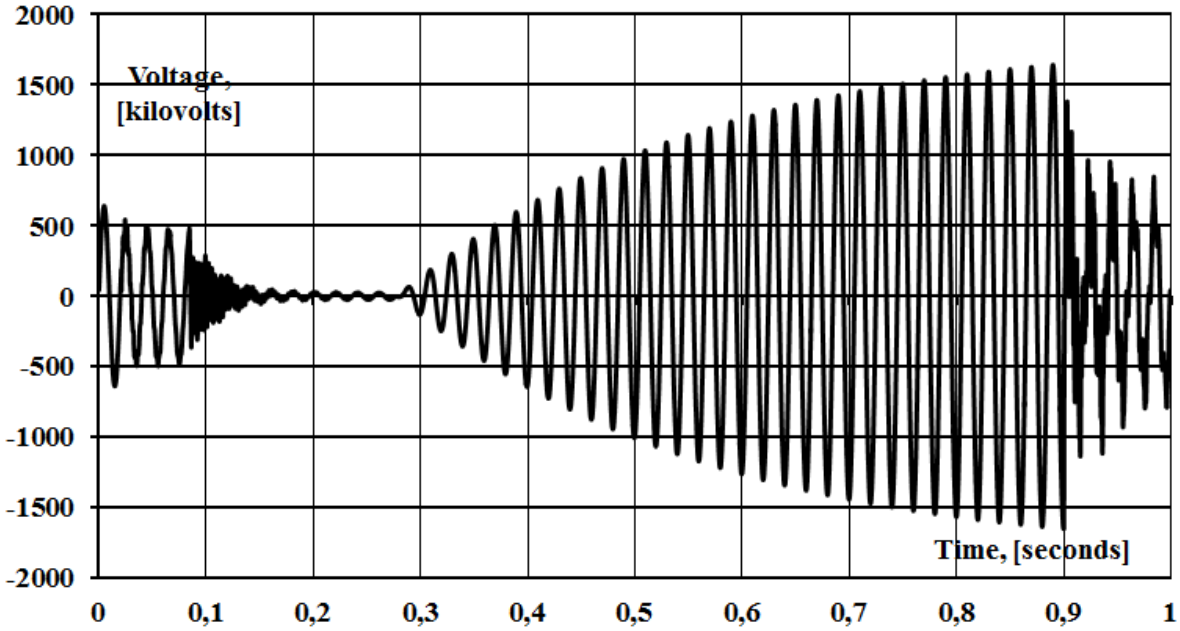

Fig. 1.14 ARO in assymetrical mode

In this case, ARO are characteristic of a mode in which the deviation of the circuit and the parameters of the elements from the phase symmetry play an essential role. As an example of such distortion, the incomplete mode of operation of the extra-high voltage transmission line is considered, which causes the appearance of resonance circuits with distributed capacities of the line and the inductances of the shunt reactors. The statement of the problem differs from the traditional design, when the criterion for choosing the inductors of the shunt reactors is the overvoltages of the normal mode, but although the causes of

overvoltages in the incomplete mode are well defined, their appearance and values depend on many factors of the abnormal regime. Therefore, when designing and operating the transmission lines EHV requires careful examination of the possibility of existence of necessary and sufficient conditions of the ARO in real electric networks.

Overvoltages arise due to the formation of a corresponding circle with distributed capacities of the line and inductance of the shunt reactors in the incomplete mode of operation of the transmission lines. For a more complete and clear understanding of the cause of the ARO in incomplete mode. As is known from the literature [8-12], shunt reactors are used to increase the line throughput, reactive power regulation and voltage in the normal operating conditions of the EHV transmission lines. The compensating reactor is used specially to compensate for the currents of secondary arc recharge at single phase auto re-closer. With a four-circuit connection circuit, the inductance of the shunt reactors compensates not only the capacitance between the ground and the phase of the line, but also the mutual capacity of overhead line.

So, we can see on Fig.1.14 that on the switched off phase of the overhead line, the process of abnormal resonance overvoltages arises, the character of which is determined by the natural oscillation frequencies of the resonant circuit with linear elements. It should be noted that an abnormal resonance voltage rise can be considered as a single-frequency process with a natural frequency, which depends on the degree of compensation of the line's charging power [15,23]. In this process, the overvoltages significantly exceed the maximum permissible values from Table 1 by several times, both in terms of both values and duration. The overvoltages in the asymmetrical mode appear slowly without distorting the shape of the voltage curve, but with significant values in the case of the current resonance condition, in contrast to overvoltages on the higher harmonic components.

The voltage arising from the formation of an appropriate range of line distributed capacitances with inductance group of shunt reactor at open-phase mode of power lines. For a more complete and accurate understanding of the

causes of resonance overvoltages at open-phase mode depicted schematic diagram and equivalent circuit of shunt reactors set in neutral compensation reactor (Fig. 1.15). As we know from the literature, shunt reactors are used to increase the capacity of lines, control of reactive power and voltage in normal modes of transmission line. The neutral compensation reactor is used specifically for suppression second arc current in pause of single phase auto-reclosure. In four-rayed connection of group (Fig. 1.15) inductance compensate not only the capacitance between the ground and also the interfacial capacitance between phases of the line. Generally the necessary conditions of resonant overvoltage at higher harmonic components are:

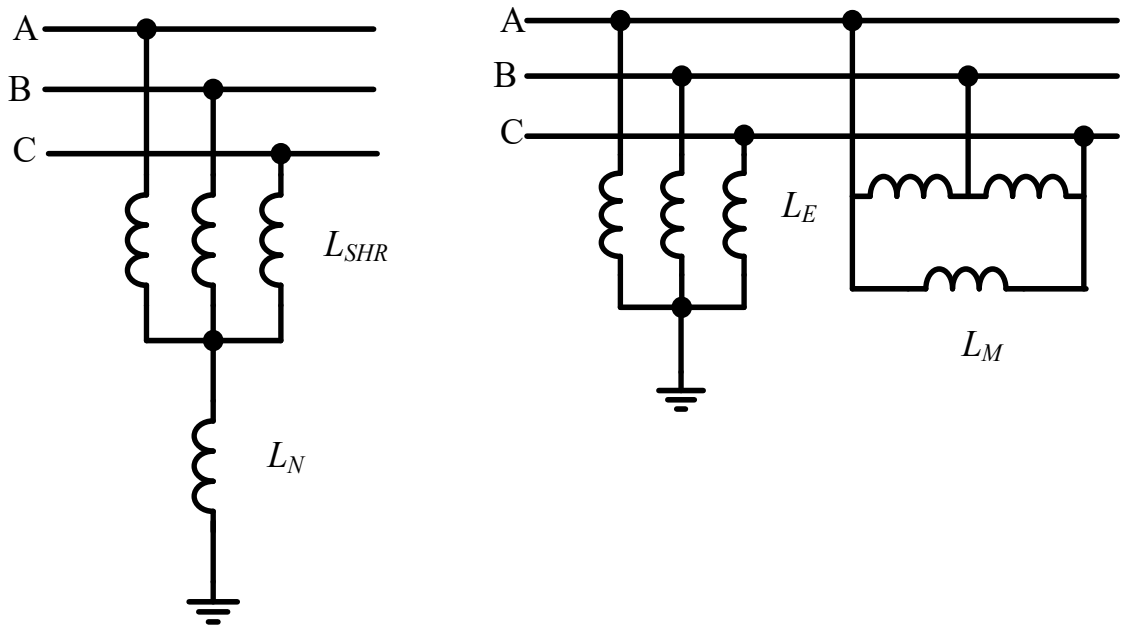

Fig. 1.15 Four-rayed connection of group shunt reactor

For better understanding of the action of four-rayed connection of group shunt reactor expressions below are constituents L_M – interphase inductance between phases and L_E – inductance between phase and earth:

$$L_M = \frac{L_P}{L_N}\left(L_P + 3L_N\right), \text{Hn} \tag{1.9}$$

$$L_3 = L_P + 3L_N, \text{Hn} \tag{1.10}$$

L_N – inductance of neutral compensator reactor, L_N – inductance of shunt reactor.

On equivevalent circuit of group shunt reactor (Fig. 1.16) it is shown that installation in neutral compensation reactor equivevalently appearance of two inductance circuit – L_E that it is inductance resistance of shunt reactor for compensation capacitance on between phase and earth and L_M – inductance for compensation mutual capacitance of the line. When value of equivalent inductance resistance L_M is tuned to full compensation mutal capacitance there is current resonance (Fig. 1.16).

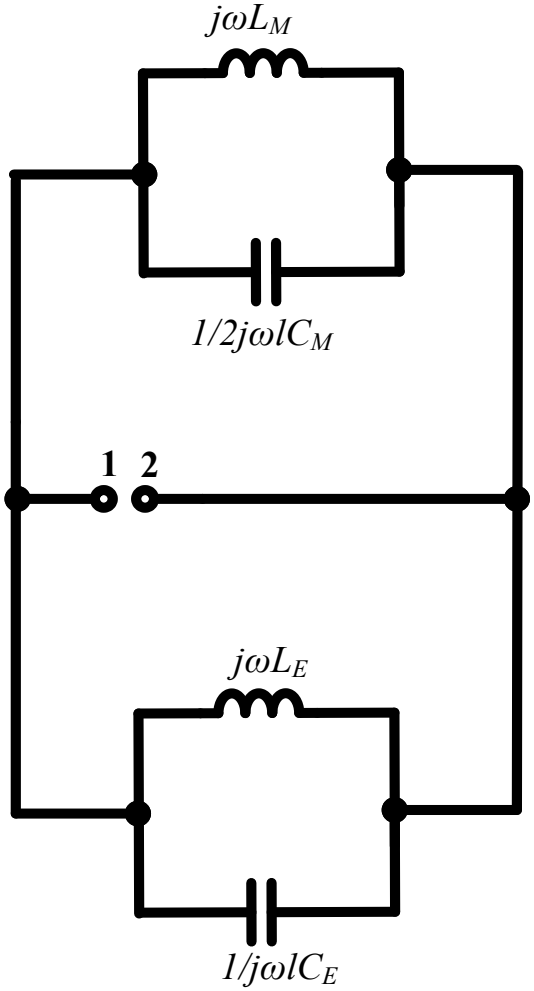

Fig. 1.16 Resonance circuit at single phase auto-reclosare

In circuit Fig. 1.16. possible existence of resonance of currents. The current resonance characterized by higher values of overvoltages in the outer circle.

Resonance current at open-phase mode of overhead line:

$$\omega^2 \cdot l \cdot L_E \cdot L_M \cdot (2 \cdot C_M + C_E) - L_M - L_E \qquad (1.11)$$

ω - rate of phase change; L_E – inductance that compensate capacitance between phase and earth; L_M – interphase inductance that compensate capacitance between phases; l – length of the line; C_M - interphase capacitance between phases; C_E - capacitance between phase and earth.

To analyze resonance overvoltages was derived formula for determining resonant lengths of line. The case of full-phase mode for any number of groups shunt reactors:

$$l_{\mathrm{Re}z} = n \frac{L_M + L_E}{L_E L_M \omega^2 \cdot (2C_M + C_E)}, \text{ km} \qquad (1.12)$$

n - number of full-phase group of shunt reactors.

Group of shunt reactor is a static electromagnetic device that has a high inductance and low active resistance. Groups of shunt reactor are used for control reactive power, voltage and transmitting capacitance by compensating capacity of extra high voltage line. Shunt reactors are connected to the line and switched to substation busbars. The reactor consumes reactive power the value of which depends on the voltage at its input.

Let is consider two circuit phase of group shunt reactor. Electric current which flows in any circuit phase of shunt reactor create magnetic flux that thread this phase Also current which flows in first circuit create through second circuit magnetic flux. By changes current the magnetic flux in first circuit will also change and thus in phase will induce electromotive force in second circuit. Circuits first and second are called coupled and phenomenon of appearance electromotive force in one of the circuit over changes current in second is called mutual inductance.

Model was developed to study the processes at single phase auto-reclose in the environment MATLAB / Simulink [14] (Fig. 1.17) that includes additional models of group shunt reactors and arc alternating current to investigate resonance

overvoltages. There were made calculations to find the effective measure to prevent this kind of overvoltages. -The three phase power system is simulated by voltage sources with fixed voltage and inductance. The overhead line is simulated by two parts with distributed parameters, which are given complex matrices with distributed elements or values on the forward and reverse sequence. By breaking the line at two parts simulates the failure in any point of the transmission line of extra high voltage.

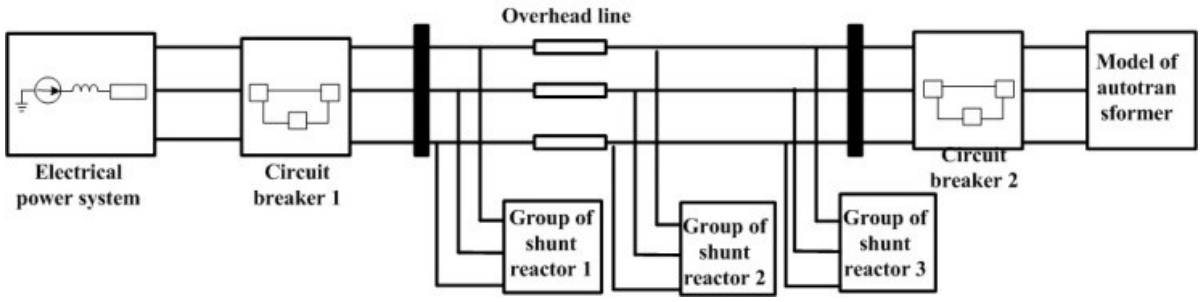

Fig. 1.17 Model of extra high voltage transmission line

As is seen from the results shown in the Table 3, disconnecting nonsimilar phase of group shunt reactor to failed phase of power line, does not lead to a significant change in the resonant length (1.1). Studies have shown [13] that dependency graph of overvoltages on the length looks like a parabola, so the line length deviation of 1-2 km would not result in significant disorder of resonance conditions corresponding to the maximum value of overvoltages. This kind of disconnecting does not achieve preventing or reducing resonance overvoltage. So disconnecting nonsimilar phase of shunt reactor according to preventing of resonance overvoltage is of no practical interest. When disconnecting the similar phase by one group of shunt reactor or similar phases of groups shunt reactor (under installed two or more groups) relative to phase of transmission line processes on which are considered, such switching lead to changes in settings of resonant circuit and overvoltage or does not occur or shift to smaller sizes, as can be seen from the table 1.3.

Table 1.3

Results of phase switching shunt reactors

The number of groups shunt reactors	Resonance length of the line, L_{Rez} (km)		
	Disconnection phase of one group shunt reactors		Mode with complete phase of shunt reactors
	Similar	Nonsimilar	
1	0	131	132
2	132	263	264
3	264	395	396

Tripping related phases led to resonance on line in the case of installing on line group shunt reactors lesser than unit:

$$l_{\mathrm{Re}z} = \frac{L_M + L_E}{L_E L_M \omega^2 \cdot (2C_M + C_E)}(n-1) \tag{1.13}$$

In table 4 compared simulation results obtained by the resonant overvoltages simulation on the model shown in Fig. 5 for incomplete phase mode and complete phase mode with and without influence of mutual inductance. When analyzing the resonance overvoltages this difference can be critical. In this case, the problem lays not so much by value, as by adequacy of the simulated results of resonance overvoltages, which makes the mutual influence between the phases of shunt reactors in the circuit configuration in the current resonance. As a corollary to this it is concluded that about investigation resonance overvoltages in extra high voltage lines (Fig. 1.18). Especially this is the case of area preventing measures this kind of overvoltages.

In Table 1.4 shown comparing results with and without the influence of the mutual inductance in incomplete and complete phase mode of group. It is clear from these results that the difference is 1.5%. Below are the results of the simulation with the same number off group with respect to the damaged phase of line. From these results it is evident that such a difference is not critical. This is

because the use of open-phase mode with disconnect similar phase relative to the damaged, significant reduce voltage by pulling out line from the resonance region.

Table 1.4

Comparison between results obtained by immitation model with and without account of mutual inductance resistance of shunt reactor X_S

Mode of group shunt reactor	**Voltages, kilovolts**		**Difference,%**
	With mutual inductance	**Without account of mutual inductance**	
Incomplete phase mode of group	118	114	1.51
Complete normal phase mode of group	811	795	2.39

Figure 1.18 shows the results of resonance overvoltage simulation of transmission lines and one of the groups of shunt reactor. This Figure 5 c shows how disconnection of similar phase of group shunt reactors to failed phase of transmission line can prevent resonant overvoltages. Also by comparison results of simulation with and without account of mutual inductance we can see that mutual inductance significant influence on resonant overvoltages.

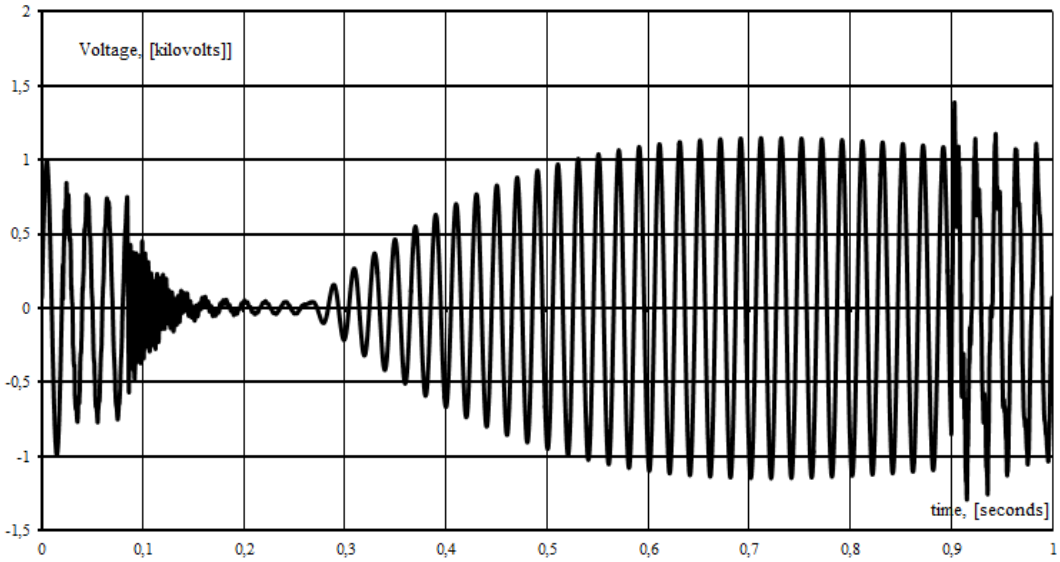

a)

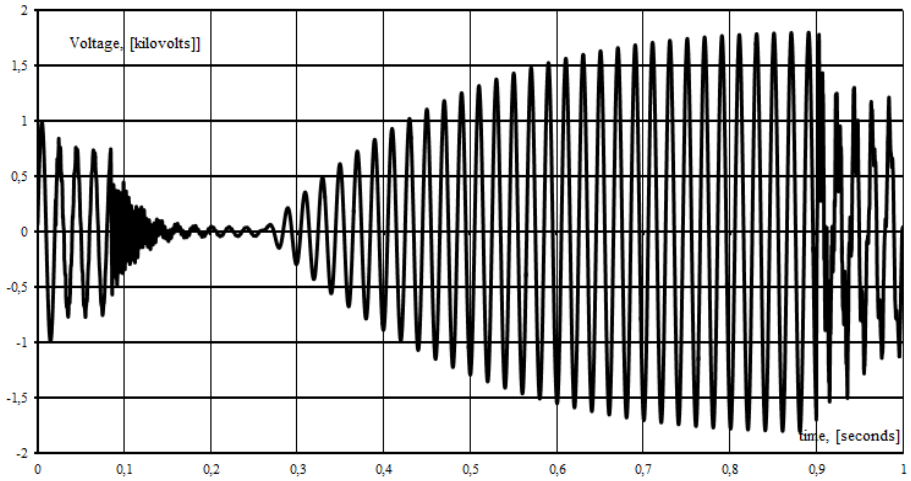

b)

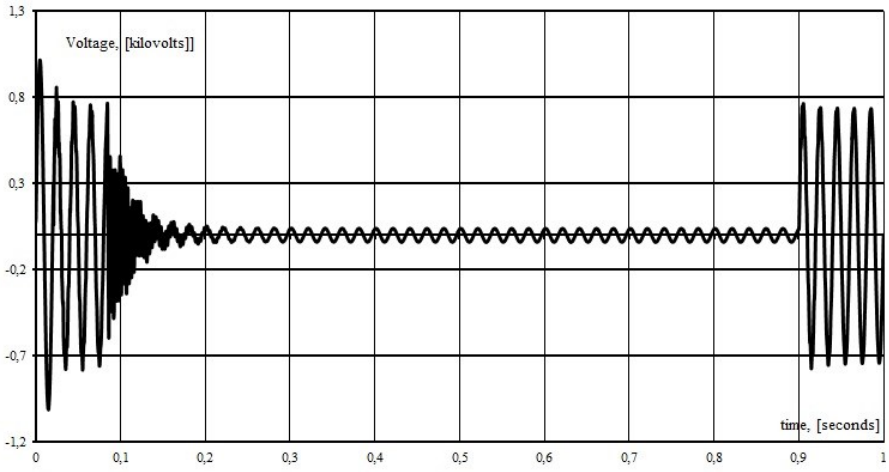

c)

Fig. 1.18 The effectiveness of disconnection similar phase of group shunt reactor with respect to failed phase of line in single phase auto reclosure. a) Overvoltages under failed phase without account of mutual inductance; b); Overvoltages under failed phase with account of mutual inductance c) disconnection similar phase of group shunt reactor with respect to failed phase of line.

In Table 1.6 the results of comparison of the resonance length in complete and incomplete phase group mode with and without the influence of the mutual inductance are shown. The resonant length of the line is calculated according to the equation. A difference of obtained results is 2.6%. Given that the length of the resonant line is widely used as a rapid assessment (references), such a difference

could significant effect on the determination of the existence region of resonance over-voltage and EHV transmission line resonance characteristics. The difference of approximately 15 km can lead to incorrect conclusions about the presence of the resonant overvoltages and cause a serious accident in the bulk energy system. Also in Table 1.5 the results of the comparison of influence mutual inductance in incomplete shunt reactor group are shown. In the case of the same name disconnecting phase of the group with respect to failed phase of the line as can be seen from Table 8 the difference in determining of the resonant length is approximately 1.5%, slightly lower than in complete mode of group. This difference can also lead to misleading when analyzing resonant overvoltages is the case with complete mode group.

Table 1.5

Comparison between results obtained by resonance length of the line $\mathbf{L_{Rez}}$ with and without account of mutual inductance resistance of shunt reactor X_S

Mode of group shunt reactor	**L_{Rez}, kilometers**		**Difference,%**
	With mutual inductance	**Without account of mutual inductance**	
Incomplete phase mode of group	264	258	1.32
Complete normal phase mode of group	396	388	2.06

1.4 Evaluation of the sources distortion influence on the quality of electrical energy of electrical networks

1.4.1 The problem of power quality in electrical power networks

In many developed countries, the deviations of electricity quality indices (EQI) from nominal values have become a permanent factor, which significantly

reduces the efficiency of electrical equipment (EE) of electric networks and consumers. In Ukraine, the situation with EQI deteriorates due to the insufficient transmission capacity of the networks (especially low voltage, the length of which reaches 50% of the total length of all lines); lack of funds for repair and modernization of the EE; obsolete methods of designing and operating networks that do not take into account (except the voltage and frequency) EQI index; the lack of modern means of measuring indicators EQI and effective devices to enhance it.

The decrease of the EQI index results, on the one hand, in increasing the losses of voltage and power in the networks, reducing their throughput, reducing the reliability of power supply, and on the other hand, to disrupting normal operation and reducing the term of service of the electrical equipment, reducing the quantity and quality of products produced, reducing labor productivity.

Authors has been developed methods for analyzing the modes of 0.4-110 kV electrical networks and above, taking into account the EQI indicators, assessing the impact of the deterioration of the EQI on electric power losses and lifetime of the EE, it was developed a number of effective methods and means of normalizing EQI indices.

The distortion of the shape of the voltage curve has a noticeable effect on the occurrence and flow of processes in the insulation of electrical machines and transformers [4]. In the presence ionization occurs, the essence of which consists in the formation of space charges and their subsequent neutralization. Neutralization of charges is associated with energy dissipation, the result of which is an electrical, mechanical and chemical effect on the surrounding dielectric. As a result, local defects in the insulation develop, which leads to an increase in dielectric losses and, ultimately, to a shorter service life. With allowable values of voltage unbalance of 2% and non-sinusoidal 5%, the service life of asynchronous motors is reduced by 21%, synchronous - by 32%, transformers - by 8%, capacitors - by 40%.

When reducing the voltage by 10% in the same way as with asymmetry

4%, the service life of electric motors is reduced by half, and with an increase in voltage by 10%, the service life of lighting installations is reduced by 4 times. The electric power losses in networks due to non-sinusoidal, asymmetry and voltage imbalance almost doubles.

The specific impact on various types of equipment, relay protection systems, automation, remote control and communication is worked differentially and depends on the amplitude spectrum of voltages (currents), parameters of electrical networks and other factors [2]. Thus, in the general case, there is no relationship between the energy of the harmonic interference and the degree of its impact on the electrical network.

This circumstance, apparently, led to the widespread use of the indicator characterizing the distortion of the mains voltage curve, called the voltage non-sinusoidal factor and determined by the ratio of the effective value of voltage to nominal or (more often) first harmonic voltage. For the same reason, in various countries there are often significantly different standards (norms, guidelines, regulations, etc.), in which, however, there is a tendency to limit the nonsinusoidality in the connection points of the sources and their penetration into the network of other voltages.

Analysis of the results of measurements of electricity quality indicators in networks with a rated voltage of 6-35 kV is presented in this materials.

The asymmetry of voltages in electrical networks arises due to the asymmetry of the phase parameters of its elements, for example overhead lines, autotransformers and shunt reactors. Voltage asymmetry is characterized by the magnitude of the voltage asymmetry coefficient by reverse order $K_{2U} = \frac{U_2}{U_1}$

Let an unbalanced EE Y be connected to a certain node of the electrical network (EN) through the resistance of the system Z_S to the generator. Connecting to the EN asymmetric EE causes the flow of asymmetric currents through its elements. This, in turn, leads to different values of the voltage drop in the phases of the EN and voltage unbalance at the point of attachment of the load.

$$\dot{U} \quad \cdot \quad \cdot$$
$$\dot{U} \quad \cdot \quad \cdot \qquad (1.14)$$
$$\dot{U} \quad \cdot \quad \cdot$$

Substituting $\dot{I}$, $\dot{I}$ in (1.14):

$$\dot{U} \quad \cdot \quad \cdot$$
$$\dot{U} \quad \cdot \quad \cdot \qquad (1.15)$$
$$\dot{U} \quad \cdot \quad \cdot$$

Considering that the generator does not create a negative-sequence electro motive force, and the resistances of the direct and reverse sequences are equal, the negative-sequence voltage at the connection point of the asymmetrical EE:

$$\dot{U} \quad \cdot \qquad (1.16)$$

$$K_{2U} = \frac{U_2}{U_1} = \frac{|Z_S \cdot}{|\dot{I} \cdot} \qquad (1.17)$$

We put Z_S out for brackets and get

$$\dot{U} \quad \cdot \quad , \qquad (1.18)$$
$$(Z_S \quad)$$

where $\dot{I}$ - short circuit current value. It is known that $\dot{I} \gg$. Then we can write

$$\dot{U} \quad \cdot \qquad (1.19)$$

Substituting (1.18) into (1.17) we get

$$K_{2U} \approx \frac{I_2}{I_{SC}} \qquad (1.20)$$

Normally permissible and maximum permissible value at the points of common connection to the EN according to all-Union State Standard 13109-97 is 2% and 4%. The quality of electricity at the point of general connection is

considered to comply with all-Union State Standard 13109-97, if the highest of all measured values within 24 hours does not exceed the maximum permissible value, and the value corresponding to a 95% probability for a specified period should not exceed the normally allowed values.

So that the asymmetrical EE connected to the EN does not lead to the appearance of unacceptable values at the point of common connection, the following conditions must be met:

$\frac{I_2}{I_{SC}} \le 0,02$ with probability 95 %; $0,02 < \frac{I_2}{I_{SC}} \le 0,04$ with probability 5 %.

If we assume that the normally allowed and maximum allowed value K_{2U} is determined for the condition $U_1 = U_{NOM}$, then taking into account the normal (5%) and maximum (10%) allowable value of the voltage drop and the constant value of the load current by the reverse sequence of I_2 inequality.according to the condition of normally acceptable value of voltage asymmetry in reverse order $\frac{I_2}{I_{SC}} \le 0,019$ with a probability of at least 90.25% with a decrease U_1 of 5% and $\frac{I_2}{I_{SC}} \le 0,018$ with a probability of at least 4.75% with a decrease U_1 of 10%;

according to the condition of the maximum permissible value of voltage asymmetry in reverse order $0,019 < \frac{I_2}{I_{SC}} \le 0,038$ with a probability of no more than 4.75% with a decrease U_1 of 5% and $0,018 < \frac{I_2}{I_{SC}} \le 0,036$ a probability of no more than 0.25% with a decrease U_1 of 10%.

Express the values of the phase currents through symmetrical components.

. . . .

(1.21)

Given that in three-phase networks with isolated neutral zero-sequence currents are missing, we get

(1.22)

1.4.2 Evaluation of the influence asymmetrical distortion sources on the quality of electrical energy in electrical networks with distributed generation

The main task of electric networks is providing effectively the needs of consumers in energy of the appropriate quality at minimum costs and sufficient level of reliability. This causes a constant increase in the size of the grids and the complexity of the structure. They have become the only complex for the transformation, stabilization of parameters and transport of electricity. At the same time, with the development of new technological processes, the share of asymmetric, nonlinear and dynamic consumers of electricity is continuously increasing. In practice, all this leads to the fact that in electricity networks such factors of distortion of the electricity quality as deviation, oscillation, asymmetry and non-linearity of voltage have become permanent disturbances. They significantly reduce the efficiency of both the power supply system's themselves and consumers which are power supplied from them.

Generation from renewable sources of energy: distributed generation (connected to networks of distribution companies) with a stochastic generation schedule. Increase in the volume of this energy would result in a fundamental change of the mode of power grids (stochastic generation in distribution depth) and the mode of balancing the whole power system. In general, the principles of construction, development of modern and The main goal of the article is to

determine the degree of influence of sources of distortions on the quality of frequency regulation and electricity of networks with distributed generation. The research was based on the developed model of the electric power system, which includes a 750 kV extra-high voltage power line and an electrical network with a wind turbine.In BEPS, the failures are almost entirely determined by accidents on the overhead lines. In this case, in lines 750 kV the overwhelming part of the trips is caused by single-phase short circuits (SC). From the point of view of distorting effects on adjacent systems, measures of liquidation of short circuits on a line are essential.

Emerging on the line unstable single-phase SC are accompanied by minimal disturbances on adjacent systems if they are eliminated in a cycle of single-phase automatic re-closure (SPAR) . In this case, the damaged phases of the line are disconnected from the two sides by the switches (fig. 1.20), and then, after a certain time, the so-called powerless pause, are automatically re-closed.

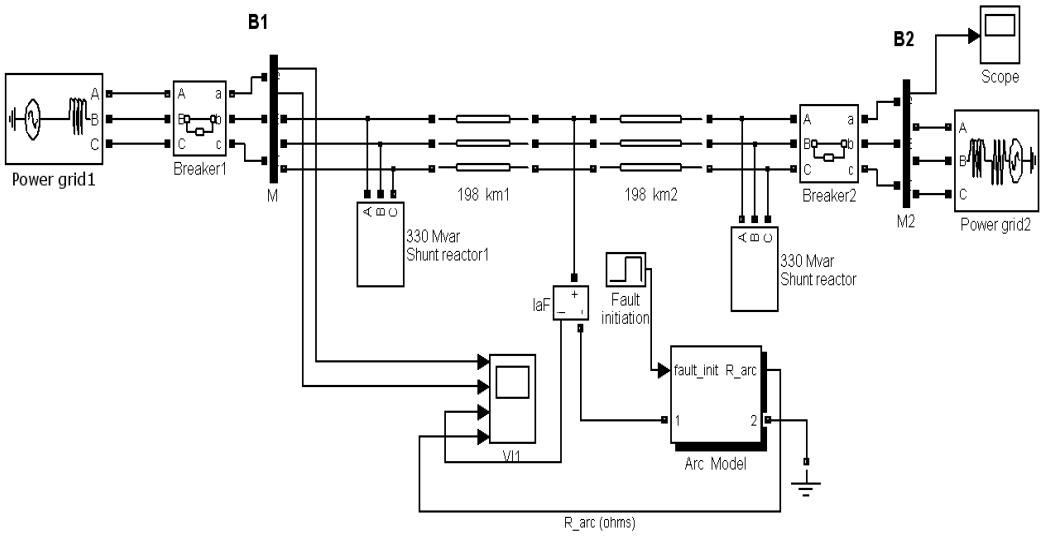

Fig. 1.20 Imitation model for investigation asymmetric modes

This example uses an initial state vector to start the simulation from steady-state. When you make changes to the model, the initial state vector needs to be regenerated or disabled; otherwise Simulink signals an error when the simulation is started. In turn, the wind turbine and the wind generator together form a wind unit. The turbine blades are combined into a rotor.

The principle of operation of the wind energy unit is related to the conversion of the kinetic energy of air molecules into the kinetic mechanical energy of the rotor. The kinetic energy of the turbine rotor is transformed into the kinetic energy of the wind generator (electric generator) using the transmission.

The electrical network induced in (fig.1.21) is taken as symmetrical, and the coefficients in the reverse and zero sequence are assumed to be zero to determine the effect of only sources of distortion of the backbone electrical system.

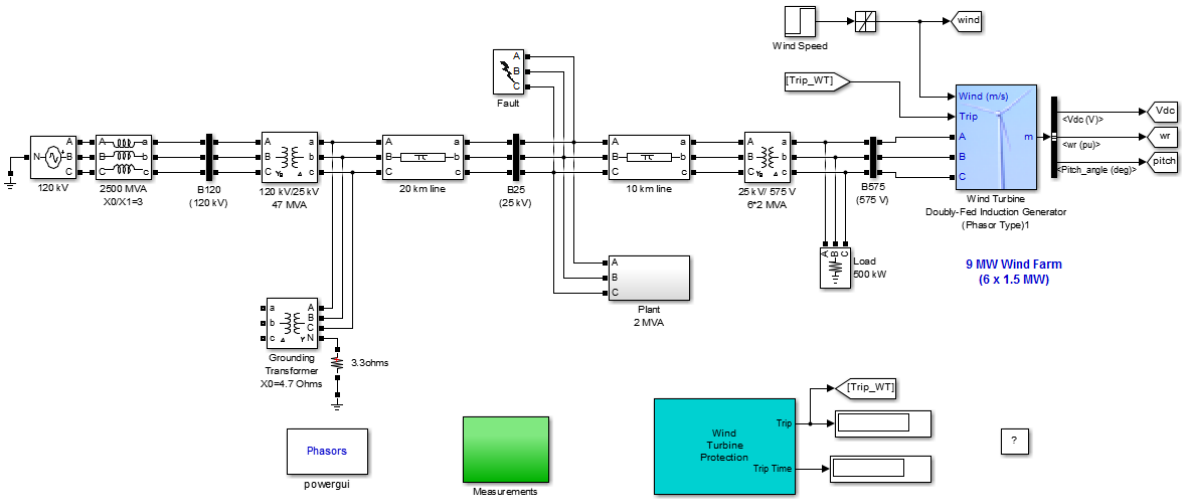

Fig. 1.21 Electrical network with wind farm

Voltage unbalance: The state of a three-phase alternating current power supply system in which the rms values of the main components of the interfacial voltages or phase angles between the main components of the interphase voltages are not equal to each other.

The voltage unbalance factor in the reverse sequence is the effective voltage value of the negative sequence voltage of the fundamental frequency, referred to the nominal effective voltage value. The coefficient of asymmetry of the voltage $k_{2U_i},\%$ by the negative sequence component for the i-th observation is determined by the formula:

$$k_{2U_i} = \frac{U_{2(1)i}}{U_{Nom}} \cdot 100,\%$$

where $U_{2(1)i}$ is the effective value of the negative-sequence voltage of the fundamental frequency in the i-th observation; U_{Nom} – nominal value of voltage.

The normal allowable value of the voltage unbalance factor in the reverse order is 2%. The maximum permissible value of the stress asymmetry coefficient by the reverse sequence is 4%.

The zero-sequence voltage unbalance factor is the ratio of the effective value of the zero-sequence voltage of the fundamental frequency to the nominal effective value of the phase voltage. The asymmetry coefficient for the zero sequence $k_{0U_i},\%$, for the i-th observation is determined by the formula:

$$k_{0U_i} = \frac{U_{0(1)i}}{U_{Nom}} \cdot 100,\%$$

where $U_{0(1)i}$ is the effective value of the zero-sequence voltage of the fundamental frequency in the i-th observation.

Changes in the value of the voltage unbalance factor with decreasing load power values are shown on table 1.6.

Table 1.6

Changes in the value of the voltage unbalance factor with changing places of SC on extra high-voltage transmission line.

Distance of CS, km	The coefficient of asymmetry of the voltage in distributed electrical network 25 kV, $U_{2(1)i}$, %
358	4.7
298	4.5
254	3.8
214	3.1
187	2.5
150	2.1
87	1.1

The reduction of systematic asymmetry in networks is carried out by rational distribution of single-phase loads between the phases so that the resistances of these loads are equal to each other. If the voltage unbalance cannot be reduced by circuit solutions, then balancing devices are used. As such devices used asymmetrically included capacitor banks.

Measures to reduce asymmetry of voltage:

1. The use of symmetrical devices (fig. 1.22). Resistances in the phases of the symmetrical devices are selected in such a way as to compensate for the negative sequence current generated by the open-phase mode as a source of distortion. Application of voltage balancing device. This is the most effective event, but it requires creativity in the design of electrical installations and decisiveness in operation.

2. The usage of uniform distribution of the load across the phases.

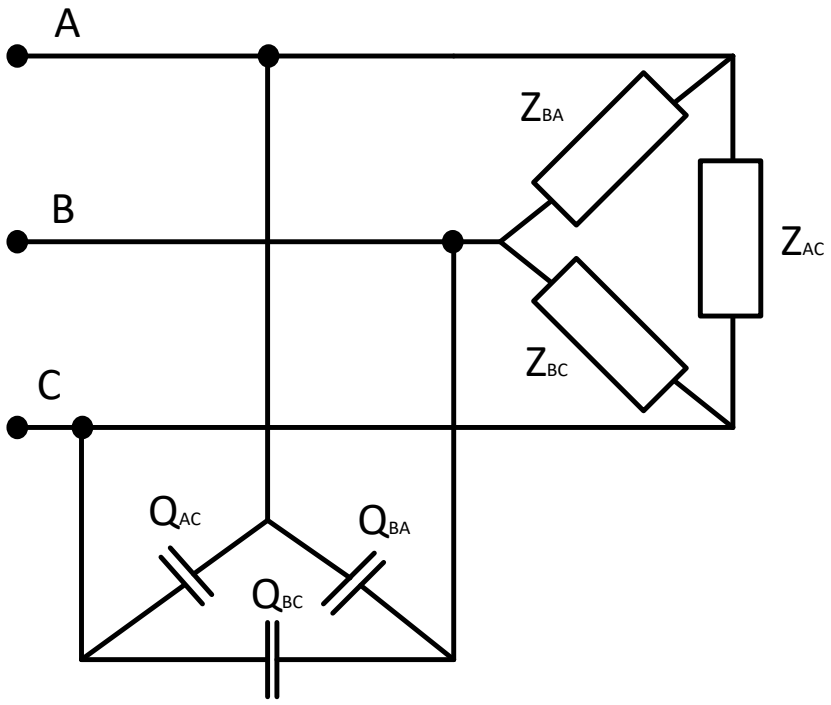

Fig. 1.22 Symmetrical device

2. MATHEMATICAL MODELING OF INFLUENCE OF DIFFERENT REGIONS ON ELECTRICAL APPLICATIONS, MODES AND LOSSES IN MICROGRID

2.1 The impact of renewable energy sources on the quality of electrical energy

In the energy sector of Ukraine, new technologies are being developed, informational and diagnostic systems are being implemented, modern means of measurement and management are implemented. In our time, consumers have a choice: to focus on centralized sources or to use autonomous power [24]. Ukraine is implementing distributed generation based on the active use of alternative energy sources of water, sun, wind, etc. As of January 1, 2015, in Ukraine, the installed capacity of renewable energy facilities with a green tariff was 1462.2 MW, of which 280.6 MW were introduced in 2014. Different scattered energy sources in 2014 produced 2.01 billion kWh. of electricity, which is 32% more than in 2013 [25].

This generation is actively developing in many countries of the world [26].

By the end of 2013, the share of renewable energy in the world energy balance was almost 22.1% (as shown in Fig. 2.1, a) and is increasing every year, due to the rapid increase in fossil fuel prices. Also, every year the power of photovoltaic systems in the world increases, and by the end of 2013 it was 139 GW (Fig. 2.1, b). In developed countries such as the Netherlands, Japan, Denmark, Germany and others, even entire towns using solar panels on roofs of buildings are created (Fig. 2.2) [27, 28].

However, in networks where RESs are actively installed and operated, namely PV, there is a deterioration in electricity quality indicators. This is, for example, more than the normalized voltage deviation on the bus of substations 10 / 0.4 kV, and such an indicator of electric energy quality as the coefficient of distortion of the voltage sinewave (Ku) [29-32].

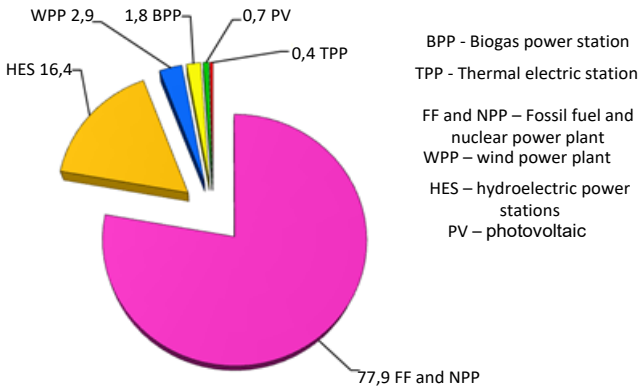

a)

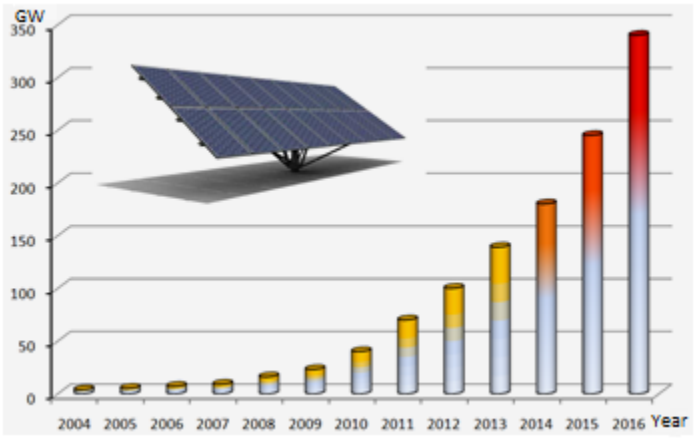

b)

Fig. 2.1. Development of renewable energy in the world: a) share of renewable energy in the world energy balance; b) the installed power of photovoltaic systems in the world (2004-2012 data [30], 2016 - [31], 2014-2015 - approximated)

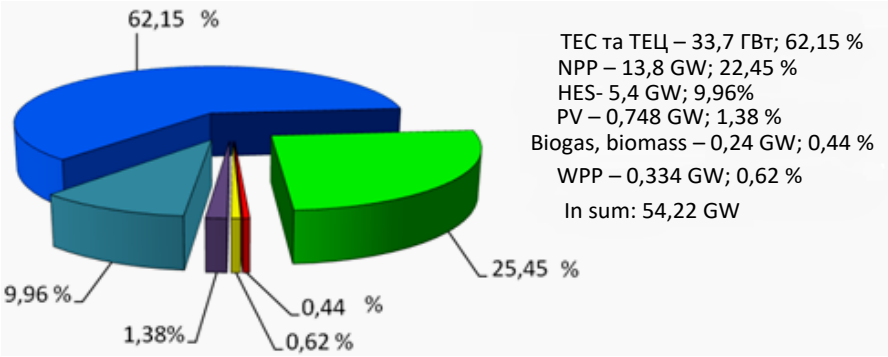

Fig. 2 2 The diagram of the installed capacity of the power industry of Ukraine by the end of 2013

Therefore, the task of developing mathematical and computer models of LES with RESs is relevant, which allows us to investigate the processes of changing the quality indices of electrical energy in these systems, in order to use the results of such studies in developing methods and tools for ensuring optimum utilization of LES equipment [29]. For this purpose Software tools such as Matlab (Simulink), PS Cad and others are widely used.

Analysis features of existing controllers inverter PV

The technological scheme of PV is shown in Fig. 2.3 [33]. The main elements of the PV are solar panels, inverter, collective transformer substation and switchgear. An important device of the PV is an inverter, the main purpose of which is to convert a constant voltage to a three-phase voltage, track the maximum power tracking point (MPTP), automatically phase-locked loop-PLL voltage synchronization, and others.

Fig. 2.3 Technological scheme of PV

Different control laws are implemented in the PV inverters, such as: proportional-integral (PI), proportional-resonant (PR) and DB (deatbeat) laws (Fig. 2.4).

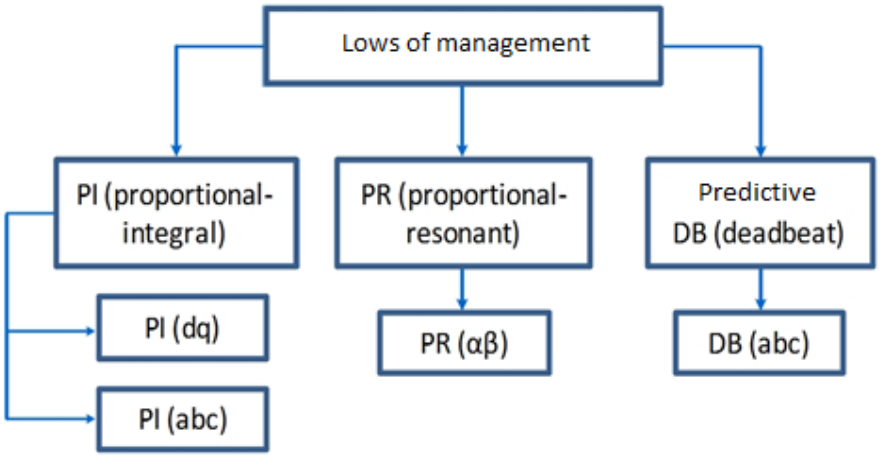

Fig. 2.4. Classification of the laws governing the inverters PV

Each of the PV inverters has its advantages and disadvantages.

It is known that the quality of electric energy in LES depends on parameters, state, mode of RES (renewable energy sources) in general and PV, as one of the types of RES. At the same time, the inverters of these stations and controllers have a significant influence on the quality indices of electric energy. In operation there are PV, many manufacturers which implement different laws of controlling their inverters. Therefore, the task of studying the influence of design features and laws of control of PV inverters on indicators of quality of electric energy in LES (local electric system) is actual.

Features of the proportional integral controller of PV inverters.

In the proportional-integral (PI) controller of PV inverters, the transformation of voltages and currents from the abc coordinate system in dq is usually realized.

coordinate system. The transfer function of the control system of the inverter, which operates under the IR of the control, is determined by the expression (2.1):

$$G_{PI}(s) = K_p + \frac{K_i}{s} \qquad (2.1)$$

where K_p, K_i is the proportional and integral coefficients of the gain of the controller, s is the Laplace operator.

The block diagram of control of the inverter PV with RI controller is shown in Fig. 2.5

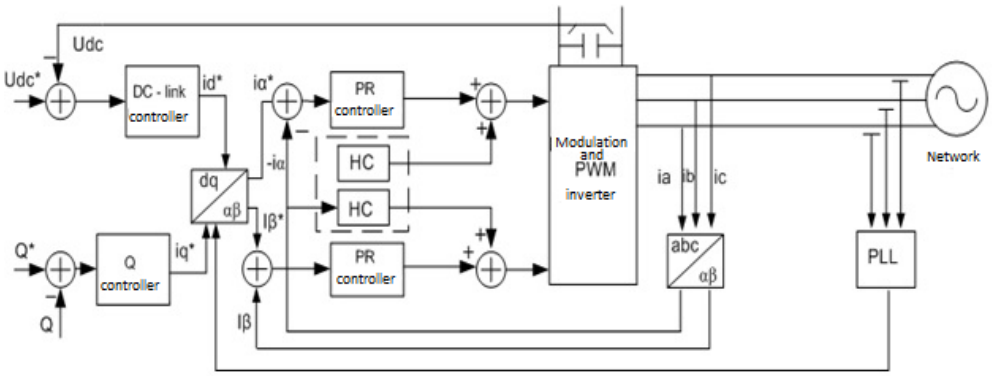

Fig. 2.5 The block diagram of control of the inverter PV using the PI of the controller [27]

In order to improve the PV characteristics, the controller software that manages the PV inverter is being improved. Thus, in particular, the transfer function (in abc coordinates) of the control system of the PV inverter, in which the PI control law is applied, is in the expression (2.2):

$$G^{(abc)}{}_{PI}(s) = \frac{2}{3}\begin{bmatrix} K_p + \frac{K_i s}{s^2+\omega^2{}_0} & -\frac{K_p}{2} - \frac{K_i s + \sqrt{3}K_i\omega_0}{2(s^2+\omega^2{}_0)} & -\frac{K_p}{2} - \frac{K_i s - \sqrt{3}K_i\omega_0}{2(s^2+\omega^2{}_0)} \\ \frac{K_p}{2} - \frac{K_i s - \sqrt{3}K_i\omega_0}{2(s^2+\omega^2{}_0)} & K_p + \frac{K_i s}{s^2+\omega^2{}_0} & -\frac{K_p}{2} - \frac{K_i s + \sqrt{3}K_i\omega_0}{2(s^2+\omega^2{}_0)} \\ -\frac{K_p}{2} - \frac{K_i s + \sqrt{3}K_i\omega_0}{2(s^2+\omega^2{}_0)} & -\frac{K_p}{2} - \frac{K_i s - \sqrt{3}K_i\omega_0}{2(s^2+\omega^2{}_0)} & K_p + \frac{K_i s}{s^2+\omega^2{}_0} \end{bmatrix} \quad (2.2)$$

where K_p, K_i is the proportional and integral coefficients of the gain of the controller, s is the Laplace operator, $\omega_0 = 2\pi f$ is the angular velocity and f is the frequency.

In fig. 2.5 shows the structural scheme of control of the inverter PV with PI controller, in which (using the Park-Gorev transformation) the transformation of signals of currents and voltages from a three-phase abc system of coordinates into a rotating dq coordinate system is realized. The PV inverter controller carries out

an agreed power supply to the PV on the bus control of the inverter, in such a way that the switch-on of the PV becomes impossible in the absence of tire voltage. In the control circuit of the inverter, the current signals after converting from the abc coordinate system to the coordinate system dq are converted to blocks that operate under PI control laws. Further converted signals are fed to PWM inputs (pulse width modulation) - pulse width modulator. At the output of PWM we get three-phase voltage. Also, the schematic (Fig. 2.5) uses the PLL (Phase-Locked Loop) automatic phase adjustment, whereby the inverter PV synchronizes with the voltage in the network.

The advantage of controller PI lies in the simplicity of its implementation and in the smallest harmonic distortion of the signal at its output in the normal operating conditions of the LES.

The disadvantage of controller PI is that it is a controlled voltage of LES on PV tires. Consequently, if there is a distortion of the voltage or current sinewave in the network (for example, when switching on and off other RESs, or high loads, etc.), there is a distortion of the voltage and phase currents sinusoid at the output of the inverter.

Features of the proportional-resonant controller of the inverter PV

Proportional-resonance (PR) controllers of PV inverters have become more widespread in the past decade, due to the fact that they use filters of harmonic components. These controllers react to the resonance frequency of the filter and eliminate the static error when adjusting the sinusoidal signal. They have a simple harmonic low-harmonic harmonic that does not affect the dynamic characteristics of the PV controllers of the PV that are used in the LES, connected to the EPS (Fig. 2.6). The transfer function of the PR controller G_{PR} is determined by the expression (2.3):

$$G_{PR}(s) = K_p + K_i \frac{s}{s^2 + \omega^2} \tag{2.3}$$

where K_p, K_i is the proportional and integral coefficients of the gain of the controller, s is the Laplace operator, $w = 2 \cdot \pi \cdot f$ is the resonance frequency.

The transfer function of the low-pass filter G_{HC} is expressed by (2.4):

$$G_{HC}(s) = \sum_{h=3,5,7} K_i \frac{s}{s^2 + (\omega^2 h)} \tag{2.4}$$

where h - serial number of the harmonic.

In fig. 2.6 shows a schematic diagram of the control of the PV inverter with the PR controller.

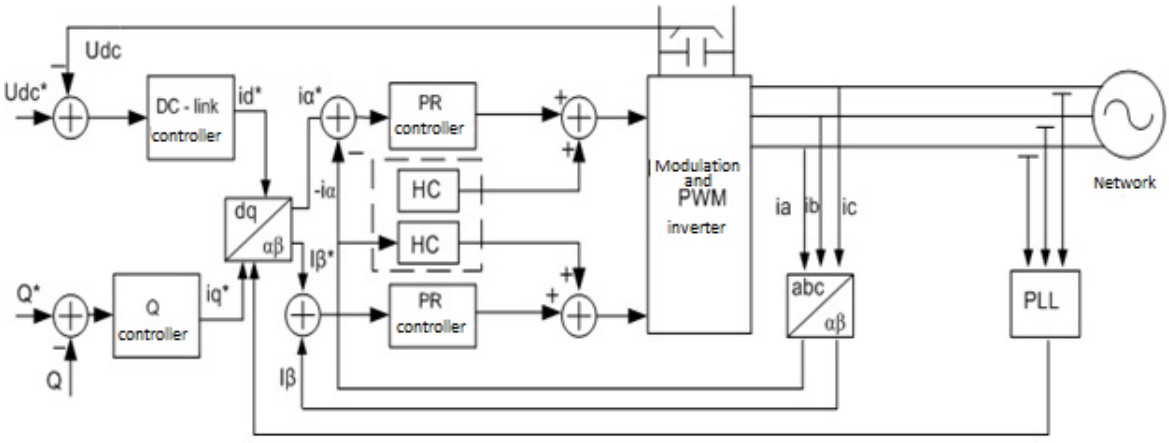

Fig. 2.6 Structural diagram of PV with PR controller [5]

Unlike Fig. 2.5, in Fig. 2.6, a block of transformation of currents from abc of a three-phase coordinate system in *abc* stationary coordinate system is used. The PLL block (Fig. 2.6) allows using the phase voltages in a three-phase coordinate system to find the angle of displacement on which to adjust the signal at the output of the inverter according to the reference signal (the voltage on the LES on the PV tires). In the conversion unit dq / αβ, the currents in dq of the coordinate system are converted into currents in the αβ coordinate system. Compared with the scheme in Fig. 2.5 in the structural scheme of Fig. 2.6 additionally used HC (harmonic compensator) harmonics harmonics, which perform functions of reducing the effects of 3, 5, 7 harmonics in the voltages on the output of the inverter PV.

The disadvantage of the PR controller inverter PV is the need for a complicated system of inverter synchronization with the network. The law of controlling this controller does not eliminate the effect of harmonics of high order (above 11 harmonics) on the voltage at the output of the inverter PV.

The transfer function of the control system of the SPS inverter, in which the PR controller is used (in abc of the coordinate system) is in the expression (2.5):

$$G^{(abc)}{}_{PR}(s) = \begin{bmatrix} K_p + \frac{K_i s}{s^2 + \omega^2{}_0} & 0 & 0 \\ 0 & K_p + \frac{K_i s}{s^2 + \omega^2{}_0} & 0 \\ 0 & 0 & K_p + \frac{K_i s}{s^2 + \omega^2{}_0} \end{bmatrix} \quad (2.5)$$

Features of the predictive (DB) controller inverter PV. One of the properties of the predictive DB (deadbeat) of the PV inverter controller is that in its software, the mathematical apparatus of fuzzy logic is used to predict the signal at the output of the controller. To explain the transfer function of the control system inverter PV, which uses the predictive controller in Fig. 2.7 shows a one-line scheme with the DB controller (Fig. 2.7).

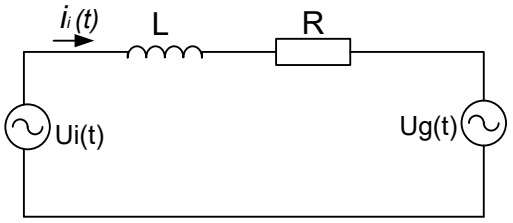

Fig. 2.7 Single-line schematic of PV with DB controller

In Fig. 2.7 shows: inductance L = + Lg and active resistance R = Ri + Rg, where Ri, Li - inductive and active resistance of the inverter, Lg, Rg - inductive and active network resistance).

The current in the electric circuit of the inverter is determined by the expression (2.6).

$$\frac{di_i(t)}{dt} = \frac{R}{L} i_i(t) + \frac{1}{L}(U_i(t) - U_g(t)) \tag{2.6}$$

where ii is the current in the circle of the inverter, R is the total active resistance, L is the total inductance, Ui is the voltage on the busbar of the inverter, Ug is the voltage in the PV bus.

After conversion, we obtain the expression (2.7):

$$i_i((k+1)T_s) = e^{-(R/L)T_s} i_i(kT_s) - \frac{1}{R_T}(e^{-(R/L)T_s} - 1)(U_i(kT_s) - U_g(kT_s)) \tag{2.7}$$

where Ts is a constant inertia, R is the total active resistance, L is the total inductance.

Transfer function DB is defined by the expression (2.8):

$$G^{(abc)}{}_{DB} = (\frac{1}{b})(\frac{1 - az^{-1}}{1 - az^{-1}}), \tag{2.8}$$

where $a = e^{-(R/L)T_s}$, $b = -\frac{1}{R}(e^{-(R/L)T_s} - 1)$, T_s –constant inertia.

This controller uses the LCL filter and block, which implements a simplified calculation model of the LES and parameters of the regime on the PV tires. This enables the controller to be sensitive to the non-compliance of the model parameters with the parameters of the current LES regime on the PV bus. The disadvantage of this controller is the delay in time, which greatly impairs its performance and the quality of the reaction to changing the regime parameters in the LES.

2.2 Study of operating modes and parameters of PV inverters on harmonic components in microgrid

PVs are being actively built in the Vinnytsia region, for example, there are PV such as Sloboda-Bushnaya PV, Galzhbievska PV, Tsekinivska PV and

Pomeranian PV in the Yampilsky District Electric Networks. Consider a fragment of the microgrid scheme of the Yampil REM and the connection of Sloboda-Bushnaya PV to them (Fig. 2.8).

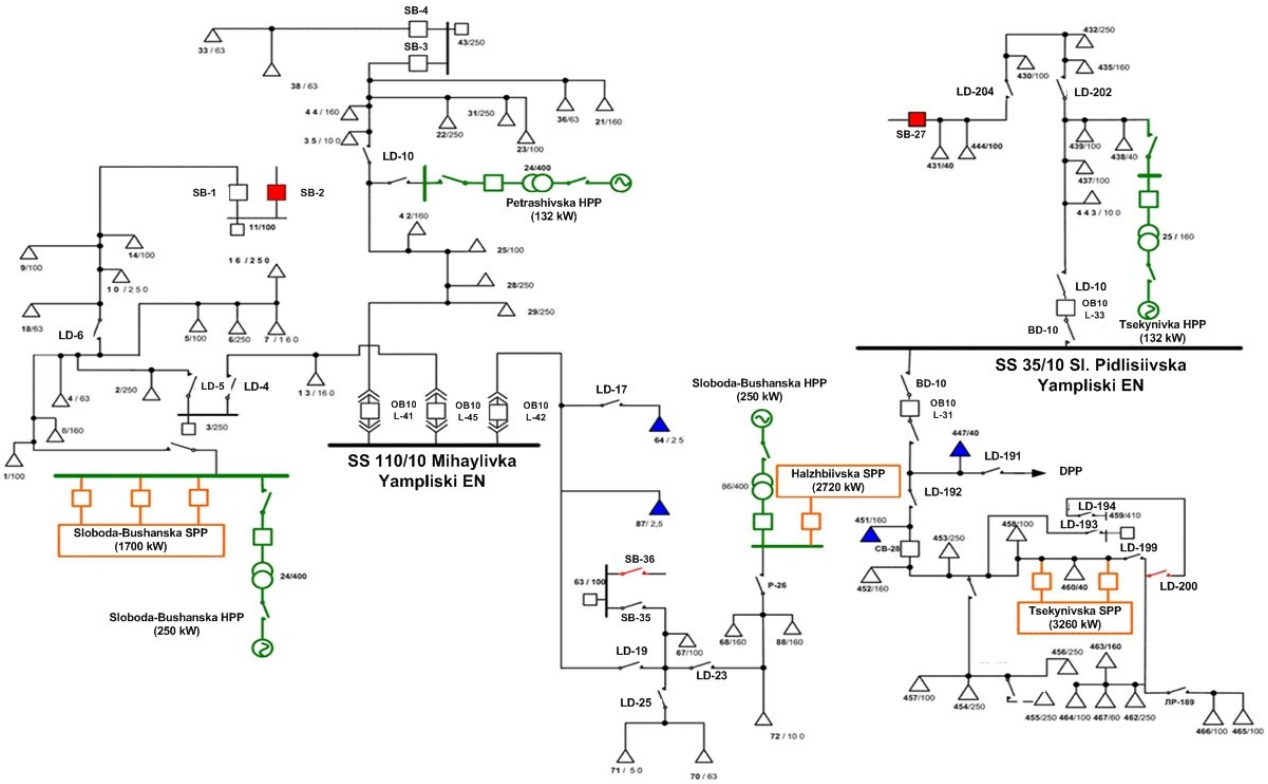

Fig. 2.8 A fragment of the scheme of the Sloboda-Buhanskaya PV and the HES in the Yampolski DEN

In order to analyze the processes occurring in the PV LES, a model of LES 110/10 / 0.4 kV voltage was created in the software environment PS CAD (Power System Simulation) shown in Fig. 2.9. In the computer model, the scheme of which is shown on rice 9, as power supplies, the following power systems are used: the power system connected to the 110 kV Lumber, PV_1 and PV_2 tanks (the capacities of which were selected within the range of 0.5 to 1 MW). Also shown in the diagram are a battery of static capacitor (BSC) for reactive power compensation, three lowering transformers (110/10 kV and 10 / 0.4kV) and two elevating transformers (0.4 / 10 kV) at substations of PV, as well as two lines 10 kV for the power supply of consumers (during the simulation the load power varied within the range of 0.3 MW to 1.23 MW). The scheme of the PV, in which

the controller of the inverter, implementing the PI control law in dq of the coordinate system, is shown in Fig. 2.10

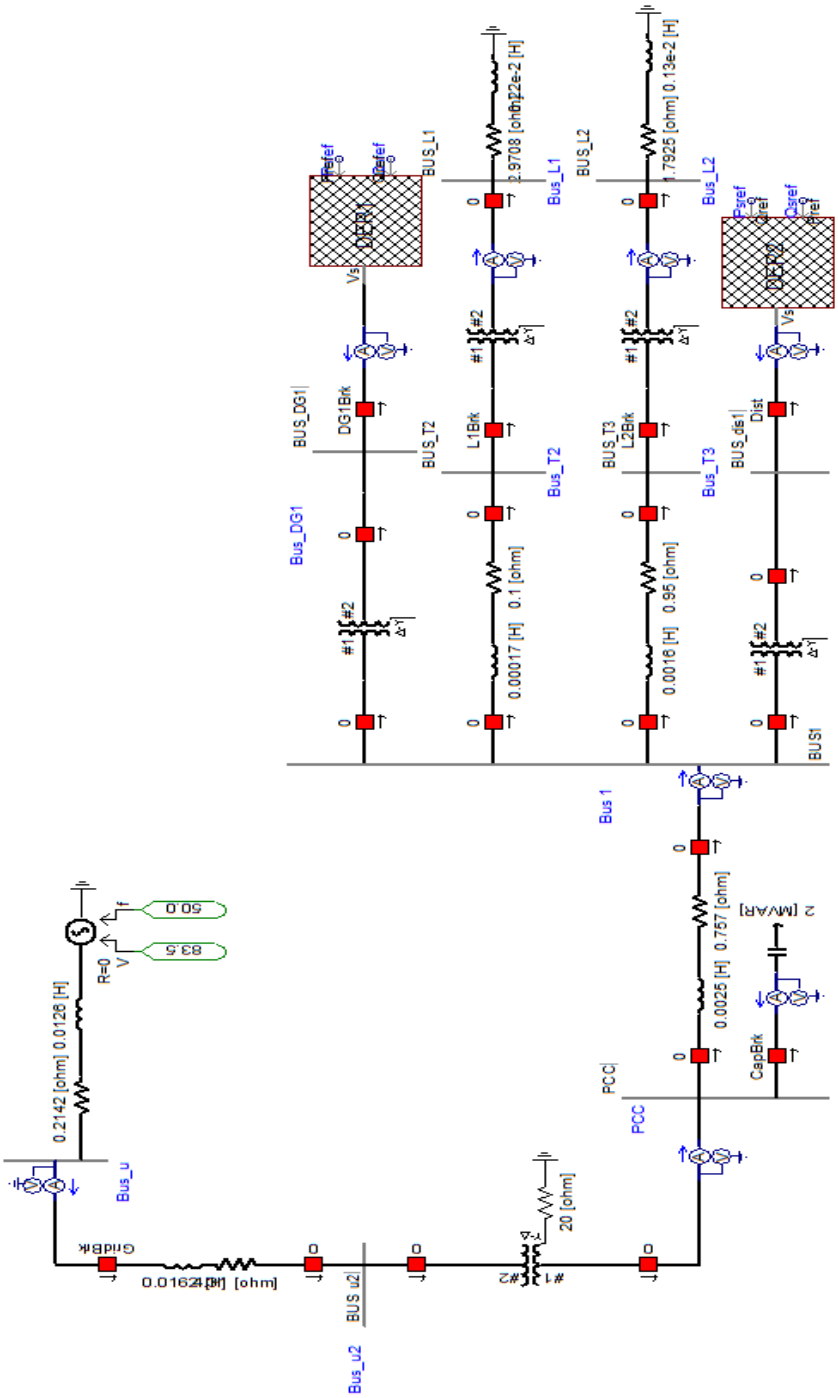

Fig. 2.9 Scheme of the microgrid model 110/10 / 0.4 kV voltage in the software environment PS CAD

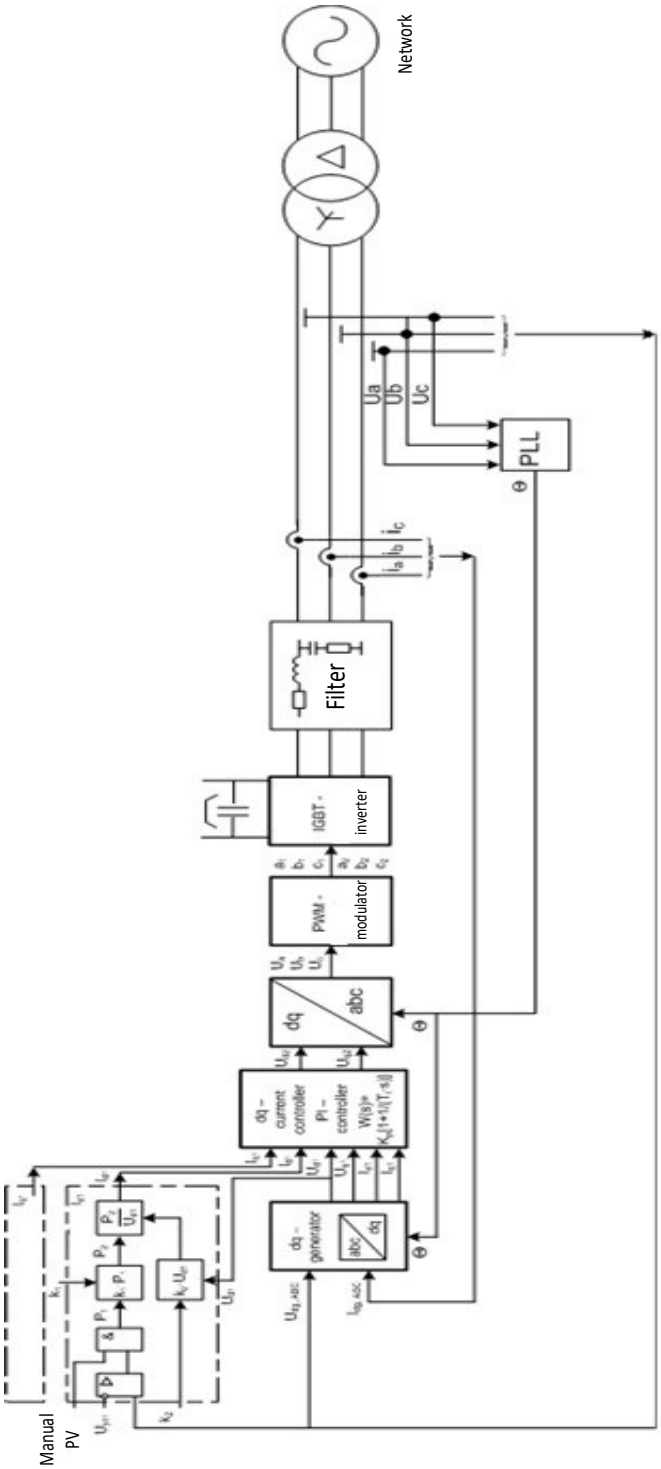

Fig. 2.10 Scheme of PV model with PI controller in software environment PS CAD

As an indicator of the quality of electric energy, we suggest using a harmonic component

voltage (K_u), which is determined by the expression (2.9):

$$K_u = \frac{\sqrt{\sum_{n=2}^{\infty} U_n^2}}{U_1} \times 100\% \qquad (2.9)$$

where U_1 is the amplitude of the fundamental harmonic, $_{Un}$ is the amplitude of the nth harmonic component.

Using in the scheme of the two PV Fig. 2.9 provides an opportunity to analyze the coefficients of harmonic components in stress on LES tires under different laws of control of PV inverters. In Fig. 2.11 shows the results of research of harmonic components in stress on PV buses, which use controllers of inverters operating under different control laws.

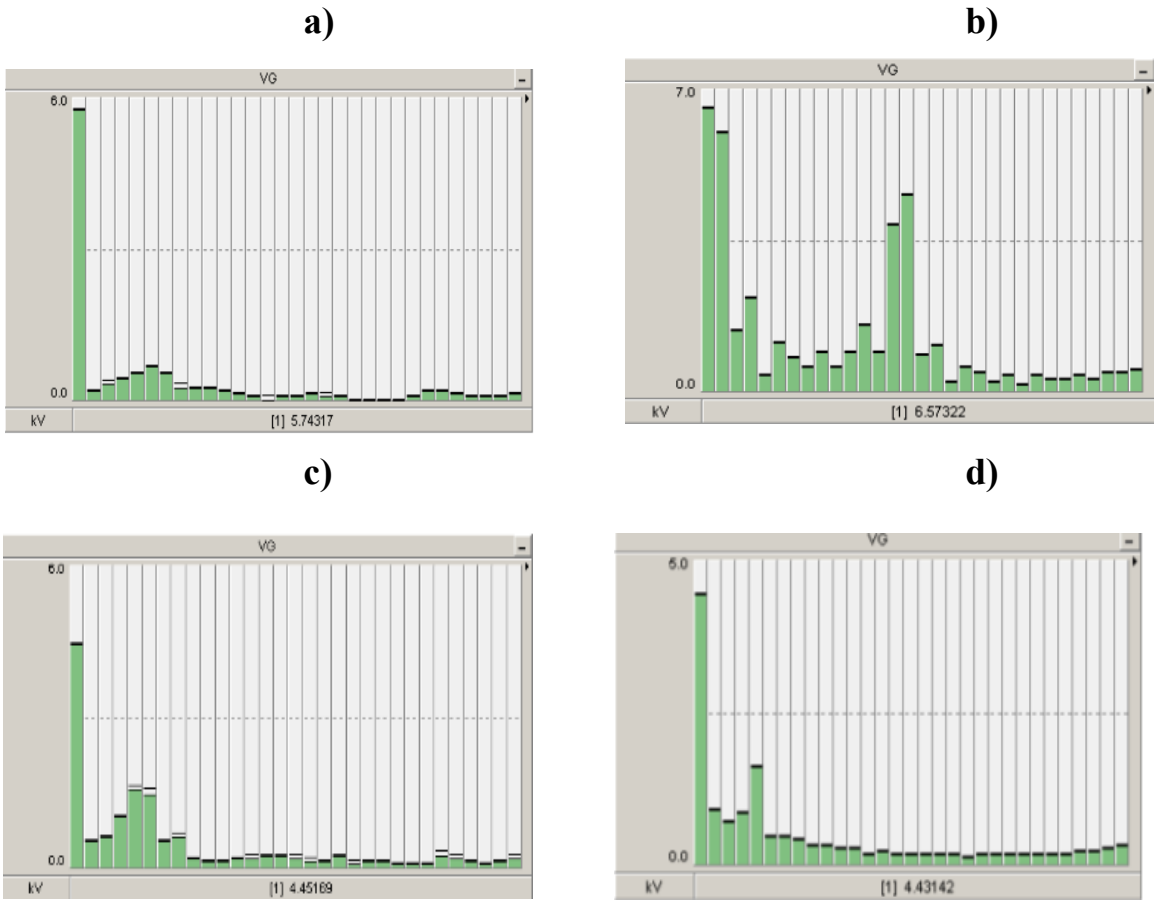

Fig. 2.11 Spectrum of harmonic components in voltage on PV buses

Figure 2.11 shows the harmonic components in the voltage on the coefficient K_u buses, provided that they are used on the PV: a) the PI of the controller, which uses the transformation of the coordinate system into dq; b) PR controller, which uses the transformation into coordinate system αβ; c) PI of the controller, which uses the transformation of the coordinate system into abc; d) using the DB controller, in which the transformation of the coordinate system into abc is used. The results of the studies are presented in table 2.1.

Table 2.1.

The value of the coefficient of harmonic distructions

Controller control law and coordinate system	Value of coefficient K_u,%
PI (abc)	6,3
PI (dq)	6,9
DB (abc)	7,5
PR (αβ)	7,8

Consequently, comparing the obtained results it can be concluded that the least harmonic distortion of the voltage sinewave will be when using the controller PI, which implements the transformation of the coordinate system into abc, and the use of the PR controller, implementing the transformation into the αβ coordinate system, will produce the most harmonic distortion at the output of the inverter. In further research, PI controllers were used on both PVs. The results of computer simulation indicate that the greatest distortion of the shape of the voltage and current sinusoid at the outlet of the PV causes the transient processes associated with the switching on and off of powerful consumers, the PV itself, a powerful BSC, etc. Particularly significant distortions occur in mode the inclusion of different PV and powerful consumers with a short interval of time between them

(for example, in the case of successful dumping on different LES sites). The results of the research are shown in Fig. 2.12 and 2.13.

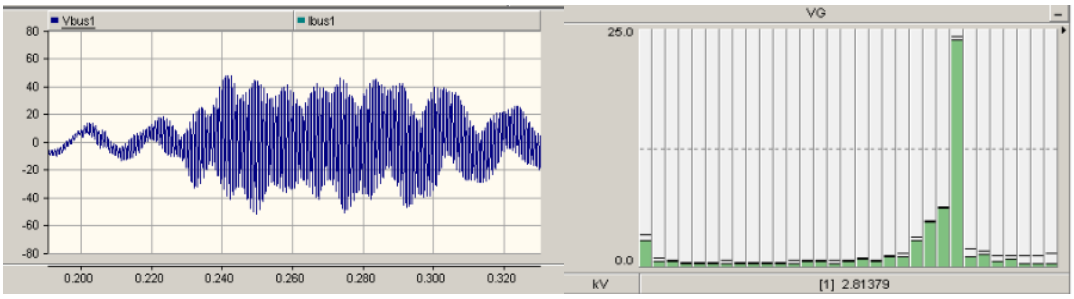

Fig. 2.12 Continuous activation of PV_1 and PV_2, and a powerful consumer: a) distortion of voltage sine wave on 10 kV SS (substation) buses; b) spectrum of harmonic components of voltage at 10 kV substation.

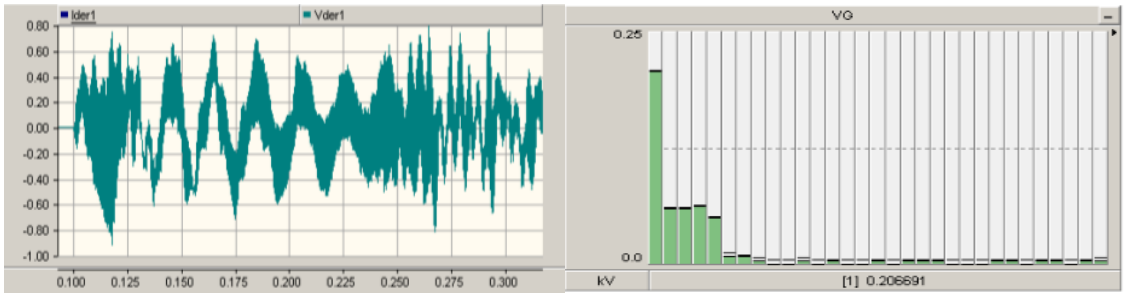

Fig. 2.13 Simultaneous activation of PV_1 and $_{PV2}$, and a powerful consumer (with successful automatic restart): a) distortion of the voltage sine wave on the bus PV_1 0.4kV; b) spectrum of harmonic components of voltage at PV_1 0.4kV

As can be seen from Figs. 2.12 and 2.13, resonance and ferroresonance phenomena occur in networks with RESs. On the distortion of the voltage sinewaves, both the load power and the parameters of the PV inverters themselves are affected. One of the parameters characterizing the PV is the constant inertia (T) in the control laws. The results of the studies indicate that, when T decreases, the harmonic components in the voltage on the PV are increasing (Fig. 14).

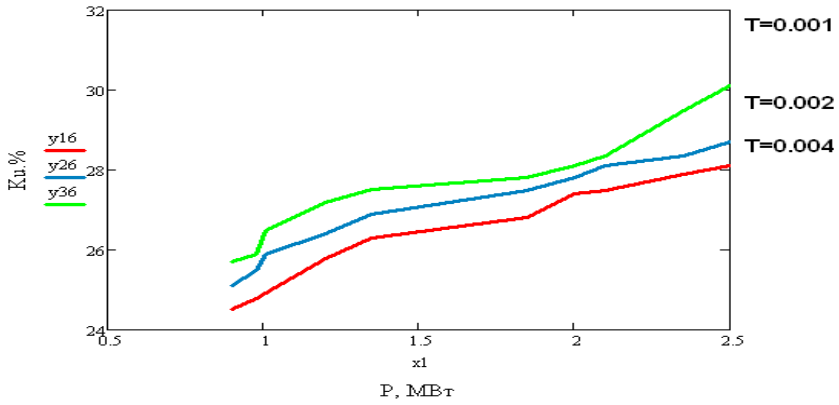

Fig. 2.14 Dependence of K_u on constant inertia T and load of PV R.

Research of the influence of harmonious components of voltage on the technical condition of high-voltage equipment of microgrid

High-voltage equipment of distribution electric networks quickly ages [34, 35]. Under such conditions, the task of studying the effect of harmonic components of voltage on the technical condition of high-voltage equipment of LES is to become actual in order to develop measures for the rational use of the residual resource and its trouble-free operation. As an example, we investigate the effect of harmonic voltage components on the technical condition of high-voltage measuring voltage transformers and cable clutches.

It is known that cable lines (CL) have a larger insulation capacity than air power lines. Large capacity of isolation especially in cable ties. Therefore, to calculate the effect of increasing the frequency of harmonic components in the voltage phases of cable lines on the current through the isolation of their cable clutches, the simplified scheme shown in Fig. 2.15 was used.

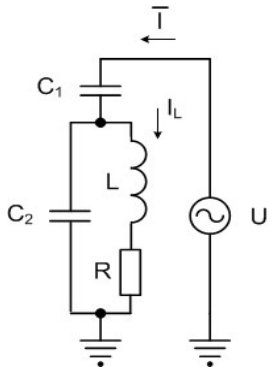

Fig. 2.15 The following diagram of the electrical network with the CL

In the diagram shown in Fig. 15, the circuit diagram C1 - the intercontact capacitance of the switch, C2-capacity of the cable line, R - the total active resistance grid, L - load inductance, for example, measuring voltage transformer, etc.

The current flowing through the insulation of the cable is determined by the expression (2. 10):

$$\bar{I}_{C_2} = \frac{\bar{U} \cdot \omega \cdot C_2 \cdot (\omega \cdot L + R)}{z_{\Sigma}(\omega \cdot L \cdot C_2 - j\omega \cdot R \cdot C_2 - 1)} \tag{2.10}$$

where I_{C2} – current flowing through the isolation of the CL; $\omega = 2\pi \cdot f$ is the angular velocity, *f* is the frequency in the network.

For 10 kV CL with a capacity of 0.0016 μF with an increase in frequency up to 300 Hz, the current in the isolation of the CL will be 10.56 A, with a maximum permissible value of 300 μA, and therefore it can lead to premature damage to the isolation of the CL.

Studies show that with the order of harmonic components in the voltage phases of cable lines, the value of the current strength flowing through the isolation of the CL increases. The dependence of current in the isolation of the CL from the frequency is shown in Fig. 2.16.

Another type of equipment under investigation was measuring voltage transformers. To calculate the current flowing in the transformer winding, a generalized substitution scheme was used (Fig. 2.15).

The current in the transformer winding is determined by the expression (2.11):

$$\bar{I}_L = \frac{\bar{U}}{z_{\Sigma}\left[(R + j\omega \cdot L) \cdot j\omega \cdot C_2 + 1\right]} \tag{2.11}$$

where I_L - current flowing through the transformer winding; C_1 - intercontact capacitance of the switch, C_2 - inter-circuit capacity of the transformer winding, R -active resistance of the transformer winding, L-inductance of the transformer winding.

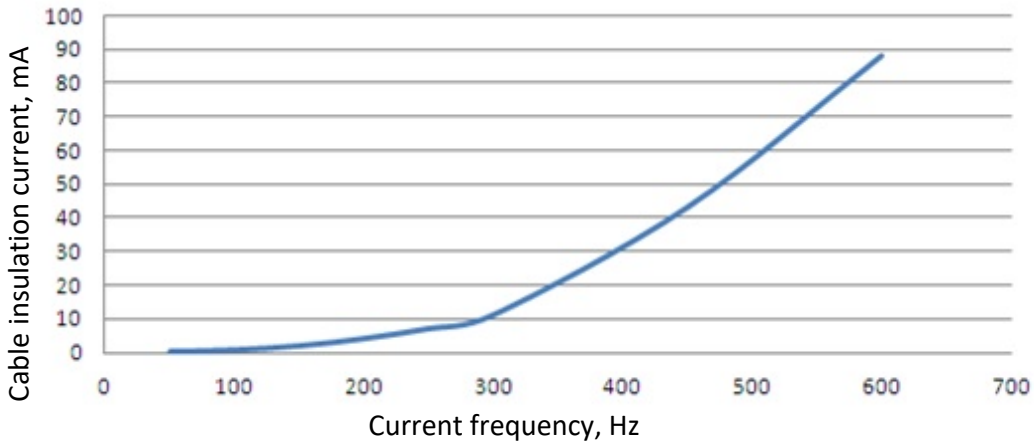

Fig. 2.16 Dependence of the value of current in the isolation of the CL from the frequency in the network

The maximum permissible current through the transformer winding must not exceed 0.3 A for a transformer of the type NTMI-10. Substituting the passport data of the transformer NTMI-10 (C2 -200 -400 pF, R-1800 ohm, L -74 Gn) in expression 11, the dependence of the current in the TN winding on the frequency of this current, as shown in Fig. 2.17, was obtained.

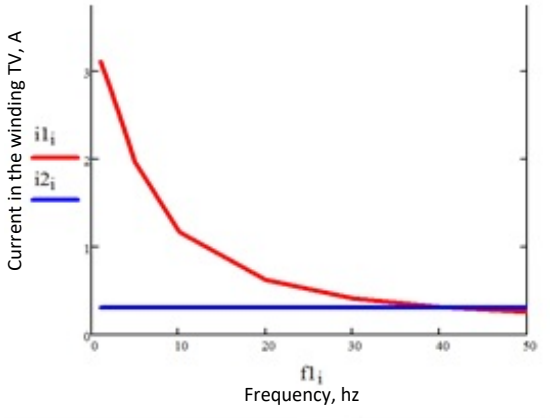

Fig. 2.17 Dependence of current in NTMI winding on the frequency of this current

The analysis of the research results suggests that, as the current frequency decreases in the winding, the current will increase, therefore the appearance of the current in the voltage of the voltage transformer of the harmonics of low frequencies (less than 50 Hz) may lead to an increase in current that significantly exceeds the maximum permissible limits that certain conditions) can damage the transformer winding.

2.3 Models of distribution electric networks with damaged high-voltage equipment

In order to reduce the loss of electric power during the transport of electricity generated by the PV, in the research, as a rule, distribution networks 6 ÷ 10 kV are considered. At the same time, foreign researchers further consider 0.4 kV networks in which PV primarily satisfy the electricity needs of their owners, and only an excess of electricity is transmitted from PV to REM and is often consumed by consumers closest to the SES. Under these conditions, several inverters of PV of different owners can be connected to one REM with RES in different nodes of 0.4 kV.

Taking into account the complexity of conducting research on the quality of electrical energy indices in REM with RESs with several different RESs, due to the lack of several RESs in one REM, it is proposed to carry out such studies using mathematical and computer models.

It is known [36] that in electrical networks of 3-35 kV with isolated neutral processes there are processes that negatively affect the work of electromagnetic devices. For example, the average lifespan of voltage transformers (TN) often does not exceed 3-5 years. For reasons causing damage to electrical equipment, it can be attributed to the ferro-resonance overvoltages, switching overvoltages, transients, neutral displacement, the presence of a constant component of the magnetic flux in the TN during self-oscillating processes in the network.

In [36] it is noted that a considerable amount of equipment damage in networks with isolated neutral (6-35 kV) is caused by ferroresonance. This phenomenon causes overvoltage or overvoltage, the impact of which equipment is not calculated and from which it is not protected. In addition, the ferroresonance occurs more often than other types of influences. It is especially dangerous because it can last a long time. Ferro magnetic elements in electric networks are power transformers, arc-jet reactors, measuring current and voltage transformers, electric motors, ie all devices in which there is a reel with ferromagnetic (steel) cores.

Under normal conditions there are no conditions for excitation of resonance, that is, non-vanishing oscillations. However, under the influence of a ferromagnetic element, which leads to saturation of the core, there is a smooth change in the inductance of this element. As a result, conditions are created for the possible occurrence of resonance and, as a consequence, damage to the insulation of electrical equipment. In some cases, damage is classified as arising due to internal overvoltages.

The statistical data given in the first section show that, besides the others, in the REM with the DER, measuring voltage transformers 6 to 10 kV, cable clutches, dischargers, etc. are often damaged. In reviews [36, 37] bugs are mentioned damages of voltage transformers, electric motors, complete distributive devices of external installation (CDDE), nonlinear overvoltage limiters (NOL) and gate arrests. It is believed that these damage occurs due to the occurrence of internal overvoltages. The reasons, among many others, may be transitional processes during switch-on / off in the electric network of the RESs, especially the SES [39, 40, 41]. The task of studying the effect of harmonic components of voltage on the technical condition of the high-voltage equipment of grid with RES is set in order to develop measures for the rational use of the residual resource and its trouble-free operation [38].

As an example, we will show what values can have harmonic voltage components and their effect on measuring voltage transformers and cable lines.

It is known that cable lines (CL) have a larger insulation capacity than air power lines. Large capacity of isolation especially in cable ties. For example, for a 10 kV CL with a capacity of 0.0016 μF with increasing frequency up to 300 Hz, the current in the isolation of the CL will be about 10 A. Since the maximum permissible value is 300 mA, this can lead to premature damage to the CL isolation.

The analysis of literary sources suggests that the equipment of the REM with the RESs is outdated [42] and often worked out its passport resource. So, it is expected to increase its damage. In other articles [37, 43] it is noted that during the operation of such RESs as PV there are temporary deteriorations in the quality of electrical energy, which are also capable of causing damage to electrical equipment. It was shown in [44-47] that in overhead electrical networks, for example, 10 kV, overvoltages arise and, under certain conditions, surges take place (resonance of currents). Therefore, it is expedient to consider, for example, PV inverters to influence such a change in the parameters of the distribution network, in which there are overvoltages in the nodes of the network, and in the branches surges take place.

Consider PV with inverters PCS-9563, which are used in the networks of PJSC "Vinnitsaoblenergo". In order to reduce the effect of higher harmonics in the output circuits of the inverters, RC filters are installed: in each phase a capacitor with a capacity of 300 μF and a coil with an inductance of 0.1 mH, is calculated on the operating current Irobe = 917 A (power of the inverter is 500 kW).

Let's consider the processes of changing the current in the primary winding of the measuring voltage transformer and voltage on the primary winding of this transformer. For this purpose in Fig. 2.18 is a forward circuit of one phase of the 10 kV network with a RC-filter of the inverter of the PV connected to it, the voltage source source, voltage source in the power supply of the distribution network, a single-phase voltage transformer and power lines.

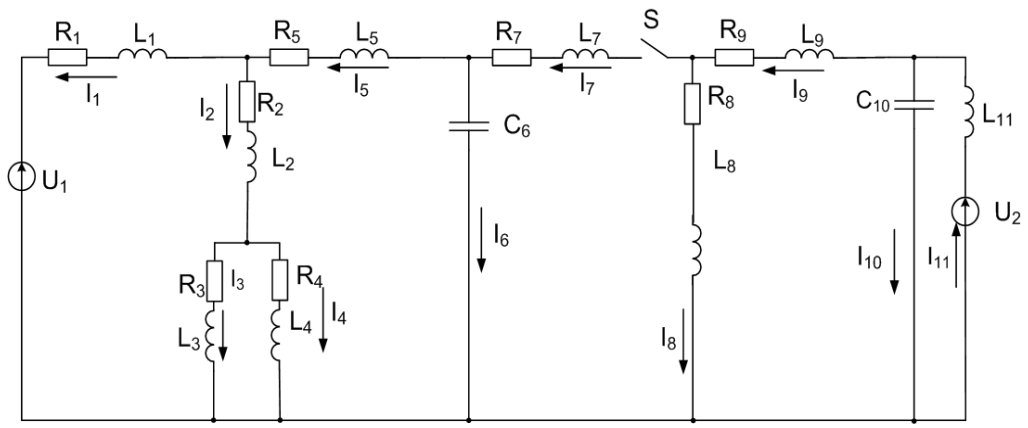

Fig. 2.18. Forward circuit diagram of the network with PV

In the diagram of Fig. 2.18 the active resistance R1 and the inductance L1 of the 110/10 kV power transformer are applied to the voltage of the 10 kV bus, to which a 10 kV measuring transformer is connected. Active resistance R_2 and inductance L_2 - parameters of the high voltage winding of the measuring voltage transformer, the active resistance R_3 and the inductance L_3 - the parameters of the magnetization field on the transverse circuit of the measuring voltage transformer, the active resistance R_4 and the inductance L_4 - the parameters of the secondary winding together with the load resistance on the circuit of the measuring transformer voltage, active resistance R_5, capacity C_6 relative to ground and inductance L5 of the power line from the bus of the substation, to which the voltage transformer is connected, to the bus of the substation her, to which is attached a power transformer 10 / 0,4 kV. Parameters of the secondary circuit of this transformer are represented by the active resistance R_7 and the inductance L_7 - the high voltage of this transformer, the active resistance R_8 and the inductance L_8 - the parameters of the magnetization field on the transverse circuit diagram, the active resistance R_9 and the inductance L_9 - low voltage winding, led to the high voltage side, active resistance C_{10} and inductance L_{11} - parameters of the inverter filter PV. The active resistance of the filter is not taken into account because its value is much less than the inductive resistance of the throttle L_{11}. U_1 and U_2 - voltage sources of the power supply and PV (down to the side of 10 kV).

In fig. 2.19 schema shown in Fig. 2.18, given in the operator form, taking into account the independent initial conditions. Consider the switching mode of the key S at the time t = 0, in which the voltage curve u1 (t) = u2 (t) = Um · sin (ω · t) passes through 0. In this case, the independent initial condition will be a real number equal to the product of the imaginary part of the complex number of the corresponding current or voltage on.

For example, instantaneous current value:

$$i_1(t) = I_1 \cdot \sqrt{2} \cdot \sin(\omega t + \psi_{i1}), \qquad (2.12)$$

where *I1* is the current value of current; *ψi1* is the initial phase of this current.

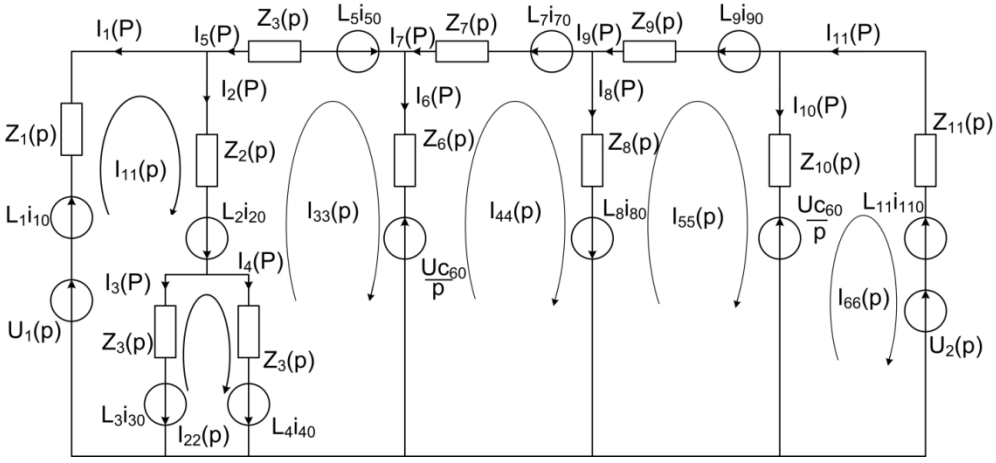

Fig. 2.19 - The calculation scheme in the operator form of the record

At time t = 0+:

$$i_1(0_+) = I_1 \cdot \sqrt{2} \cdot \sin(\psi_{i1}) = Im(\underline{I}_1) \cdot \sqrt{2}\ . \qquad (2.13)$$

In order to simplify the calculations in the circuit diagram, nonlinear properties of transformer parameters are not taken into account, which are taken into account in the works [48, 49, 50]. This causes an error in the quantitative results of the mathematical model, but allows for a qualitative analysis of the processes in the studied circles of the underlying and calculation schemes.

Independent initial conditions are determined from the calculation of the steady-state operation of the scheme to the switching performed by the symbolic method, namely: currents in the inductances L1 ÷ L5, L7 ÷ L9, the voltages on the capacities C6 ÷ C10.

In order to study the change of current in the high voltage winding of the measuring transformer voltage transient process that occurs during the connection of the PV to the network of LES with renewable energy sources, we calculate the calculation of the contour currents in the operator form in accordance with the scheme shown in Fig. 2.19.

emf sources $U_1(s)$ and $U_2(s)$ – this is the operator representation of sinusoidal functions $u_1(t)$ та $u_2(t)$: $U_1(s)= [U_{m1}\cdot\omega]/(s^2+\omega)$ та $U_2(s)= [U_{m2}\cdot\omega]/(s^2+\omega)$.

System of equations in operator form:

$$\begin{cases} I_{11}\cdot((L_1\cdot s+R_1)+(L_2\cdot s+R_2)+(L_3\cdot s+R_3))-I_{22}\cdot(L_3\cdot s+R_3)-I_{33}\cdot(L_2\cdot s+R_2)= \\ =U_1+L_1\cdot I_{10}+L_2\cdot I_{20}+L_3\cdot I_{30} \\ I_{22}\cdot((L_3\cdot s+R_3)+(L_4\cdot s+R_{4)})-I_{11}\cdot(L_3\cdot s+R_3)-I_{33}\cdot(L_4\cdot s+R_4)=L_4\cdot I_{40}-L_3\cdot I_{30} \\ I_{33}\cdot((L_2\cdot s+R_2)+(1/(C_6\cdot s))+(L_4\cdot s+R_4)+(L_5\cdot s+R_5))-I_{11}\cdot(L_2\cdot s+R_2)- \\ -I_{22}\cdot(L_4\cdot s+R_4)-I_{44}\cdot(1/(C_6\cdot s))=-L_4\cdot I_{40}-L_2\cdot I_{20}+L_5\cdot I_{50}-(U_{C6}/s) \\ I_{44}\cdot((1/(C_6\cdot s))+(L_7\cdot s+R_7)+(L_8\cdot s+R_8))-I_{33}\cdot(1/(C_6\cdot s))-I_{44}\cdot(L_8\cdot s+R_8)= \\ =(Uc_6/s)-L_7\cdot I_{70}+L_8\cdot I_{80} \\ I_{55}\cdot((L_8\cdot s+R_8)+(L_9\cdot s+R9)+(1/(C_{10}\cdot s)))-I_{44}\cdot(L_8\cdot s+R_8)-I_{66}\cdot(1/(C_{10}\cdot s))= \\ =-(U_{C10}/s)-L_8\cdot I_{80}-L_9\cdot I_{90} \\ I_{66}\cdot((1/(C_{10}\cdot s))+(L_{11}\cdot s))-I_{55}\cdot(1/(C_{10}\cdot s))=(Uc_{10}/s)-L_{11}\cdot I_{110}-U_2 \end{cases}, \quad (2.14)$$

where s is the Laplace operator.

The result of the solution of the system of equations (2.13) is circuit currents, the values of which in the operator.

The current in the primary winding of the voltage transformer in the operator form is determined by:

$$I_2(s) = I_{11}(s) – I_{33}(s); \quad (2.15)$$

$$I_2(s) = I_{11}(s) - I_{33}(s) = - (-((-R_4 - L_4 \cdot s)^2 \cdot (R_7+1/(C_6 s)+L_7 \cdot s) - - (R_3+R_4+L_3 \cdot s+L_4 \cdot s) \cdot (-(1/(C_{62} \cdot s^2))+(R_2+ R_4 + R_5+1/(C_6 s) + L_2 s+L_4 s+L_5 s) \cdot \cdot(R_7+1/(C_6 s)+L_7 s))) \cdot (-(I_{30} L_3-I_{40} L_4) \cdot (-R_2-L_2 s) + (-R_4-L_4 s) \cdot (-I_{10} L_1-I_{20} L_2-I_{30} L_3- -U_1)) + ((-R_3-L_3 s) \cdot (-R_4-L_4 s) - (-R_2-L_2 s) \cdot (R_3+R_4+L_3 s+L_4 s)) \cdot (-(I_{30} L_3-I_{40} L_4) \cdot \cdot(-(1/(C_6^2 s^2)) + (R_2+R_4+R_5+1/(C_6 s)+L_2 s+L_4 s+L_5 s) \cdot(R_7+1/(C_6 s)+L_7 s)) + (-R_4- - L_4 \cdot s) \cdot ((I_{70} L_7-I_{80} L_8-U_{c6}/s)/(C_6 s) + (R_7+1/(C_6 s)+L_7 s) \cdot (I_{20} L_2+I_{40} L_4-I_{50} L_5 + +U_{c6}/s))))) / / (((-R_3-L_3 s) (-R_4-L_4 s)-(-R_2-L_2 s) \cdot (R_3+R_4+L_3 s+L_4 s)) \cdot ((-R_2- L_2 s) \cdot D$$

$$D= (-R_4-L_4 s) \cdot (R_7+1/(C_6 s)+L_7 s) - (-R_3-L_3 s) \cdot (-(1/(C_6^2 s^2)) + +(R_2+R_4+R_5+1/(C_6 s) + L_2 s+L_4 s+L_5 s) \cdot (R_7+1/(C_6 s)+L_7 s))) - (-(-R_2-L_2 s) (-R_3 - -L_3 s) + (R_1+R_2+R_3+L_1 s+L_2 s+L_3 s) \cdot (-R_4-L_4 s)) ((-R_4-L_4 s)^2 \cdot (R_7+1/(C_6 s)+L_7 s) - -(R_3+R_4+L_3 s+L_4 s) \cdot (-(1/(C_6^2 s^2)) + (R_2+R_4+R_5+1/(C_6 s)+L_2 s+L_4 s+L_5 s) \cdot \cdot(R_7+1/(C_6 s)+L_7 s)))) - (I_{10} L_1 R_3+I_{20} L_2 R_3+I_{40} L_4 R_3+I_{10} L_1 R_4+I_{20} L_2 R_4+ +I_{30} L_3 R_4+I_{10} L_1 L_3 s+I_{20} L_2 L_3 s+I_{10} L_1 L_4 s+I_{20} L_2 L_4 s+I_{30} L_3 L_4 s+I_{40} L_3 L_4 s + +R_3 U_1+R_4 U_1+L_3 s U_1+L_4 s U_1)/(R_2 R_3+R_2 R_4+R_3 R_4+L_3 R_2 s+L_4 R_2 s+L_2 R_3 s+ +L_4 R_3 s+L_2 R_4 s+L_3 R_4 s+L_2 L_3 s^2+L_2 L_4 s^2+L_3 L_4 s^2)+(((-R_3-L_3 s)/(-R_4-L_4 s) - ((R_3+R_4+L_3 s+L_4 s)\cdot (-(-R_2-L_2 s) (-R_3-L_3 s)+(R_1+R_2+R_3+L_1 s+L_2 s+L_3 s) \cdot (-R_4- L_4 s)))/((-R_4-L_4 s) \cdot ((-R_3-L_3 s) \cdot (-R_4-L_4 s)-(-R_2-L_2 s) \cdot (R_3+R_4+L_3 s+L_4 s)))) \cdot \cdot (-((- R_4-L_4 s)^2 \cdot (R_7+1/(C_6 s)+L_7 s)-(R_3+R_4+L_3 s+L_4 s) \cdot (-(1/(C_6^2 \cdot \cdot s^2))+(R_2+R_4+R_5+1/(C_6 s)+L_2 s+L_4 s+L_5 s) \cdot (R_7+1/(C_6 s)+L_7 s))) \cdot (-(I_{30} L_3-I_{40} L_4)\cdot \cdot (-R_2-L_2 s)+(-R_4-L_4 s) \cdot (-I_{10} L_1-I_{20} L_2-I_{30} L_3-U_1))+((-R_3-L_3 s) \cdot (-R_4-L_4 s)-(-R_2-L_2 s) \cdot \cdot(R_3+R_4+L_3 s+L_4 s)) \cdot (-(I_{30} L_3-I_{40} L_4) \cdot (-(1/(C_6^2 \cdot \cdot s^2)) + (R_2 +R_4+ +R_5+1/(C_6 s)+L_2 \cdot s+L_4 s+L_5 s) \cdot (R_7+1/(C_6 s)+L_7 s))+(-R_4-L_4 s) \cdot ((I_{70} L_7-I_{80} L_8 -U_{c6} / s)/(C_6 s)+(R_7+1/(C_6 s)+L_7 s) \cdot (I_{20} L_2+I_{40} L_4-I_{50} L_5+U_{c6}/s)))))/(((-R_3-L_3 s) \cdot (-R_4--L_4 s)-(-R_2-L_2 s) \cdot (R_3+R_4+L_3 s+L_4 s)) \cdot ((-R_2-L_2 s) \cdot (-R_4-L_4 s) \cdot (R_7+1/(C_6 \cdot s)+L_7 s)-(- R_3-L_3 s) \cdot (-(1/(C_6^2 s^2))+(R_2+R_4+R_5+1/(C_6 s)+L_2 s+L_4 s+L_5 s) \cdot \cdot(R_7+1/(C_6 s)+L_7 s)))-(-(-R_2-L_2 s) \cdot (-R_3-L_3 s)+(R_1+R_2+R_3+L_1 s+L_2 s+L_3 s) \cdot (-R_4- L_4 s)) \cdot ((-R_4-L_4 s)^2$$

$\cdot\cdot(R_7+1/(C_6\,s)+L_7\,s)-(R_3+R_4+L_3\,s+L_4\,s)\cdot(-(1/(C_6^{2\cdot}s^2))++(R_2+R_4+R_5+1/(C_6\,s)+L_2\cdot s+L_4\,s+L_5\,s)\cdot(R_7+1/(C_6\,s)+L_7\,s)))).$

On the received expressions it is possible to analyze how time currents in the branches of the circuit change. Perform further calculations taking into account the parameters of the scheme:

active supports in the branches of the circuit: R_1=2,52 Ohm; R_2=1800 Ohm; R_3=3420 Ohm; R_4=207000 Ohm ; R_5=1,26 Ohm ; R_7=1,28 Ohm; R_8=7482 Ohm; R_9=3,28 Ohm;

inductance in the branches of the circuit: L_1=0,0736 H; L_2=10,032 H; L_3=56,70 H; L_4=10,032 H; L_5=0,00 H; L_7=0,001 H; L_8=23,83 H; L_9=0,01 H; L_{11}=0,36 H; capacitor in brances in scheme: $C_6=10^{-10}$ F; $C_{10}=8{,}335\cdot10^{-8}$ F.

In order to determine the currents in the inductive branches of the circuit and the voltages on the capacitors at the time of closing the contacts of the switch in accordance with the laws of commutation, we convert the circuit as shown in Fig. 2.21. Accordingly, the integrated supports of the branches are expressed by the expressions:

$$Z_1 = R_1 + j\cdot\omega\cdot L_1 = 2.52 + j\cdot 314\cdot 0{,}0736 = 2{,}52 + j23{,}122\ (\text{Ohm}),$$
$$Z_2 = R_2 + j\cdot\omega\cdot L_2 = 1800 + j\cdot 314\cdot 10{,}032 = 1800 + j3151{,}646\ (\text{Ohm}),$$
$$Z_3 = R_3 + j\cdot\omega\cdot L_3 = 3420 + j\cdot 314\cdot 56.7 = 3420 + j17812{,}83\ (\text{Ohm}),$$
$$Z_4 = R_4 + j\cdot\omega\cdot L_4 = 207000 + j\cdot 314\cdot 10{,}032 = 2{,}07\cdot 10^5 + j3151{,}646\ (\text{Ohm}),$$
$$Z_5 = R_5 + j\cdot\omega\cdot L_5 = 1{,}26 + j\cdot 314\cdot 0{,}0024 = 1{,}26 + j0{,}754\ (\text{Ohm}),$$
$$Z_6 = -j\cdot\frac{1}{\omega\cdot C_6} = -j\cdot\frac{1}{314\cdot 10^{-10}} = -j3{,}183\cdot 10^7\ (\text{Ohm}),$$
$$Z_7 = R_7 + j\cdot\omega\cdot L_7 = 1{,}28 + j\cdot 314\cdot 0{,}001 = 1{,}28 + j0{,}314\ (\text{Ohm}),$$
$$Z_8 = R_8 + j\cdot\omega\cdot L_8 = 7482 + j\cdot 314\cdot 23{,}83 = 7482 + j7486{,}415\ (\text{Ohm}),$$
$$Z_9 = R_9 + j\cdot\omega\cdot L_9 = 3{,}28 + j\cdot 314\cdot 0{,}01 = 3{,}28 + j3{,}142\ (\text{Ohm}),$$
$$Z_{10} = -j\cdot\frac{1}{\omega\cdot C_{10}} = -j\cdot\frac{1}{314\cdot 1{,}667\cdot 10^{-7}} = -j19094{,}774\ (\text{Ohm}),$$
$$Z_{11} = j\cdot\omega\cdot L_{11} = j\cdot 314\cdot 0{,}36 = j113{,}097\ (\text{Ohm}),$$

$$Z_{56} = Z_5 + Z_6 = 1{,}26 + j0{,}754 + -j3{,}183 \cdot 10^7 = 1{,}026 - j3{,}183 \cdot 10^7$$

$$Z_{34} = \frac{Z_3 \cdot Z_4}{Z_3 + Z_4} = \frac{(3420 + j17812{,}83) \cdot (2{,}07 \cdot 10^5 + j3151{,}646)}{3420 + j17812{,}83 + 2{,}07 \cdot 10^5 + j3151{,}646} =$$

$$= 4800{,}938 + j17096{,}214 \,(\text{Ohm}),$$

$$Z_{234} = Z_2 + Z_{34} = 1800 + j3151{,}646 + 4800{,}938 + j17096{,}214 =$$

$$= 6600{,}938 + j20247{,}86 \,(\text{Ohm}),$$

$$Z_{23456} = \frac{Z_{234} \cdot Z_{56}}{Z_{234} + Z_{56}} = \frac{(6600{,}938 + j20247{,}86) \cdot (1{,}26 - j3{,}183 \cdot 10^7)}{6600.938 + j20247.86 + 1.26 - j3.183 \cdot 10^7} =$$

$$= 6609{,}344 + j20259{,}376 \,(\text{Ohm}),$$

$$Z_{123456} = Z_1 + Z_{23456} = 2{,}52 + j23{,}122 + 6609{,}344 + j20259{,}376 =$$

$$= 6611{,}864 + j20282{,}498 \,(\text{Ohm}).$$

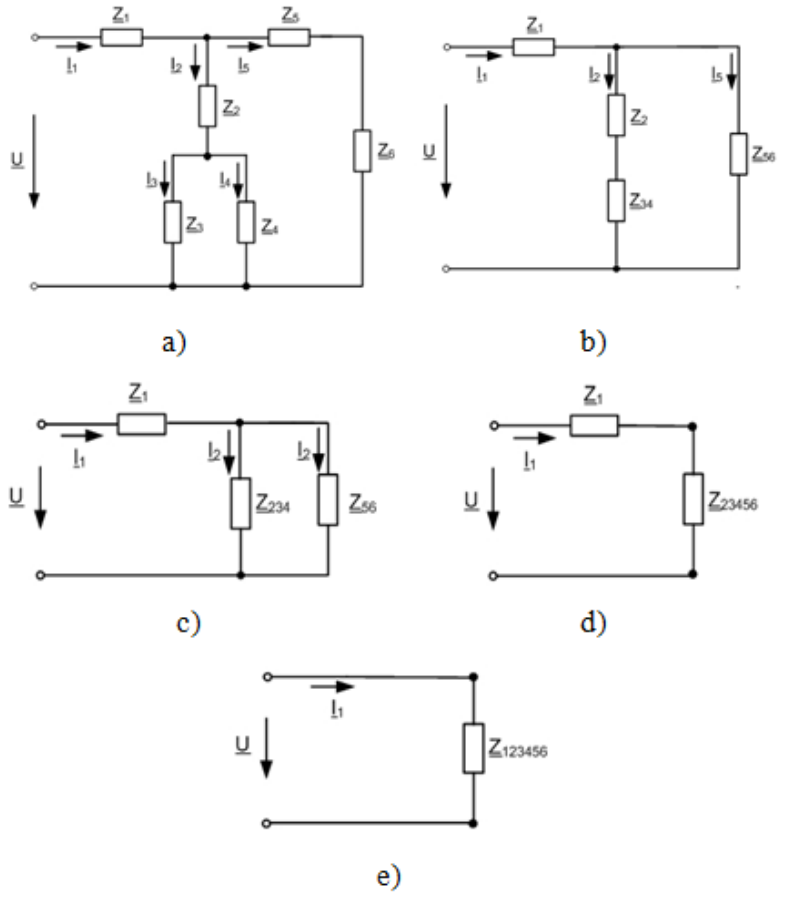

Fig. 2.20 Variants of sub-schemes during successive transformations of the scheme LES

Further calculations are carried out under the following initial conditions:

currents in the inductive elements of the circuit in accordance with the first law of commutation at t = 0 c:

$I_1 = U/Z_{123456} = 0,084 – 0,257 \cdot i,\ I_1(0+) = I_{10} = -0,257\ A;$

$U_{234} = U_{234}/Z_{234} = 5767,342 – 1,291 \cdot i,\ I_2(0+) = I_{20} = -0,257\ A;$

$I_2 = U_{234}/Z_{234} = 0,084 – 0,257 \cdot i,\ I_2(0+) = I_{20} = -0,257\ A;$ i m. n. $I_3(0+) = I_{30} = -0,258\ A,\ I_4(0+) = I_{40} = 0,001A\ ;\ I_5(0+) = I_{50} = 0\ A;\ I_7(0+) = I_{70} = 0\ A;\ I_8(0+) = I_8(0+) = I_{80} = -0,387\ A;$

$I_9(0+) = I_{90} = -0,387\ A;\ I_{11}(0+) = I_{110} = -0,236\ A.$

Voltage on capacitors according to the second switching law: $U_{C6(0+)} = U_{c6} = -1,291V;\ U_{C10(0+)} = U_{c10} = -43,192V.$

Current in the primary winding of the voltage transformer in the operator form of recording, taking into account the initial conditions:

$$I_2 = -\left\{\begin{pmatrix} 8,36447\cdot 10^{44} + 2,16396\cdot 10^{43}s + 1,8235\cdot 10^{41}s^2 - 8,26273\cdot 10^{37}s^3 - \\ -7,94195\cdot 10^{35}s^4 - 2,13715\cdot 10^{32}s^5 - 2,12433\cdot 10^{28}s^6 - 9,1229\cdot 10^{23}s^7 - \\ 1,42876\cdot 10^{19}s^8 + 43267,4s^9 + 1,75442\cdot 10^{-9}s^{10} \end{pmatrix} \Big/ \right.$$
$$\left(\begin{pmatrix} (207000 + 10,032s)(98596 + s^2)(1,0876\cdot 10^9 + 1,40023\cdot 10^7 s + 1238,27s^2) \\ \begin{pmatrix} 1,13851\cdot 10^{25} + 3,20509\cdot 10^{23}s + 2,26043\cdot 10^{21}s^2 + 3,062\cdot 10^{17}s^3 + 9,56713\cdot 10^{12}s^4 \\ +31414,7s^5 + 0,944215\cdot s^6 \end{pmatrix} \end{pmatrix} + \right.$$
$$+ \left(\begin{pmatrix} -(1,0867\cdot 10^9 + 1,40023\cdot 10^7 s + 1238,27s^2) \\ \begin{pmatrix} -1(207000 + 10,032s) \\ (2.5) \end{pmatrix} \begin{pmatrix} -\left(\left(1\cdot 10^{10}(9,22221 + 1,291/s)\right)/s\right) - \\ 1(-2,56819 - 1,291/s)\begin{pmatrix} 7483,28 + \\ 1\cdot 10^{10}/s + 23,831s - 1 \end{pmatrix}\begin{pmatrix} 7482 + \\ +23,83s \end{pmatrix} \end{pmatrix} \\ +14,6386\left(10^{20}/s^2 - 1\right)\left(208801 + 1\cdot 10^{10}/s + 20,0664s\right) \\ \left(7483,28 + 1\cdot 10^{10}/s + 23,831s - 1\right)\left(7482,0 + 23,83s\right) \end{pmatrix} + \right.$$
$$+1\left(-14,6386\left(1800 + 10,032s\right) - 1\left(207000 + 10,032s\right)\left(17,2257 - 2,5638\cdot 10^6\right)/\begin{pmatrix} 98596 + \\ +s^2 \end{pmatrix} \right) -$$
$$-1\left(207000 + 10,032s\right)\left(0 + 1\left(207000 + 10,032s\right)\begin{pmatrix} 7483,28 + 1\cdot 10^{10}/s + 23,831s - 1\cdot \\ \cdot 7482 + 23,83\cdot s \end{pmatrix} \right) -$$
$$-1\left((210420 + 66,732s\right)\left(\begin{pmatrix} 1\cdot 10^{20}/s^2 - 1\left(208801 + 1\cdot 10^{10}/s + 20,0664\cdot s\right)\cdot \\ \left(7483,28 + 1\cdot 10^{10}/s + 23,831s - 1\left(7482 + 23,83s\right)\right) \end{pmatrix} \Big/ \right.$$
$$\left. \begin{pmatrix} 3,20509\cdot 10^{23} + 1,13851\cdot 10^{25}/s + 2,26043\cdot 10^{21}s + 3,062\cdot 10^{17}s^2 \\ +9,56713\cdot 10^{12}s^3 + 31414,7s^4 0.944215s^5 \end{pmatrix} \right),$$

In expression (2.5), the Laplace operator r is denoted by the letter s.

After a Laplace transformation, the mathematical model of the current *i2(t)* is written in the form of the following expression:

$$I_2 = -239{,}213 \cdot e^{-20634 \cdot t} + 239{,}213 \cdot e^{-20633{,}9 \cdot t} - 6{,}82362 \cdot e^{-11229{,}8 \cdot t} + 7{,}16698 \cdot e^{-11228{,}5 \cdot t} -$$
$$-4{,}50157 \cdot e^{-78{,}2618 \cdot t} + 3{,}90903 \cdot e^{-78{,}488 \cdot t} + 0{,}4989 \cdot e^{-65{,}32 \cdot t} +$$
$$+0{,}04 \cdot \sin(100 \cdot \pi \cdot t - 55{,}845^{o}) + e^{-632{,}223 \cdot t} 0{,}237 \cdot 2 \cdot \sin(3{,}18309 \cdot 10^{6} \cdot t - 90{,}136^{o}).$$

The proposed mathematical model makes it possible to study the process of changing the current in the primary winding of the measuring voltage transformer in time. Chart of current change in TN is shown in Fig. 2.21.

As you can see from the graph, high-frequency oscillations arise when switching on the PV in the distribution network. The amplitude value of high-frequency current fluctuations in the primary winding of the measuring voltage transformer far exceeds the amplitude value of the current in the primary winding in the steady state and leads to significant overvoltages.

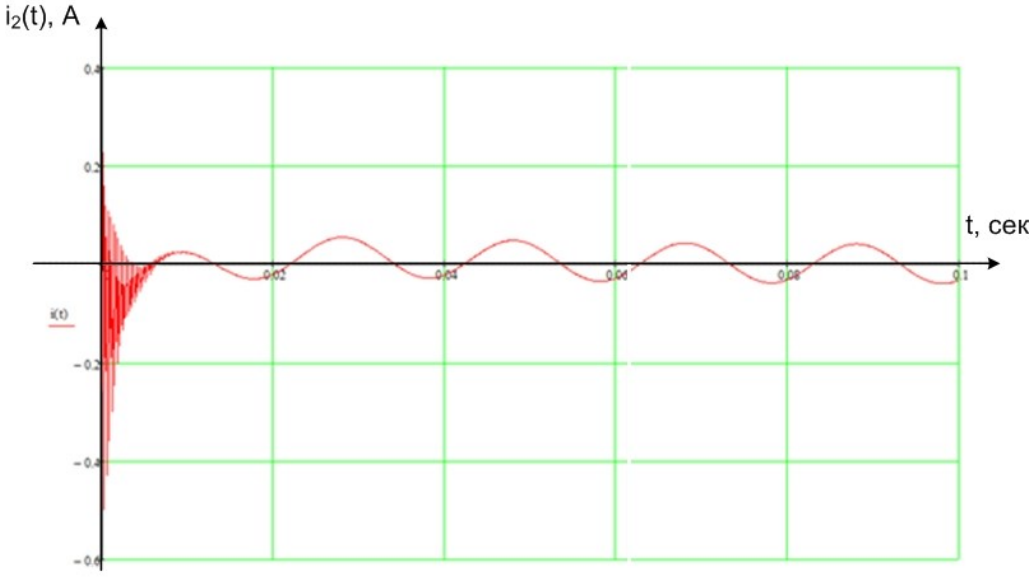

Fig. 2.21 Current dependence in the primary winding of the voltage transformer on the time during switching on the SES to the network

Burden of calculations shows the expediency of further creation of computer models of distribution networks with SES that will reduce the modeling error due to simulation of modes in three-phase networks and through the use of already developed computer models of measuring and power transformers, which take into account the nonlinearity of their parameters. So commonly recognized software is PS CAD [50].

2.4 Optimal control of small hydroelectric plants power generation in local electrical systems

A sign of today is the ever-increasing use of renewable energy sources (RES), which are considered as one of the most promising ways to solve growing energy supply problems. Often, such features of RES as ecological cleanliness and inexhaustible resource base become crucial to their benefits in the face of increasing rates of environmental pollution and a rapid reduction of organic fuel resources.

Ensuring the country's energy independence and joining the European Union are two of the most important strategic tasks for the development of modern Ukraine. One of the conditions for a successful solution to both tasks is the maximum increase in the share of energy in the strategic balance, produced at the expense of its own energy resources, including RES. Ukraine has a great potential for a variety of RES.

It is also known that there are problems in Ukraine due to the use of traditional energy sources. The reasons are outdated technologies and the exhaustion of equipment resources in the power industry, which together with the low efficiency of fuel usage lead to considerable increase of harmful emissions. Significant losses during transportation, distribution and use of electricity and heat, as well as a monopoly dependence on imports of energy carriers, complicate the situation on the energy markets of Ukraine. However, an increase in the generation of distributed energy sources (DES) without taking into account the peculiarities of

their operation in power grids can lead to deterioration of the electric energy quality, and sometimes to deterioration of equipment reliability indices in local electrical systems.

Consequently, the reduction of electricity losses in local electrical systems by means of coordinated control over the generation of solar power stations and small hydroelectric stations and the optimization of power flows in local electrical systems (LES) with RES are relevant, designed to ensure reduction of electricity losses in electrical networks, maintain balance reliability and improve the quality of electric energy supply.

Characteristic feature of today is the ever-increasing use of renewable energy sources (RESs), which are considered as one of the most promising ways of solution growing energy supply problems. Such features of RES as ecological cleanliness and inexhaustible resource base become their main advantages in conditions of increasing rates of environmental pollution and a rapid reduction of organic fuels resources.

Providing the country's energy independence and joining the European Union are two of the most important strategic tasks of the development of modern Ukraine. One of the conditions of a successful solution of both tasks is the maximum increase in the strategic balance of the share of energy produced at the expense of its own energy resources, including RES. Ukraine has a great potential of various RES.

It is also known that there are problems in Ukraine due to the use of traditional energy sources. The reasons of this are outdated technologies, the exhaustion of equipment resources in power industry, all this together with the low efficiency of the fuel use leads to significant amounts of harmful emissions. Significant losses in the process of transportation, distribution and use of electric energy and heat, as well as a monopoly dependence on imports of energy carriers, complicate the situation in the energy markets of Ukraine. However, increase of generation volume by distributed energy sources (DESs) without taking into account the peculiarities of their operation in power grids can lead to deterioration

of electric energy quality, and sometimes to deterioration of reliability indices of the equipment of local electrical systems

In [51] M.P. Anand; W. Ongsakul; Jai Govind Singh; S. Golshannavaz state that in order to reduce electric energy losses and improve its quality indices, it is expedient to pass to solution of the complex problem of district electric grids (DEG) , which involves the implementation of efficient design solutions and the introduction of operational reconfiguration systems of RES connection by means of Smart Grid. Consequently, the reduction of electric energy losses in local electrical systems by means of coordinated control of the generation by solar power plants and small hydroelectric power stations and the optimization of power flows in local electric systems (LES) with RES are urgent, intended to provide the reduction of power losses in power grids, maintain balance reliability and improve the quality of power supply

For example, in [52] the need for coordinated control of automated devices and photovoltaic generators in order to reduce the negative impact of the voltage increase in circuits of DESs by RES sources is substantiated, and an algorithm for reducing power losses and voltage stabilization by using voltage regulators and reactive power compensation devices in a microcontroller is suggested . In [53], an overview of the literature on optimal energy management and control modes of DES is presented and a hierarchical energy management architecture that requires the need for a telecommunications infrastructure for the connection of distributed control on the level of DES with the upper level of control of the energy supply company where the optimization of grid operation mode is carried out. In [54], the issues of autonomous operation of DEG in the directions of symmetric load distribution between parallel operating inverters and compliance with the requirements of electric power quality are studied . In [55], the issue of optimization of the influence of the share of RES in the balance of reactive power of DEG of wind and solar power plants is discussed. The issue of estimating the forecast characteristics of solar power plants generation is a subject of scientific work in [56]. The article proposes new economic indices for the forecasting of the

production of electric energy at solar power plants, taking into account the consequences of forecasting errors. In [57] a methodology was proposed for the development of equivalents of electric grids of low and medium voltage electric networks to study their impact on the reliability of power systems. In [58] attention was paid to the creation of intelligent electric grids based on the SMART GRID concept, taking into account the features of the energy market and RES. The ways of compensating of seasonal variations of RES generation are analyzed. In [59], it is shown that the grid configuration depends on the choice of individual generators modes, that allows to reduce the power losses in the system. Inconsistencies in operating modes can lead to excessive losses. In [60] it is said that the integration of RES in the distribution grid of rural areas can significantly improve the reliability of electric energy supply. Thus, the problem of optimal control of the generation power of small hydroelectric power stations in local electrical systems is relevant and actively studied in foreign and domestic scientific works.

2.4.1 Mathematical model of power losses in local electrical systems

In order to calculate the losses of active power in District Electric Networks the node voltage method [60] is chosen. The matrix of branches in the nodes, the matrix of the resistance of the branches and the matrix of currents in the nodes are used as the input parameters.

To calculate the steady-state DEN (distribution electric metwork) with DES, the mathematical model based on the node voltage method is adapted to the form of the output data of such networks, as well as to the tasks that being solved. The method and corresponding algorithm allow counting modes when the circuit of the network is closed and open, but some of the lines (those with the RES) are lines with two-way power supply. Moreover, individual power lines can combine several different types of DES.

The mathematical model in the matrix form, depending on the output data, is used in the form where $\mathbf{Y_n}$ –is a matrix of nodal conductivity;

$$\mathbf{Y_n} \cdot \dot{\mathbf{U}} = \mathbf{U_d^{-1}} \mathbf{S} - \mathbf{Y_b} \ \dot{\mathbf{U}}_\mathbf{b} \quad \textbf{or} \quad \mathbf{Y_n} \ \dot{\mathbf{U}} = \dot{\mathbf{J}} - \mathbf{Y_b} \ \dot{\mathbf{U}}_\mathbf{b} \tag{2.17}$$

Y_b – is a matrix-column of nodal conductivity relative to the balancing node with voltage $\dot{U}_b$; $\hat{\mathbf{S}}$ is a vector of conjugated complex capacities of nodes;

$\hat{\mathbf{U}}_\mathbf{d}^{-1}$ – inverse diagonal matrix of nodal voltage complexes; $\dot{\mathbf{J}}$ – is a vector of nodal currents.

Capacities or currents in nodes are provided as the sum of nodal loads and generation of RES:

$$\dot{\mathbf{S}} = \dot{\mathbf{S}}_1 - \dot{\mathbf{S}}_{gHES} - \dot{\mathbf{S}}_{gSES} \quad \textbf{or} \quad \dot{\mathbf{J}} = \dot{\mathbf{J}}_1 - \dot{\mathbf{J}}_{gHES} - \dot{\mathbf{J}}_{gSES} \ . \tag{2.18}$$

To study the effect of the generation of RES on power losses in the DEN and its selected fragments, an algorithm based on the matrix of the distribution of power losses on the circuit branches, depending on the power in its nodes, is used [60]:

$$\Delta\dot{\mathbf{S}}_\mathbf{b} = \dot{\mathbf{T}} \ \mathbf{S} \ , \tag{2.19}$$

where $\dot{S}_1$ $\dot{S}_{gHES}$, $\Delta\dot{\mathbf{S}}_\mathbf{b}$ – is a vector of losses in the branches of the circuit, which are determined by the capacities.

Each matrix T line is defined as

$\Delta\dot{\mathbf{S}}_\mathbf{b}$ – is a vector of losses in the branches of the circuit, which are determined by the capacities .

Each matrix T line is defined as

$$\dot{\mathbf{T}}_i = (\dot{\mathbf{U}}_t \mathbf{M}_i)\mathbf{C}_i \mathbf{U}_d^{-1}, \qquad (2.20)$$

where $\mathbf{M}_i$ – is the matrix of branches connection in the nodes; $\widehat{\mathbf{C}}_i$ – is the i line of the matrix for the distribution of currents in the nodes $\dot{\mathbf{J}}_1$ $\dot{\mathbf{J}}_{gHES}$ $\dot{\mathbf{J}}_{gSES}$ on the branches of the circuit. For a fragment of a network with dedicated HES, expression (2.21) is converted to

$$\Delta\dot{\mathbf{S}}_{bf} = \dot{\mathbf{T}} \quad \mathbf{S}_{\breve{}} \quad , \qquad (2.21)$$

where $\dot{\mathbf{T}} = \dot{\mathbf{T}} \quad \dot{\mathbf{T}}$ – is the power loss distribution matrix in the fragment of the network. As a rule, the dependence of losses of active power and electricity from generation of hydroelectric power stations is interesting. If the power of the HES tires is balanced in such a way that it does not consume or generate reactive power, then the expression (2.22) for the analysis of the impact of the HES on the loss is considerably simplified:

$$\Delta P_b = T_{fa} \cdot P_{gHES}. \qquad (2.22)$$

Expressions (2.17 ÷ 2.22) is a mathematical model of LES modes that enables to study the impact of HES and SES capacities on power losses in them and determining the optimal by losses criterion generated power taking into account voltage constraints, transmission capacities and installed HES power.

Unplugging the trunk of the network at the point of flow distribution provides a minimum of power losses [61]. However, network segmentation at this point is associated with a number of problems. First, optimal location of power losses may not coincide with the location of the segmentation determined from the conditions of reliability. Secondly, the point of flow distribution in the network can

"float," depending on the load, in addition, the point of flow distribution of active and reactive power may not coincide. The task is to ensure that in a power network open in accordance with the requirements of reliability, provide power fluxes that correspond to the point of flow distribution in a closed network. Thus, a reduction of electric power losses in DEN without reducing its reliability is achieved. In DEN with RES, it is possible to influence on power flows by modifying the generation of small HES and SES [61, 62]. However, considering that the optimal point of power flow and, accordingly, the calculated optimal power flows may change, this task can only be realized with the help of Industrial control system (ICS). To create the normal conditions for the functioning of the ICS it is necessary to establish for it a zone of insensitivity to the input parameters, which are the power load of consumers and the generation of DES.

By its physical content, this zone of insensitivity corresponds to the optimality region of electric energy losses in the DEN when the power load of consumers and the generation of DES change.

2.4.2 Determination of insensitivity zones of optimal points of power flow deviations to load power and generation of DES.

The insensitivity zone of the functioning of the ICS can be determined in relative units in accordance with the procedure outlined in [59]. To obtain criterial model that relates the relative total active power losses in DEN with currents, set in the nodes, the following equation is written in matrix form:

$$\Delta P = \dot{I}_t \, r \, I. \qquad (2.23)$$

Let us express the losses $\Delta\mathbf{P}$ by the currents in the nodes. The currents in the network branches, if emf is missing, are defined as $\dot{\mathbf{I}} = \dot{\mathbf{C}}\dot{\mathbf{J}}$, where $\dot{\mathbf{C}}$ –is matrix of current distribution coefficients, $\dot{}$ –is current in the nodes of load and DES generation . Then (2.23) will be rewritten:

$$\Delta\mathbf{P} = \dot{\mathbf{J}}_t\left(\dot{\mathbf{C}}_t\mathbf{r}\hat{\dot{\mathbf{C}}}\right)\hat{\dot{\mathbf{J}}} \tag{2.24}$$

Rewrite (2.24) as follows: $\mathbf{B}_a = Re\left(\dot{\mathbf{C}}_t\mathbf{r}\hat{\dot{\mathbf{C}}}\right)$; $\mathbf{B}_p = Im\left(\dot{\mathbf{C}}_t\mathbf{r}\hat{\dot{\mathbf{C}}}\right)$ are valid symmetric matrices.

$$\Delta\mathbf{P} = \dot{\mathbf{J}}_t\,\mathbf{B}_a\,\mathbf{J} + \mathbf{j}\,\dot{\mathbf{J}}_t\,\mathbf{B}_p\,\mathbf{J}. \tag{2.25}$$

Further, according to the method described in [58], expression (2.24) is rewritten in a canonical quadratic form and by the method of integral analogues [57] the value of power losses in relative units is written:

$$\Delta P* = \sum_{i=1}^{m} \pi_{ja}\,\bar{J}^2_{ja*} + \sum_{i=1}^{m} \pi_{jp}\,\bar{J}^2_{jp*}\,. \tag{2.25}$$

Or

$$\Delta P_* = \sum_{j=1}^{m} \pi_{ja}\left(\sum_{i=1}^{m} v_{ji\mathrm{a}}\frac{J_{i\mathrm{ao}}}{\bar{J}_{j\mathrm{ao}}}J_{i\mathrm{a}*}\right)^2 + \sum_{j=1}^{m} \pi_{j\mathrm{p}}\left(\sum_{i=1}^{m} v_{ji\mathrm{p}}\frac{J_{i\mathrm{po}}}{\bar{J}_{j\mathrm{po}}}J_{i\mathrm{p}*}\right)^2 \tag{2.26}$$

Rewrite (8) as follows: $\mathbf{B_a} = Re\left(\dot{C}_t \mathbf{r} \hat{\hat{C}}\right)$; $\mathbf{B_p} = Im\left(\dot{C}_t \mathbf{r} \hat{\hat{C}}\right)$ are valid symmetric matrices.

$$\Delta \mathbf{P} = \dot{\mathbf{J}}_\mathbf{t}\, \mathbf{B_a}\, \mathbf{J} + \mathbf{j}\, \dot{\mathbf{J}}_\mathbf{t}\, \mathbf{B_p}\, \mathbf{J}. \tag{2.27}$$

Further, according to the method described in [58], expression (2.27) is rewritten in a canonical quadratic form and by the method of integral analogues [57] the value of power losses in relative units is written:

$$\Delta P* = \sum_{i=1}^{m} \pi_{ja}\, \bar{J}^2_{ja*} + \sum_{i=1}^{m} \pi_{jp}\, \bar{J}^2_{jp*}\,. \tag{2.28}$$

Or

$$\Delta P_* = \sum_{j=1}^{m} \pi_{ja} \left(\sum_{i=1}^{m} v_{ji\mathrm{a}} \frac{J_{i\mathrm{ao}}}{\bar{J}_{j\mathrm{ao}}} J_{i\mathrm{a}*} \right)^2 + \sum_{j=1}^{m} \pi_{jp} \left(\sum_{i=1}^{m} v_{ji\mathrm{p}} \frac{J_{i\mathrm{po}}}{\bar{J}_{j\mathrm{po}}} J_{i\mathrm{p}*} \right)^2 \tag{2.29}$$

$\pi^{J}_{ja} = \frac{b_{ja}\, \bar{J}^2_{jao}}{\Delta P_{min}}$; $\pi^{J}_{jp} = \frac{b_{jp}\, \bar{J}^2_{jpo}}{\Delta P_{min}}$, where caused by the active and reactive components of currents in the nodes, respectivfrom the general expression for the DEN with the DES (2.30), we can obtain the expression for analysis of the effect on relative power losses $P*$ in the network, caused by the generation of the DES.For example, for j-th DES with (2.30) we obtain:

$$\Delta P_{*j} = \pi_{ja} v^2_{aj} J^2_{ja*} + \pi_{jp} v^2_{pj} J^2_{jp*}\,, \tag{2.30}$$

Another possibility of determining relative power losses, depending on the power of a small hydroelectric power station is the usage of the expression (6). In this case, the influence of the HES (hydro electric station) capacity on the losses of

power is determined in the part of the electrical network on which this HES is operating. In practice, as a rule, the task is set precisely because it is necessary to determine the zone of insensitivity for ICS of HES, corrective effects of which are determined by the local parameters of the mode [58].

To construct the dependence of power losses on the power of the HES and further analysis of the sensitivity, calculations are carried out according to (6). Dependence is formed in tabular form. When using the criterion method, as the basis of the algorithm for assessing the sensitivity of optimal solutions, the dependence of losses on the power of HES is approximated in the criterial form. In particular, we obtain certain advantage if the dependence $Pf(P_{g\ HES})$ is approximated in the form of a binomial posynomial:

$$\Delta P*j(P_{g\,HES*}) = a_j P_{g\,HES*\,j}^{\alpha_j} + b_j P_{g\,HES*j}^{b_j},$$

where $\Delta P*j(P_{g\,HES*})$ – is the value of the target function (minimum losses of active power in the network or its part) in relative units;

$$P_{g\,HES*j} = P_{g\,HES\,j} / P_{g\,HES\,jo}$$

generation capacity of HES, with the help of which the LES modes are optimized, in relative units. (as the basic optimal values of generating capacity of HES are taken); aj, bj, αj, βj − are constant coefficients reflecting the dependence and the degree of influence of HES generation on the value ΔP_{*j}. The advantage of approximating the target function in the form (2.30) lies in the fact that thedirect and inverse task of sensitivity is solved in simplified manner. If there is no problem with the direct task – $\Delta P*j(P_{g\,HES*})$ in the right side of equation (2.30) the set deviation of the generation is substituted and corresponding value of the losses is calculated, then the inverse task of sensitivity ΔP_* is more difficult. Since the equation (2.30) is nonlinear, the inverse problem of sensitivity

refers to incorrect problems . Fig. 2.22 illustrates the determination of optimal solutions area, i.e., the inverse problem of sensitivity.

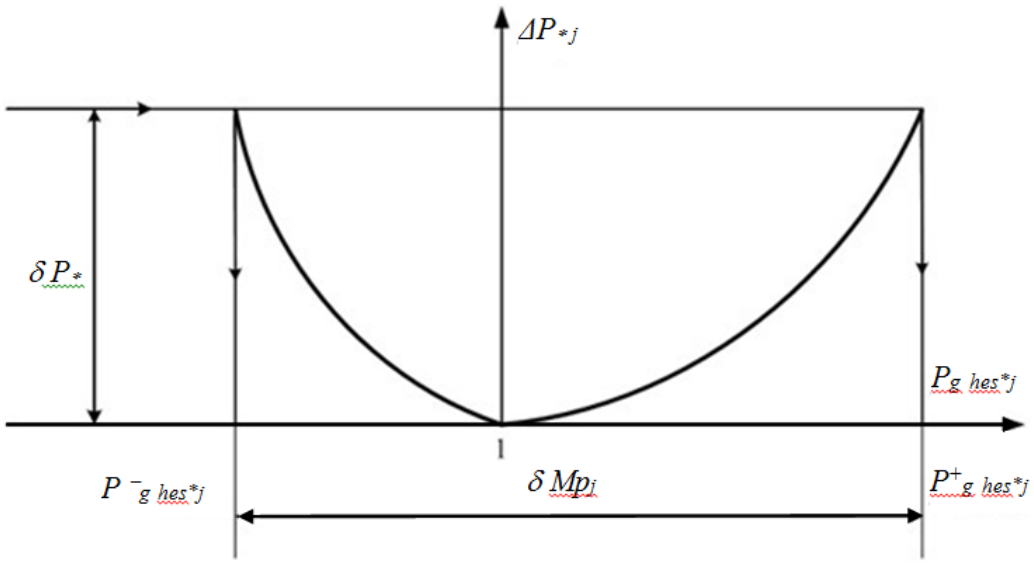

Fig. 2.22 − Definition of optimal solution area (inverse sensitivity problem)

Limiting values of generating power with a given allowable deviation of power δP_* losses in a selected fragment of the DEN [58]:

$$P^{-}_{g\,HES*j}=\left(\frac{1}{\pi_{j1}}\cdot\frac{a_j}{1+\delta P*}\right)^{-1/\alpha},\qquad P^{+}_{g\,HES*j}=\left(\frac{1}{\pi_{j2}}\cdot\frac{b_j}{1+\delta P*}\right)^{-1/\beta}. \tag{2.31}$$

The values of similarity criteria can be determined from the optimality conditions of the dual problem of crite- rion programming relatively the direct problem. For (2.31):

$$\begin{cases}\alpha_j\pi_{j1}+\beta_j\pi_{j2}=0;\\ \pi_{j1}+\pi_{j2}=1.\end{cases} \tag{2.32}$$

From the system of equations (2.32) we obtain

$$\pi_{j1} = \frac{-\beta_j}{\alpha_j - \beta_j}, \quad \pi_{j2} = \frac{\alpha_j}{\alpha_j - \beta_j}. \tag{2.33}$$

Substitute in (2.32) the value of the similarity criteria (2.33) and finally observe:

$$P_{g\,HES*j}^{-} = \left(\frac{\alpha_j - \beta_j}{-\beta_j} \frac{a_j}{1+\delta P*} \right)^{-1/\alpha}, \quad P_{g\,HES*j}^{+} = \left(\frac{\alpha_j - \beta_j}{\alpha_j} \frac{b_j}{1+\delta P*} \right)^{-1/\beta} \tag{2.34}$$

The resulting δMP area of the allowable deviations of variable from their optimal values, in essence, contains a set of possible equally-economical variants of HES generation with the set accuracy. The δ_{MP} area is used to make decisions regarding the implementation of optimal modes, using HES.

3. AUTOMATIC CONTROL OF FREQUENCY AND ACTIVE POWER OF AN ELECTRICAL POWER SYSTEM WITH RENEWABLE ENERGY SOURCES

The balance between generation and load is one of the basic requirements of operation of power systems. In practice used various levels of governors to ensure the balance from the primary frequency control to planning modes.

Table 3.1

Types of frequency and active power control

Type of regulation	Time interval	The purpose of regulation
Inertial response	0-5 s	Reducing the rate of change of frequency
Primary frequency control	4-30 s	Balancing power in a transitional mode
The secondary frequency control	15 minutes 30 seconds	Balancing power in the steady state
Dispatching	5 min	A reliable system operation

Active periods of three levels of government (Fig.3.1) must take into account the capacity of the system and its dynamic characteristics. In large power systems, the primary control reserves are activated in the first 15-30 seconds while in the autonomous networks (islands) RES or small EPS this time should be significantly lower, due to increasing the share of the load on the synchronous generator with an initial allocation of unbalance

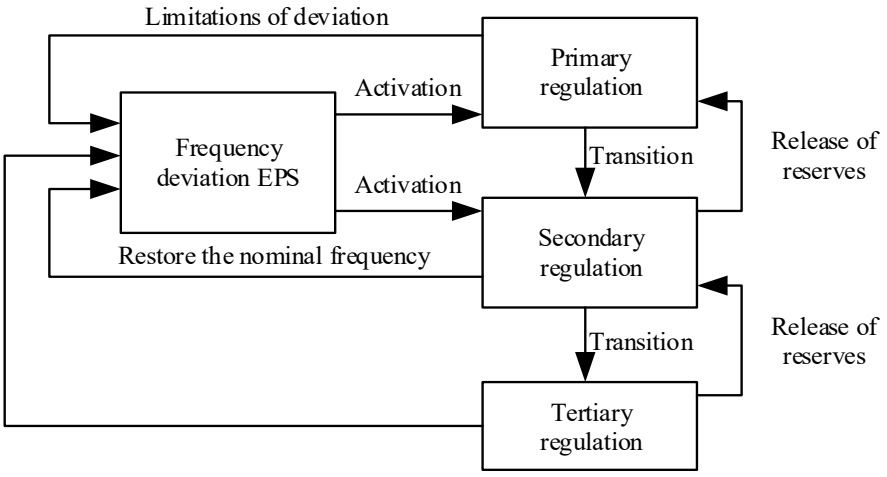

Fig. 3.1. Levels of frequency control

The most common method of administration, for classical systems and for systems with significant RES is a method based on static characteristic expressed dependence:

$$s = \frac{\Delta f_{\text{sys}}}{\Delta P_{\text{reg}}} \tag{3.1}$$

This method is used for decentralized management of partial load distribution of each block without the use of high-speed communication lines between the central controller and relevant units, while centralized management for optimal control frequency.

According to industry grid code in Ukraine primary regulation (PR) is activated when the frequency deviation of more than ± 20 MHz (the amount of error of ± 10 MHz and the dead zone regulator ± 10 MHz). PR activation time is 30 seconds (50% - in the first 15 seconds, from 50% to 100% - increases linearly). After stabilizing the transition frequency deviation shall not exceed ± 180 MHz.

According to research conducted [63] PR reserve for UES of Ukraine should make ± 185-190 MW. According to [64] range PR of each block should make up 5-10% of the installed capacity, including possible plans and emergency repairs of equipment.

Given the above, it is necessary to provide additional primary regulation at 33-35 units of 200 and 300 MW. Provision of secondary regulation (SR) must comply with 450-500 MW and 1000 MW unloading the load. Currently there is a shortage of spare capacity and maneuverability UES Ukraine, power lack reach 8000 MW during winter maximum load and about 5000 MW in the summer. [65]

In terms of integration of Ukraine in ENTSO-E, analysis of test results revealed [65] that now, in addition to the Burshtyn TPP existing thermal power characteristics, block and station control systems do not comply with ENTSO-E requirements regarding frequency and power.

The results of tests on 17 power units showed that:

- Governors dead zone exceeds ± 80 MHz (ENTSO-E normalize dead zone at ± 10 MHz).

- Sensitivity of control system - 50 - 100 MHz (as required by ENTSO-E - 20 MHz).

Secondary control (SC) aims to restore the nominal frequency and activated simultaneously with the PR, but the time constant, which characterizes its dynamics is much higher (at least ten times). Thus, these two levels of regulation are separated in time. SC is associated with proportional-integral (PI) action, which slowly sets the frequency to the set value. While in the classic grid PI controller is used for error correction control, which expresses the active power unbalance [66], in the case of small-scale networks easier to apply compensation directly to the frequency deviation. Thus, the SC model can be written in the form:

$$\Delta P_f(t) = K_{Pf} * \Delta f + K_{If} * \int \Delta f dt \,, \tag{3.2}$$

where K_{Pf}, K_{If} - proportional and integral coefficients; ΔP_f - correction on the output of the regulator; Δf - frequency deviation after the initial adjustment (static error).

Secondary regulation can be centralized [67] or decentralized – at each unit [68], but the first solution has several advantages. When working with multiple distributed PI regulator that affect one parameter, i.e. the frequency of any (even small) error in measurements that inevitably integrated over time and leads to an imbalance between the active power units.

SC applied at 6 units connected to grid. Dnieper HPP-1 total capacity of 432 MW, enough to compensate for the loss of 1000 MW.

In the absence of the required amount of reserve automatic secondary frequency and power UES Ukraine rebalancing while lowering power plants or during fluctuation of consumption in Ukraine partly compensating input hydroelectric power reserves connected during automatic secondary regulation, and by changing the load of thermal power plants and hydroelectric operating units manually by NPC "Ukrenergo".

To ensure a reserve of 500 MW on the basis of planned and emergency repairs to the automatic secondary regulation must connect about 30 new thermal units.

With the integration of renewable energy is important to consider that this source characterized by low inertia, high maneuverability, low time constant. In most cases, renewable equipped by the required automatic excitation regulators however, most are not equipped with speed and active power control systems. Given the fact that over time, their impact on the balance of power will become more pronounced – there is a need to develop effective approaches to use RES power during control processes [69] [70], in order to control power flows in emergency, overloaded and transient conditions.

3.1 Analysis of the impact of renewable energy sources on the frequency of the electric power system

In Ukraine, the requirements for the operation of renewables as a part of the EPS partly described in [71], according to [72] renewables must maintain a specified level of voltage at the point of connection and participate in the regulation of frequency and power of EPS under normal and emergency conditions.

Requirements for parallel operation of renewable energy from the power grid considered in the feasibility study, the results of which conclude about the impact of renewables on network operation and the need for additional measures to reduce the negative effects of joining RES.

Note that when RES connected to network, network operators facing the problems that are related to retooling the electrical network:

- modification of existing relaying systems and replacing some of them with new ones;
- change in short-circuit levels, replacing switching equipment;

- development of operational procedures and technical support for renewables in autonomous mode [73].

Research conducted in [74] showed that depending on the type, structure and capacity of RES, there are three main options of connection:

- RES power up to 5 kW - connected to 0.4 kV bus. In this case connecting to an 0,4 kV electrical network provides backup power consumers. This renewable energy can work both independently and in parallel to the electrical network. Since the capacity of renewables low, there is no significant effect on a power grid.
- RES with capacity up to 600 (1000) kW - 6..10 kV bus connected. In this case it is necessary to solve the problem of optimizing the choice of connecting renewables by calculation of network modes and develop new approaches to the selection of types of relay protection and automation;
- RES group (virtual power plants) with a total capacity 150 MW and above – substations of 35..110 kV. In this case, working in a parallel with RES and EES influence the modes of electricity system and traditional power stations [75].

3.1.1 Assessing the impact of renewable energy on the frequency of the electric power system

Parallel operation with RES complicates the calculation of static and dynamic stability margins, while renewables can increase system stability limits, since the introduction of renewables can reduce the burden of large synchronous generators (SG) and power lines, reduce the unbalance between load and generation in the disruption of the network.

At the same time, there are a number of events related to integration of renewables, which have a negative impact on the stability of the system. First, a low inertia of a small generator sets compared to the powerful SG and unstable power output of some types of renewable energy (wind farms, solar power stations), which makes it difficult to use them during the centralized regulation

[76].

Given the variety of types and characteristics of dispersed generation, especially renewable energy, the nature of transients in systems with RES requires further research. At the level of distribution network RES turns it into an active power component, resulting in the need to change management principles and operation of the power grid.

In the study of processes of frequency is important to identify the main factors affecting the dynamic behavior of the research object.

Simplistically, electromechanical transient frequency change in EPS, which can be described by the following relationship:

$$2H\frac{\partial^2\delta}{\partial t^2}\frac{S_{inst}}{{\omega_s}^2} = T_{mech} - T_{max} * si\,n(\delta) - D * \left(\frac{\partial\delta}{\partial t}\right) = \Delta T \qquad (3.3)$$

where ΔT - the difference between mechanical and electrical torque of an equivalent generator; H - equivalent inertia constant of a generator (2.5-3.5s for UES of Ukraine); S_{inst} - installed capacity of equivalent generator; T_{mech} - mechanical torque of equivalent generator; δ – change of the angle of rotation of the rotor of the equivalent generator; T_{max} - the maximum torque of equivalent electric generator; D - damping factor of equivalent generator.

Equation (3.3) can identify the main parameters that influence the dynamics of the process of change of frequency:

- ΔT unbalance in the power points;
- inertia constant H;
- speed controller parameters that affect the mechanical moment (time constants rise and decline of power, electrohydraulic servo time constants, etc.);
- T_{max} - depends on the resistance of the equivalent electrical path, type and parameters of the automatic voltage regulator, the use of FACTS. Transfer to a weak section (with relatively low bandwidth) can delay the response of frequency regulators or pressure transmitters;
- D damping factor;

- regulating effect of the load has a significant impact on control process. It is determined by the frequency load dependency (4 %/ Hz for UES of Ukraine) and power load regardless of the voltage.

The value of the constant inertia of the system is determined by quantitative and qualitative characteristics of synchronous machines, which mainly consist of synchronous generators in nuclear, thermal and hydro power plants [77]. Synchronous machines are electrically connected to the grid and the rotor is mechanically connected to the turbine. When disturbance that leads to change power balance in the system appears it forces the change of the synchronous machines rotation frequency. When an imbalance of power occurs, kinetic energy changes reaction typically seen in countering changes in connected to the network synchronous generators rotor speed.

Equation (3.4) determines the amount of energy that is released when the frequency changes from the nominal value ω_n to ω_i as inertial response.

$$\Delta E_k = E_{k0} - E_{k1} = \frac{1}{2} J(\omega_n^2 - \omega_i^2) \tag{3.4}$$

where J - the equivalent moment of inertia of the generator [kg m²].

Given that consumption and generation constantly changing, system operators conduct operational planning or the redistribution of power to maintain levels to generate appropriate levels of power flows, which leads to changes in the time value of system constant inertia. This process is a natural feature of the electrical system. When generator is disconnected from the network, its kinetic energy is not available. Study of EPS with RES in island mode in terms of stochastic renewables generation has shown [78] that low system inertia (lack of kinetic energy reserves) increases the particle load of synchronous generators with an initial allocation of unbalance (during disturbances) (Fig.3.2).

It’s important that the kinetic energy of each generator is independent of the current generation unit, and depends on the physical characteristics of the machine and current frequency network.

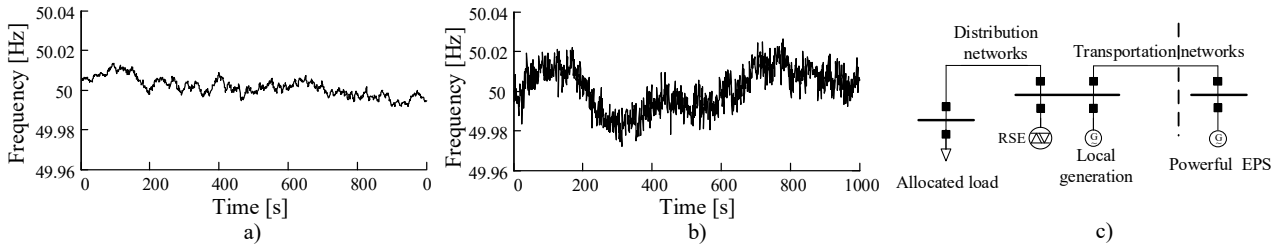

Fig.3.2. Results of frequency calculation: a) parallel operation; b) islanded mode

Thus the importance of particular note of the influence of renewables on frequency and dynamic characteristics of EPS as a whole and its individual parts. Reduced inertia leads to acceleration of EPS electromechanical transients (changing SG rotor speed), leading to the need to improve performance requirements of relay protection and automatics. Addressing the EPS kinetic energy depletion requires the development of new mathematical models and justification of EPS power supply systems, the analysis of their regimes and management.

3.2 Power systems WAMS based analysis

3.2.1 Analysis of power systems transient modes

Analysis of the data from the WAMS necessitates assessment of the nature of dynamic processes occurring in the power system. To assess the dynamic performance of multi-generator system transient conditions during unbalance divided into 3 stages:

- $t_0 - t_1$ - EPS mode transition is defined by electromagnetic transients;
- $t_1 - t_2$ - EPS mode is defined by electromechanical transients;
- t_2^+ - EPS transition mode defined by the work of automatic control.

In case of emergency distribution imbalance between generators is heterogeneous, this leads to the fact that some transient changes in operational parameters, including frequency and power flows, has an oscillatory character. Fluctuations of operational parameters, especially active power, angles and frequency, reflecting the transition between the criteria of distribution imbalance.

Immediately, at the time of imbalance ($t_0 +$) the balance of power in the system is maintained based on the accumulated electromagnetic energy. Average balance between generators is performed on the criterion of the electrical distance to the point where imbalances occurs. Generators take part in imbalance ratios depending on their capacity, synchronizing power $P_{s\_ij} = \frac{\partial P_{ij}}{\partial \delta_{ij}} = E_i E_j \left(B_{ij} cos\delta_{ij0} + G_{ij} sin\delta_{ij0}\right)$. If dynamic stability maintains then frequency oscillation and generators active power have fading nature. Generators that closer to the point of unbalance get most of the imbalance power.

If after perturbation system keeps synchronous operation during $t_1 \rightarrow t_2$ period, center of inertia frequency ($\bar{\omega}$) and equivalent angle ($\bar{\delta}$) for a coherent group is calculated as:

$$\bar{\delta} = \frac{\sum_{i=1}^{n} H_i \delta_i}{\sum_{i=1}^{n} H_i}, \ \bar{\omega} = \frac{\sum_{i=1}^{n} H_i \omega_i}{\sum_{i=1}^{n} H_i} \tag{3.5}$$

where H_i - synchronous unit inertia constant; δ_i - synchronous unit loading angle; ω_i - synchronous unit angular frequency.

3.2.2 Analysis of the renewables inertial response requirements

Currently, the Electric Reliability Council of Texas is working on requirements for inertial response [79] and has developed technical complex to evaluate the existing stock of kinetic energy in a given area at a given interval and dispatch schedule in real time. Inertial response is calculated as the ratio of the power loss (perturbation) to the difference of frequency and to maximize its rejection. When the dispatch schedule correction system automatically determines working conditions with inadequate response inertia allowing the operator to adjust the distribution of power [80].

In its turn HydroQuebec company has developed a series of standards for wind turbines installed capacity for over 10 MW [81], which among other things define the requirements for participation in frequency control by providing inertia response. Requirements of HydroQuebec primarily concerned with making the

necessary (expected) dynamic performance of wind turbines that would not harm a reliable power supply. During research Hydro-Quebec concluded that the best solution would be to increase wind turbine power by 5% for 10 seconds [82]. In studies examined two main forms of report: Hopping and linearly increasing (Table 3.2)

Table 3.2

Configuration for virtual inertia regulators standardized by Hydro-Quebec

Parameter	Explanation	Linear relationship	Hopping relationship
Dead zone	Rejection frequency with which the control activates.	0.3 Hz	0.5 Hz
The level of increase in active power	The minimum level to which station should increase their power.	6%	6%
The issuance of additional power	The minimum time for which the station must fix additional power transition to the stage of recovery.	10 s	10 s
Time activation	Maximum time after the disturbance before the issuance of additional power.	1 s	1 s
Time of transition	Minimum recovery phase transition in an effective rotational speed of the turbine.	3.5 sec	3.5 sec
The maximum level of reduction of the generation of the recovery	The maximum level of reduction of generation during the phase of recovery.	20%	20%

3.2.3 Modeling of wind power plants virtual inertia

Typical wind farm consists of groups of turbines that are made by the same technology [83] [84]. These technologies vary in cost, complexity, efficiency and equipment used. In [85][86] wind turbines have been divided into four main types: turbine at a constant speed; turbine with variable speed; turbine with asynchronous generator excitation double; full-converter turbine.

Modern wind farms are complex electromechanical devices controlled through programmable controllers (PLCs) are fed to the input information on the operation of electric network, weather conditions, setting of central regulators. The main objectives of the PLC is to control wind turbines power converters, inverters, the position of the blades, established control and transient voltage, active and reactive power, cosφ, frequency and so on.

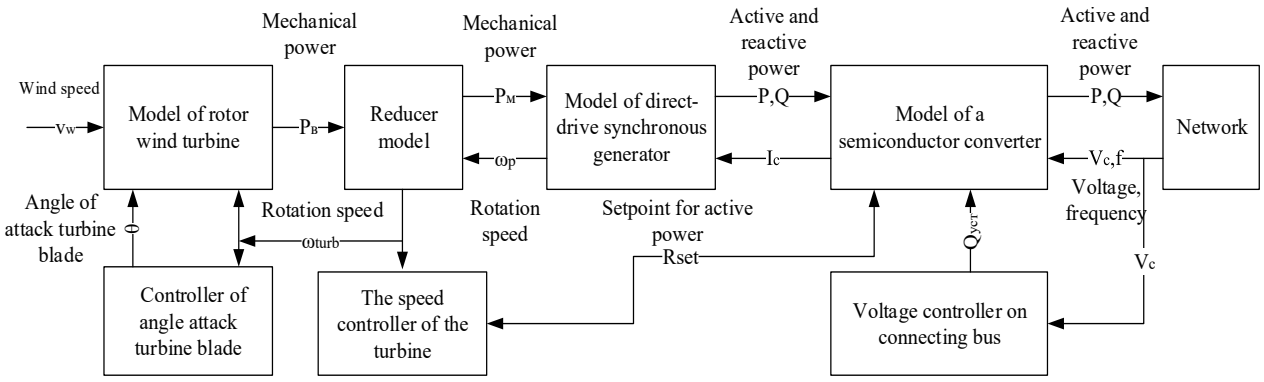

Fig.3.3. The structural model of a wind power station

Implementation of inertial response to wind turbine design algorithm provides more energy from the wind turbine by using kinetic energy of the rotating masses or through restrictions generation. Promising considered using the kinetic energy of wind turbines rotating masses (variable speed) in combination with an easy to implement discrete control.

To describe the problems of implementation of inertial response (IR) of wind power plant functional core of the PLC is defined. The subsystem is responsible for the formation of IR – regulator of virtual inertia (RVI).

The main task is to develop wind turbine RVI inertial response form implementation is based on information available from kinetic energy reserves of wind farms, the nature and quality of the EPS transition process and EPS information, relay protection algorithms set point and automatic control of electrical networks. If the inertial response formation is too strong / weak, any inconsistency of RVI time activation, etc. inertial response may adversely affect the EPS transitional regime.

Provisions for inertial response representing additional energy ΔE_{add}, which can be obtained from a given wind turbine and power grid to stabilize the transitional regime. It is important to note ΔE_{add}, considered as provision for loading and unloading. For the "safe" use of WPP inertial response necessary to determine: the value of the additional energy can be generated / consumed from the grid wind turbines ΔE_{add} , time (T_{add}) of generation / consumption of extra energy.

When virtual inertia regulator activated, the energy balance will look like:

$$\Delta E_{wind} - \Delta E_e - \Delta E_l - \Delta E_k = 0 \tag{3.6}$$

where ΔE_{wind} - the change in energy derived from wind energy; ΔE_e - change in the power generated to the grid; ΔE_l - change in energy losses; ΔE_k - change and energy from the kinetic energy of the rotating parts of the wind farm.

Then using dependencies for power derived from one wind turbine

$$P_{mech}(\lambda, V_{wind}) = C_p\left(\frac{1}{2}\rho A V_{wind}^3\right) = \frac{1}{2}\rho\pi R^2 V_{wind}^3 C_p(\lambda, \beta) \tag{3.7}$$

where P_{mech} - mechanical energy derived from wind; ρ - air density; C_p - wind turbine power factor (λ - relative speed of the blades end); β - the blade angle; A - wind capture area.

Neglecting losses in the mechanical part of WPP [87] and higher order derivatives at constant wind speed and turbine speed of rotation yields:C_p

$$\left(\frac{K_{wind} R_t {V_{wind}}^2 T_{add} \frac{\partial C_p}{\partial \lambda}}{2} - J_t \omega_t^0\right)\Delta\omega_t - \frac{J_t}{2}{\Delta\omega_t}^2 = \Delta E_{add} \tag{3.8}$$

where K_{wind} - an adjustment factor that takes into account the area of capture wind, air density and mathematical constants; R_t - radius of the wind

turbine; V_{wind} - wind speed; J_t - wind turbine moment of inertia; $\frac{\partial C_p}{\partial \lambda}$ - wind turbine power factor sensitivity to changes in angular velocity.

It is important to note that according to (3.8) change in the rotational speed of the turbine $\Delta\omega_t$ - depends not only on ΔE_{add} but also on T_{add}. And with a decrease at constant ΔE_{add}, $\Delta\omega_t$ - decreases.

Dependence (3.8) is used to calculate the T_{add} optimum values taking into account possible WPP technological constraints: the minimum speed of rotation of the turbine, the maximum permissible (short) rotational speed of the turbine, the maximum overload power, maximum overload on mechanical point of minimum electric power, the maximum rate of change set point to power, and so on.

To control the WPP kinetic energy reserves should be used method of limiting the efficiency of wind farms. With controlled wind turbine blades, WPP converts power air mass flow into mechanical energy with different efficiency. The efficiency of energy conversion depends on the aerodynamic characteristics of the blades and characterized numerical index λ:

$$\lambda = R\omega / V_{wind} , \qquad (3.9)$$

where V_{wind} - the speed of the wind; R- turbine radius (working area); ω - angular speed of rotation of the turbine.

Efficiency curve of wind energy is shown on Fig.3.4. This nonlinear dependence$C_p(\lambda)$ [88] and has a maximum point at an optimum ratio .

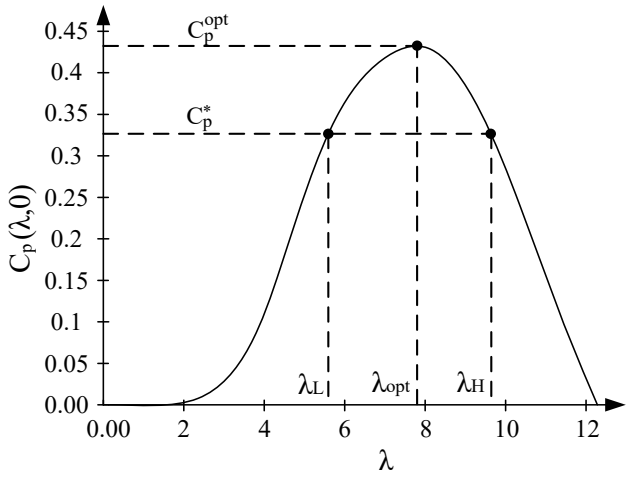

Fig. 3.4. The efficiency curve of power conversion $C_p(\lambda)$.

When the turbine is not at the optimal wind energy $\lambda \neq \lambda_{opt}$, turbine running at reduced power rate which characterized by α [87]. In the range $\lambda_l \cdots \lambda_h$ of the efficiency coefficient of wind energy is $C_p^*(\lambda)$ and more. Then α can be defined as

$$\alpha = \left(1 - \frac{C_p^*(\lambda)}{C_p^{opt}(\lambda)}\right) \cdot 100 \tag{3.10}$$

For a given wind speed V_{wind} - for a given α, the angular speed of the turbine can be reduced in a range of $\omega_l \rightarrow \omega_h$

$$[\omega_l, \omega_h] = \frac{V_{wind}}{R}[\lambda_l, \lambda_h] \tag{3.11}$$

The effect of this decrease shown in Fig.3.4. The difference in kinetic energy can be used for the issuance of the network ΔE_{add} over time T_{add}. Thus the transition to sub-optimal provision $C_p^*(\lambda)$ creates WPP kinetic energy reserve [87].

Ammount of kinetic energy depends on the operating speed of the turbine and rotor inertia with accordance to 3.12

$$\Delta E_K(V_{wind}, \lambda_h) = \frac{1}{2} J \left(\frac{V_{wind}}{R}\right)^2 (\lambda_h{}^2 - \lambda_l{}^2) \tag{3.12}$$

where $\lambda_{\text{н}}$ corresponds to λ such that $C_p(\lambda_{\text{в}}) = C_p(\lambda_{\text{н}})$.

After inertial response (impact energy ΔE_{add}) WPPs aerodynamic efficiency decreases according to a decrease in rotational speed of the turbine. In this case, to restore optimum conditions for generating wind farm electrical power necessary to reduce wind farms power output to the level at or below the current mechanical load.

To support network during disturbances that result in significant power imbalance, as required by Hydro-Quebec, wind turbines should provide inertial feedback "control system issuing power should provide an inertial response at equivalent synchronous generator with a time constant 3.5s. At the request of inertial response regulating stations should increase its active power by at least 5% of the time for at least 10 seconds. "

As required by ENTSO-E the additional power required must be in a form as Fig.3.5 "for reducing the frequency rate of change during the loss generation." The reaction must be implemented within 200 ms and "primary issuance of additional capacity to be consistent with the level of the rate of change of grids frequency." System operators must determine the timing and implementation of network support recovery interval "reserves". Inertial control unit should include setting the dead zone to the rate of change of frequency and power limitations.

Grid codes identifies two main forms of inertial response. The first - on the basis of proportional law on the criterion of the rate of change of frequency, the second - from abrupt law that allows the most efficient use of the kinetic energy of wind turbine.

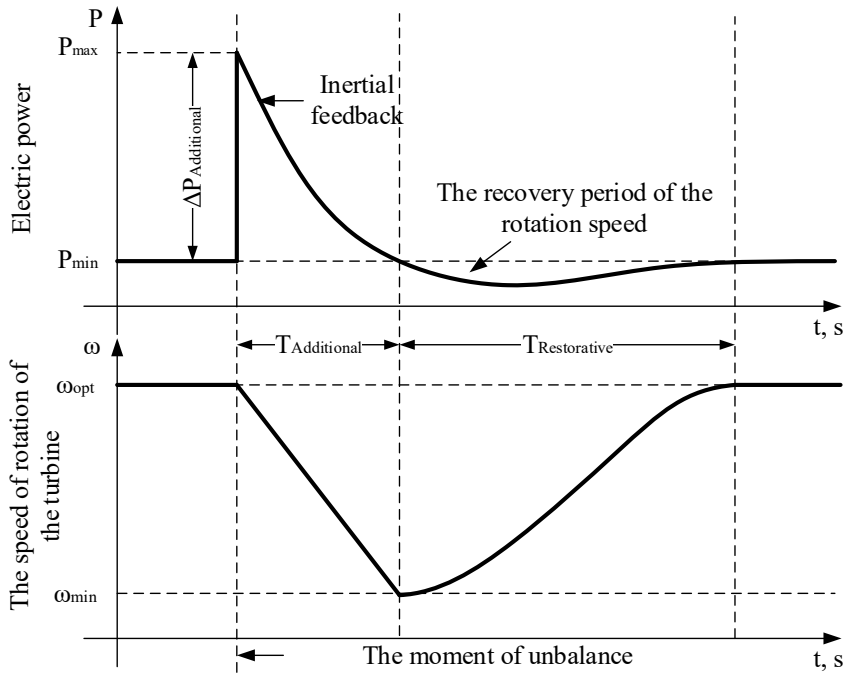

Fig.3.5. Inertial response forms as required by ENTSO-E

For wind farms $\frac{df}{dt}$-controller determines the "optimal" set point adjustment time for a specific mode. Implementation of $\frac{df}{dt}$ inertia controller shown on Fig. 23.

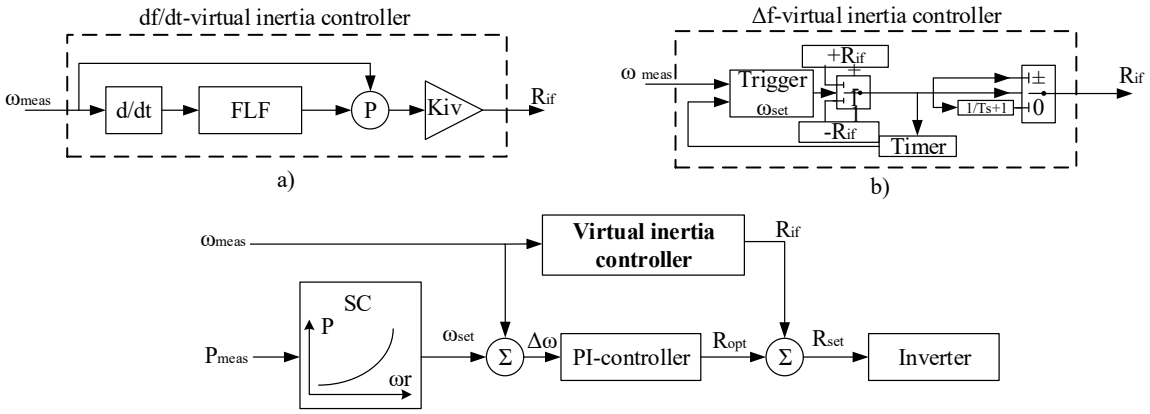

Fig. 3.6. Block diagram of the regulator as part of wind turbine virtual inertia control

Dynamical increase the moment set point on the turbine control effectively releases the stored kinetic energy in it, leading to a decrease in the rate of rotation. Immediately thereafter activates controller support for maximum power extraction that counteracts the $\frac{df}{dt}$-regulator. However, the time constant of the turbine blades

rotate much higher then inertial response so operational frequency support task at the initial time the $\frac{df}{dt}$-controller executes successfully.

An alternative approach to providing managed inertial response RES is to use a discrete Δf-regulator that enhances the generation of wind farms to a predetermined value (ΔP_{add}) at a time T_{add}. Compared with $\frac{df}{dt}$ −control, Δf-controller – more simple to implement, but needs more fine-tuning and settings of ΔP_{add} and T_{add}.

The structure of wind turbines automatic control system (Fig.3.6) with integrated RVI ($\frac{df}{dt}$-regulator and Δf-regulator) is shown in a PowerFactory software interface.

For the study of RVI in EPS dynamic mode WPP was chosen in standard 14 Bus IEEE test model network (Fig.3.7). WPP installed with RVI at bus №5. Perturbations introduced on 20th second, by an abrupt increase of the load on the bus №2 (+ 10MW). Generators that are connected to the bus №1 and №2 participate in primary frequency control.

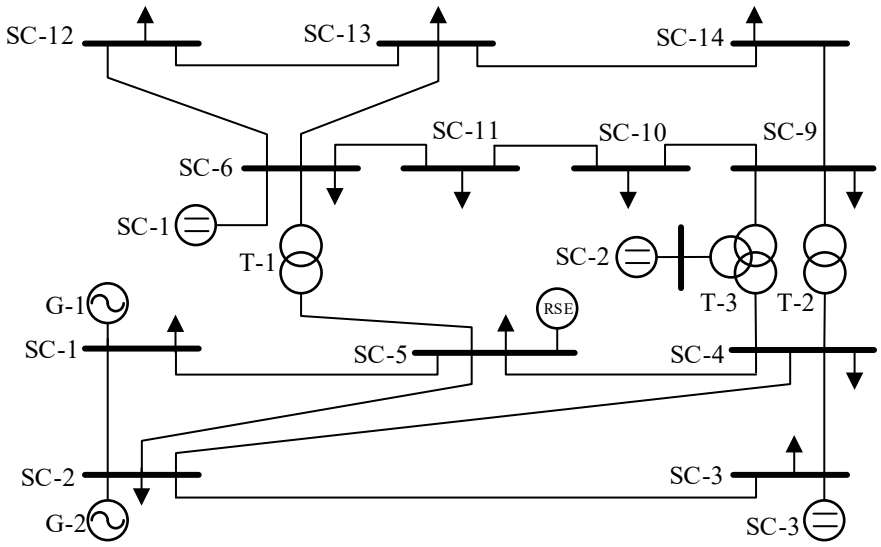

Fig. 3.7. IEEE 14-bus test network for the study of regulators virtual inertia

The scheme includes a network with voltage class 10, 115 and 230 kV, and the following elements:

- synchronous generators G-1, G-2;
- wind farm;
- synchronous compensators SC-1, SC-2 and SC-3;
- 2-winding transformers T-1 and T-2;
- 3-winding transformer T-3;
- 16 electrical power lines, 8 transmission lines - 230 kV voltage transmission lines and 8 of 115 kV;
- 12 loads.

Wind turbines automatic control system used (Fig.3.8) with integrated regulator of virtual inertia.

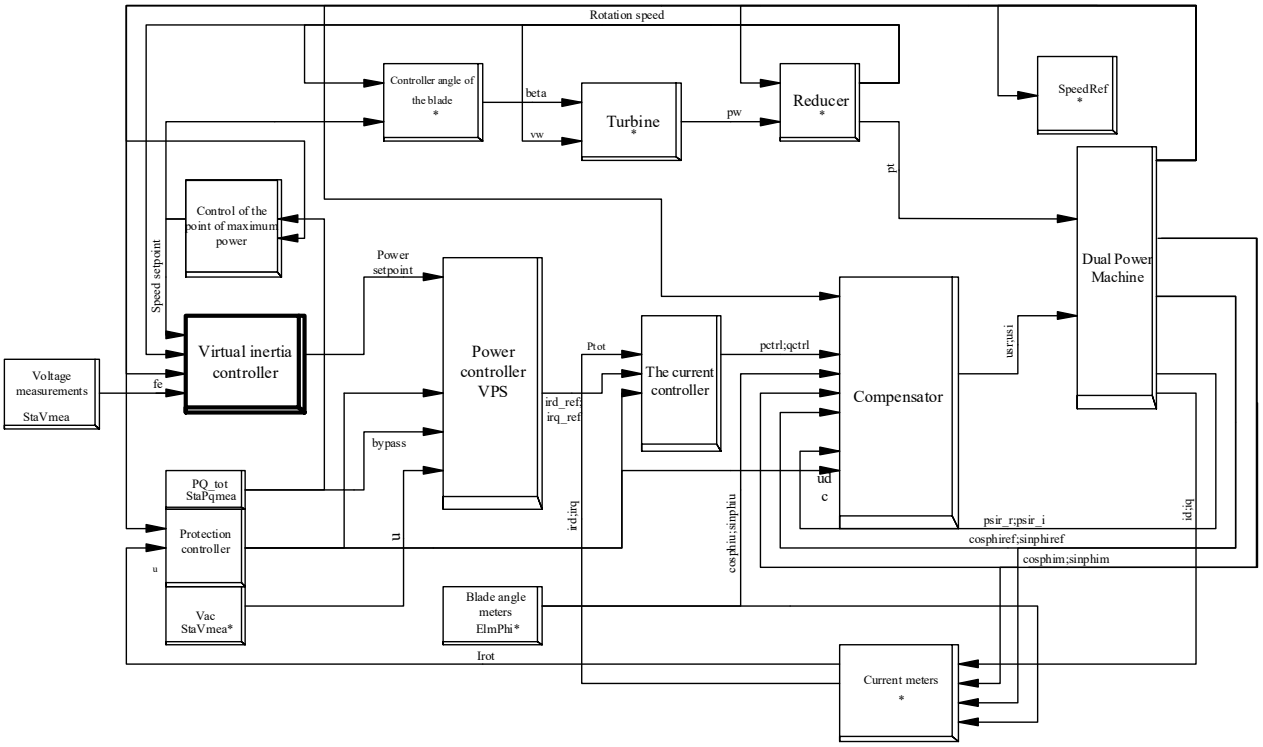

Fig. 3.8. The structure of the wind turbine automatic control system with regulator of virtual inertia

To study a work of df/dt and Δf-regulators in transient frequency modes, a series of experiments with a similar perturbation (occurrence of unbalance - load lack) and with various settings of the regulator virtual inertia. For differential regulator were chosen equivalent inertia constant at 0, 1, 5 and 10 seconds. For the

Δf-regulator issuing additional power (inertial response) was 1, 3, 5, 10 seconds. The results of calculation of the rotational speed of the wind farm turbine and power system frequency shown on Fig.3.9.

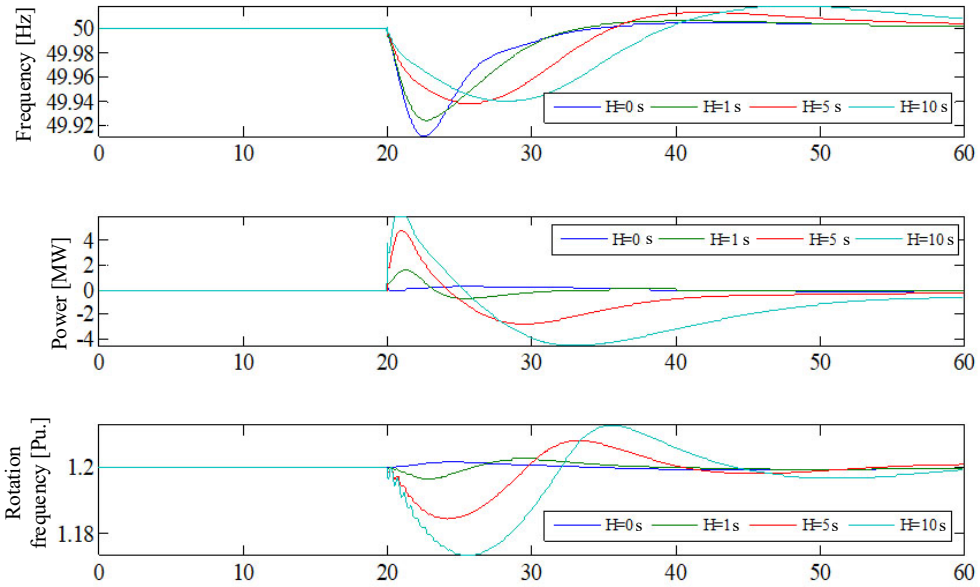

Fig. 3.9. The simulation results of the $\frac{df}{dt}$-controller settings for different virtual inertia settings

As a result of studies it was found that the use of differential regulator of virtual inertia maximum frequency deviation was decreased to 0.2 Hz, with RVI set point - 10s. The use of the operational reserve was 6 MW. When using the relay virtual inertia controller, the maximum deflection rate also decreased by 0.2 Hz at RVI set point - 1 sec. Thus the frequency approaching the nominal already at 3-4 second after the disturbance. However, in the phase of recovery of kinetic energy relay regulator creates unbalance of power that at 5 and 10 s set point exceeds original disturbance. Thus, the Δf-regulator needs accurate tuning (compared with differential).

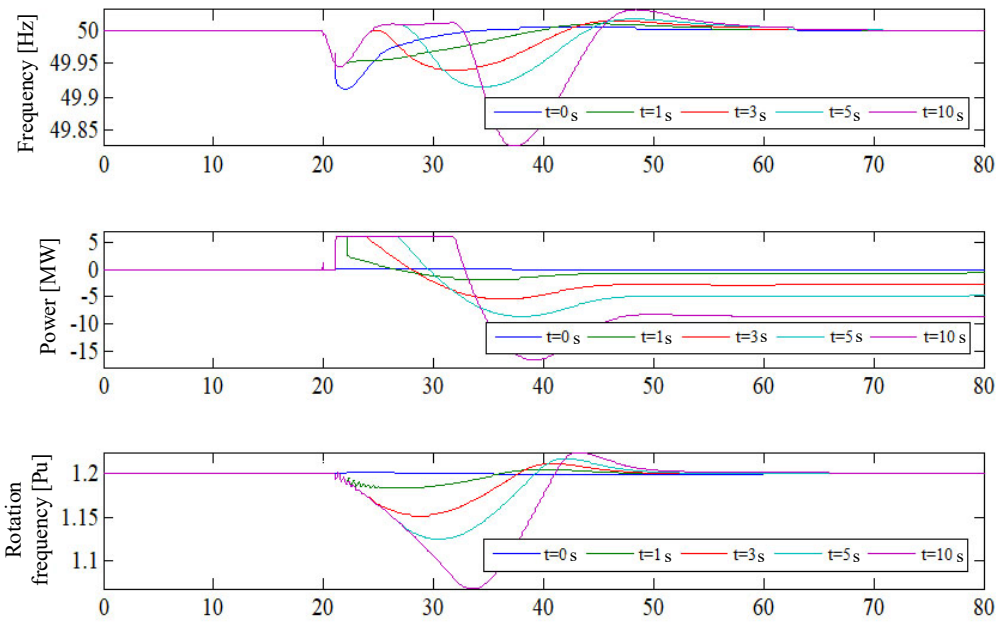

Fig. 3.10. The simulation results of the Δf-controller settings for different inertial response times

The calculation results demonstrate transient change in frequency (Fig.3.9, 3.10) by comparing the effectiveness of using wind farm virtual inertia in frequency transient mode. This data shows that the discrete wind farms RVI, as opposed to a differential, requires configuration that taking into account the current dynamic characteristics at the point of station joining.

3.2.4 Methods of generation limitations for renewables to provide reserve

Basic approaches to limit the generation of renewable energy as follows:

1) The absolute generation limitation is used to limit the active power generated by the power plant to a predefined limit at the point of connection. The absolute generation limitation generally used to protect electrical networks from overload.

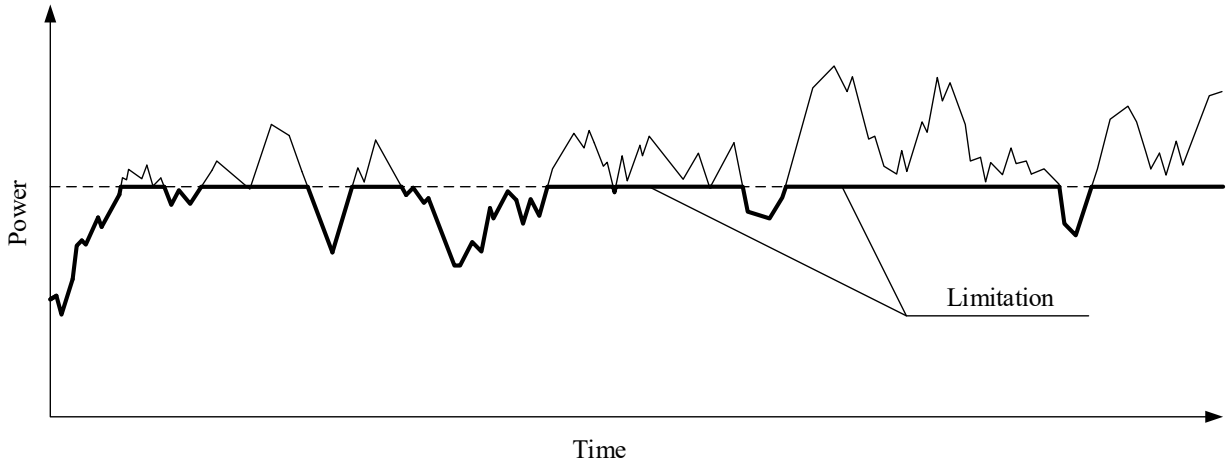

Fig.3.11. Maximum capacity of limited value and renewable energy generation at the absolute limit

2) Delta-generation limitation is used to limit the active power generated by the power plant to the desired size, which is proportional to the possible power generation. Delta-generation limitation is usually used to create a reserve of active power regulation to adjust the frequency.

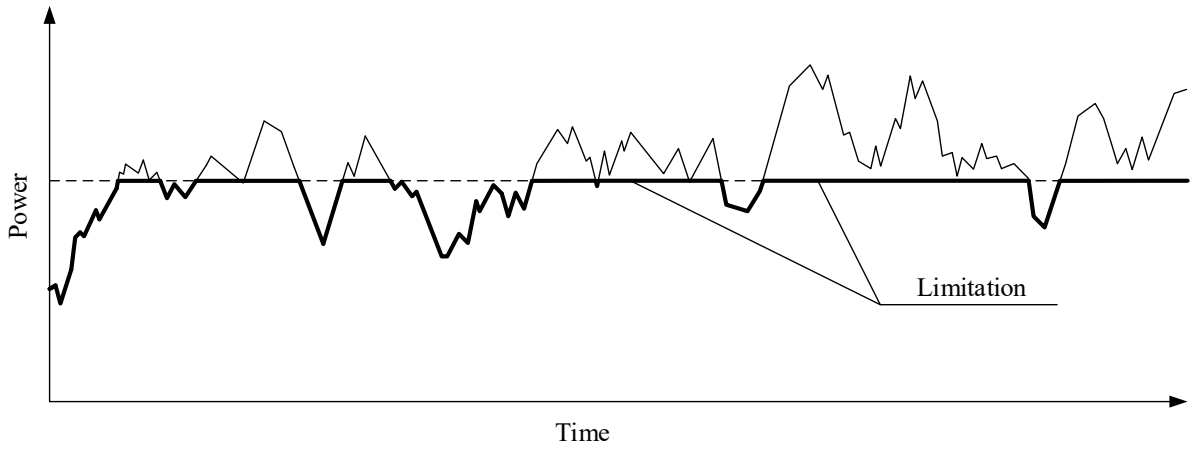

Fig.3.12. The maximum value and limited capacity of renewables during delta generating restriction

3) Limiting the power gradient is used to limit the maximum speed at which the active power can be adjusted in case of change of wind speed or intensity of solar radiation or settings for wind and photovoltaic power plants.

Gradient power limitation typically used to prevent violations of the stability of power grids due to changes in active power generation.

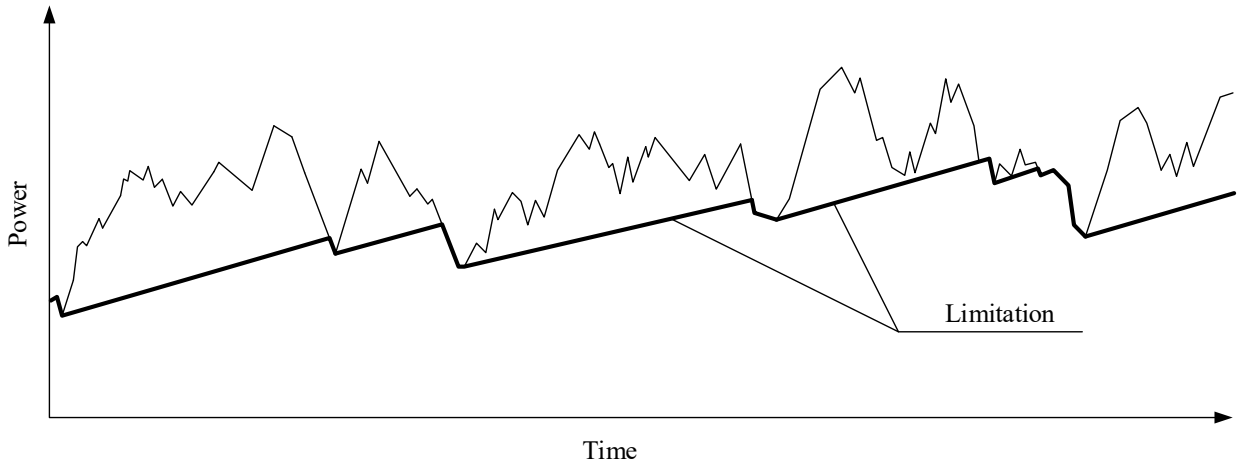

Fig. 3.13. Maximum capacity of limited value and renewable energy while limiting gradient power

In order to provide inertial response its appropriate to use delta limitation of renewable energy generation. This allowing control over time (increased predictability) of the value of additional capacity that will be used during regulation. Using gradient power limitations can reduce the rate of change of RES power - smooth generation schedule and reduce the variability of generation.

Absolute power limitation and gradient power limitation of the renewable power reserves deals with greater variability and less predictability, but the use of adaptive centralized controls that are capable of real-time change of the virtual inertia regulator setpoint makes good use of all types of managed RES conventionally reserved power.

3.2.5 Determining the optimal location of EPS frequency regulation facilities

Efficient operation means simultaneous EPS parameters registration involves the use of a powerful communication network. Given the high cost of construction and operation of WAMS, it is necessary to solve the aforementioned problem of minimizing expenses while maximizing electricity system

observability. Observability criterion can be obtained in the theory of modal analysis. As noted earlier, right eigenvector matrix system model in the form of state variables, is responsible for the "form" of mode. Transients observability, the nature of which determines the optimality criterion should be as high as possible. In addition, during the identification model of adequate specified parameters relative changes in transient conditions, it is necessary to provide high observability of characteristic features (eigenvalues) that are inherent in certain parameters.

Use of sophisticated EPS regulation requires solving the tasks of power reserve and means placement, choice of control laws and control systems configuration [89].

Stability problems of complex EPS are defined by the presence of weaknesses in these systems that can be identified based on structural analysis and assessments of mutual connectivity (including dynamic) [89]. This enables recommendation for site controls pre-installation in a complex EPS with conventionally controlled RES, on the one hand, that should strengthen weaknesses in systems, and on the other - their influence should include as much of the EPS. Thus, the recommended installation location devices are strongly related subsystems near the weaknesses of the EPS.

During the EPS identification process at clustering stage the requirement of the centroids determination showing EPS weaknesses (concerning tasks of automatic frequency control) as the intersection between coherent groups of generators (CGG). CGG are strongly connected subsystems. In terms defined CGG, establishing the optimum means of registration of operational parameters (frequency) during transients at relevant CGG centers of mass.

Described optimal placement criteria can be formalized in terms of manageability. The high observability of poorly damped events in the place of registration is weakness criterion of power system state variabes. As noted earlier left eigenvector (LE) is responsible for the energy distribution of state variables. Using the criterion of control in the power system limited by physical ability to

effect on the state variables. Therefore it is necessary to solve the problem of optimal control in terms of cost and effectiveness and choice of ways to influence the regime parameters.

Obtained from WAMS data must be converted into state variables of identified system model, while direct check of operational parameters corresponding to the identified model state variables is not always possible. In practice used estimates of state variables based on known data input-output system.$\hat{x}$

In the known system model, evaluation values of its state variables to input-output value can be obtained using a system of differential equations (3.12).

$$\dot{\hat{x}}_{\cdot} = A\hat{x} + Bu + L(y - C\hat{x}) \qquad (3.12)$$

where L - feedback matrix coefficient, the main task of which is to reduce the transition assessment process, minimizing deviation $E\{[x - \hat{x}]^T[x - \hat{x}]\}$ from the criteria $J_L = \lim_{T\to\infty} E\left\{\int_0^T (\hat{x}^T W\hat{x} + u^T Vu)dt\right\}$, where W, V - weighting matrix.

The L value is based on the expression $L = \Sigma C^T V^{-1}$ where $\Sigma = \Sigma^T \geq 0$-positive semidefinite unique solution of algebraic Rikatti equations [90].

Optimal control scheme Fig.3.14 achieved by W, V weight matrix choice, evaluation system and weight matrix Q, R of linear-quadratic regulator.

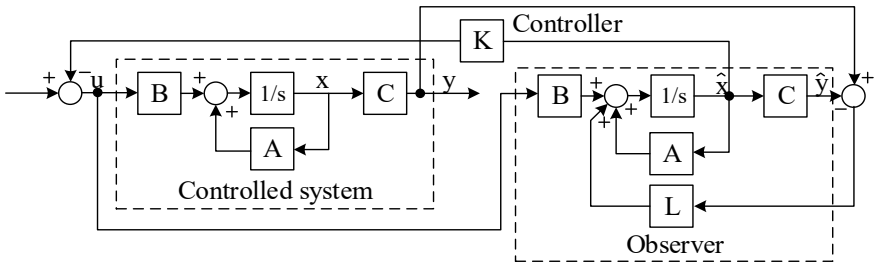

Fig.3.14. Optimal control scheme based on estimates of state variables $\hat{x}$

In the form of state space variables system (Fig.3.14) described in matrix form as (3.13):

$$\frac{d}{dt}\begin{bmatrix} x \\ x - \hat{x} \end{bmatrix} = \begin{bmatrix} A - BK & BK \\ 0 & A - LC \end{bmatrix}\begin{bmatrix} x \\ x - \hat{x} \end{bmatrix} \qquad (3.13)$$

System eigenvalues (Fig.31) are superposition of LQR system eigenvalues $(A - BK)$ and evaluation system eigenvalues $(A - LC)$.

As mentioned before linear-quadratic control aims at solving the problem while minimizing control actions and state variables deflection. Priority (weight) of each state variable and control action specified using weight matrices Q, R. However, with the task of selection criteria, which is responsible for the quality of transition or change specific dynamic characteristics of the system, the choice of weighting coefficients is transformed into the iterative process of sorting and searching.

This problem can be solved in the transformation of the original model to one of the canonical forms. The normal form of the model defines the system state variables as modal components. In this case, the choice of LQR weighting coefficients becomes a trivial task.

3.2.6 The algorithm of the central controller

Centralized control rate takes into account the mutual influence of coherent groups / zones of control. Collected WAMS information is used to identify the model and refine the dynamic characteristics of a firm subsystems and EPS as a whole.

In developing the centralized management is important to ensure that:

- maintaining efficiency of the entire system in case of failure or separation of an autonomous work of its individual parts;
- preserving the possibility of automatic frequency control and power systems in the allocation of any unit (group of units) on autonomous systems;
- the main system in the allocation it to autonomous operation should take into account the autonomous work even without continuous communication with it (fault channel).

To solve the problem of EPS frequency control two-tier hierarchical structure proposed. 3-machine EPS equivalent to UES Ukraine with three CGG (Fig. 3.15) is used, where T_{cgg} - the equivalent time constant KHH; T_t, T_g, T_{res} - the equivalent time constant of the turbine, generator and respective coherent

groups with RES; T_{ij} - the equivalent synchronizing moment ratio between the CGG; R - CGG equivalent frequency static characteristic ratio; B - equivalent frequency correction factor; ΔP_{H}, ΔP_{sec} - deviations from the planned values of loading and power interchange, respectively; Δf - CGG frequency deviation from the nominal value; ΔP_{zone} - used power reserve controls; TPR - transients recorder (synchrophasor).

Central controller forms a centralized control task while regional regulators responsible for central regulator commands implementation.

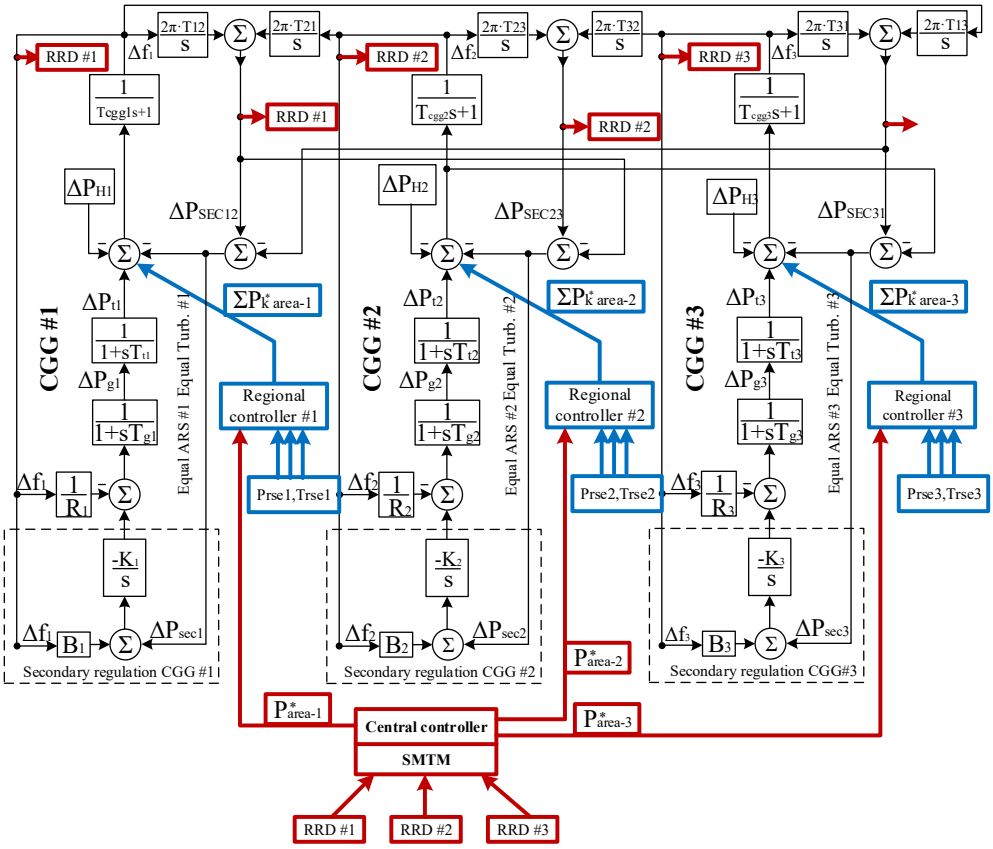

Fig. 3.15. Structure of EPSs three coherent groups of generators centralized frequency control

According to the structure (Fig.3.15) was developed central regulator algorithm (Fig.3.16) that implements modal control and allows to selectively influence the dynamic performance targets, effectively using resources for control.

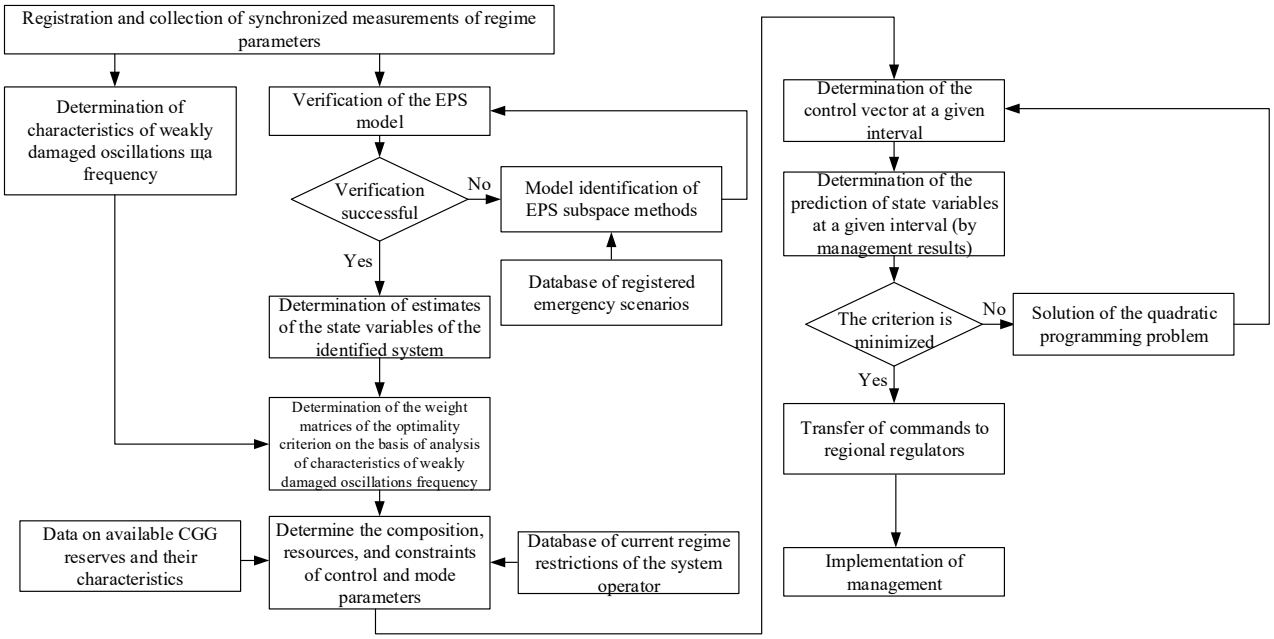

Fig. 3.16. The algorithm of the central controller

Involvement in the local / regional level aditional controls necessitates additional (local) control mode, including voltage control, automatic control systems management (synchronous compensators, relay protection, etc.) and control of existing reserves. Therefore, an important part of the implementation of centralized management is the development of structures and regional controller which is subordinate to the central.

3.2.7 The algorithm of the regional controller

The local / regional management implementation tasks set by the central regulator includes support for a given power reserves in the region and ensuring a certain flexibility of controls.

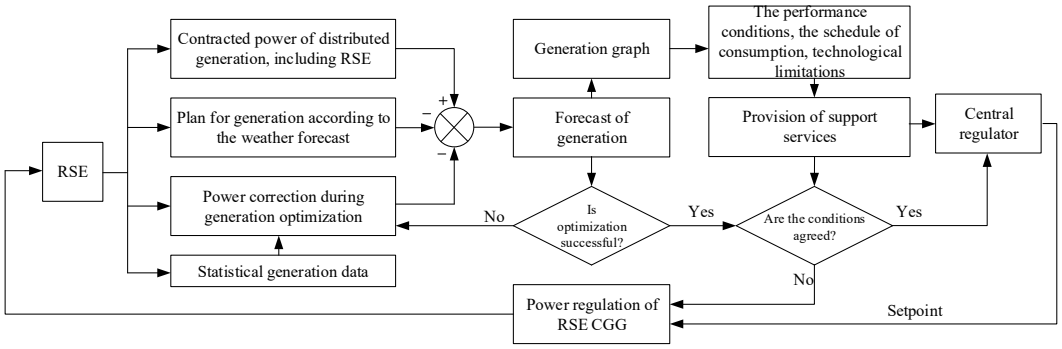

Fig. 3.17. The algorithm of the regional regulator

Previously it was found that the use of inverter-coupled renewable energy source as a control mean allows quick change of power and plays a key role in the regulation of EPS power and frequency. At the same time, studies [91] have shown the need to attract renewable energy technology to the processes of frequency and power control.

After issuing center regulator operational task for CGG capacity correction, regional(P^*_{zone-i}) regulator (LR) distributes it among its control means. The decision on each individual load control means receives LR-based operational, technological, economic constraints.

$$P^*_{zone-i} = \sum_{k=1}^{N} P^*_k \tag{3.14}$$

where $k = 1,2,3 \dots N$; P^*_k - k-th mean power change.

Corresponding central controller ($P^*_{\text{зони}-i}$) command locally distributed between regulation means in accordance with (3.15):

$$b_k(t) = \frac{\sum_{k=1}^{N} P_{\text{res}-k}(t)}{P^*_{\text{zone}-i}(t)}, \tag{3.15}$$

where $P_{\text{res}-k}$- the maximum reserve capacity for adjusting to upload or unload.

If the control element is not involved in the issuance of reactive power:

$$P_{res-k}(t) = \sqrt{S^2_{res-k}(t) - 0(t)} \tag{3.16}$$

if involved - then:

$$P_{res-k}(t) = \sqrt{S^2_{res-k}(t) - Q^2_k(t)} \tag{3.17}$$

Thus each control element is given power change command:

$$P^*_k(t) = P_{\text{res}-k}(t) * b_k(t) \tag{3.18}$$

For identifiable pattern reflecting a transient change in EPS of Ukraine frequency modal LQR synthesis was conducted. It was found changes in the character of the transient frequency and distribution of control system modes while minimizing transient changes in operational parameters optimality criterion (frequency).

The Q weight matrix criteria J according to the criterion of minimizing state variables model in normal form corresponding to poorly damped modes with a frequency of ~ 0.5 Hz gives the following results (Table 3.3, Fig.3.18-3.19).

Table 3.3

Results modal analysis uncontrolled and controlled systems

Without LQR			With LQR		
Mode	damping	Frequency [Hz]	Mode	damping	Frequency [Hz]
-0.0097 + 0.0000i	1.0000	0,0015	-0.0097 + 0.0000i	1.0000	0,0015
-0.1166 + 0.0000i	1.0000	.0185	-0.1166 + 0.0000i	1.0000	.0185
-0.3122 + 1.2879i	0.2356	.2110	-0.3122 + 1.2879i	0.2356	.2110
-0.3122 - 1.2879i	0.2356	.2110	-0.3122 - 1.2879i	0.2356	.2110
-0.4918 + 1.5722i	0.2985	.2623	-0.4918 + 1.5722i	0.2985	.2623
-0.4918 - 1.5722i	0.2985	.2623	-0.4918 - 1.5722i	0.2985	.2623
-0.0053 + 3.1397i	0.0017	.4999	-3.1854 + 0.0000i	1.0000	.4999
-0.0053 - 3.1397i	0.0017	.4999	-2.7289 + 1.7356i	0.8438	.4999
-0.0001 + 3.1403i	<0.00001	.5000	-2.7289 - 1.7356i	0.8438	.5000
-0.0001 - 3.1403i	<0.00001	.5000	-20.7256 + 1.1627i	0.9984	3.1876
-0.0022 + 3.1437i	0.0007	.5005	-20.7256 - 1.1627i	0.9984	3.2143
-0.0022 - 3.1437i	0.0007	.5005	-51.9169 + 0.0000i	1.0000	8.1210

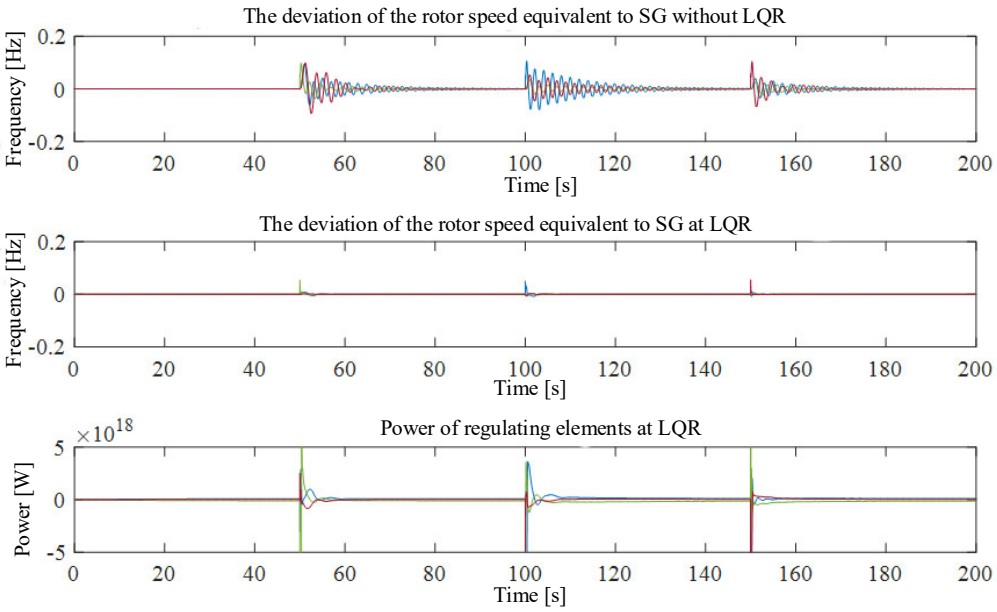

Fig. 3.18. The results of calculation of EPS transient frequency change and used controls reserve capacity with selective modal linear quadratic control

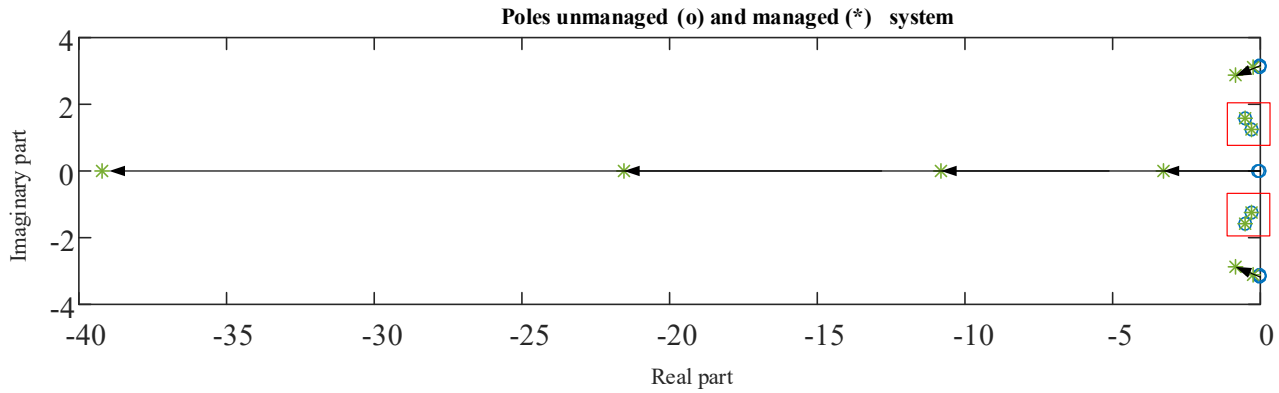

Fig. 3.19. Shifting eigenvalues with selective modal LQR

The results indicate the efficiency of quadratic linear quadratic criterion on a quality control with the exception of the necessary power reserves. The simulation showed that to achieve this task $5 \cdot 10^{18}$ W should be used, which currently can not be implemented in UPS Ukraine even with the involvement of high-speed power reserves of renewable energy virtual inertia. It is therefore necessary to adapt the approach using LQR to work within the constraints on power reserves and ranges of operational parameters change.

3.3 Electric power systems frequency control considering the limitations

Optimal control system should be consistent with the possibility of implementing defined influences. Using the linear-quadratic control for real industrial systems lack the possibility to take account of technological limitations. In case of renewables as a means of control one should take into account the physical nature of the process to generate additional power. Necessary constraints on the available reserves for loading and unloading speed, set and reset power values of operational parameters that define the boundaries of EPS stability can be formalized using model predictive control (MPC).

3.3.1 Defining state variables and system state prediction

After formalizing a mathematical model of control object one should perform the calculation for system prediction in view of future control signals. Within the optimization window (horizon) in length - N_p.

The vector of state variables $x(k_i)$, reflecting the current state information system may be received from WAMS measures [92]. Further trajectory vector of input signals defined as a sequence:

$$\Delta u(k_i), \Delta u(k_i + 1), \ldots, \Delta u(k_i + N_c - 1) \quad (3.19)$$

where k_i - the current time; N_c - control horizon that shows the length of control vector, used to determine the future trajectory of the system. Based on the current value (k_i) forecast of the system (k+) should be get from N_p samples. Let us define the resulting prediction state variables as:

$$x(k_i + 1 \mid k_i), x(k_i + 2 \mid k_i), \ldots, x(k_i + m \mid k_i), \ldots, x(k_i + Np \mid k_i), \quad (3.20)$$

where $x(k_i + m \mid k_i)$ the predicted state variable in time $k_i + m$ given the known $x(k_i)$ and known model. State variables calculated consistently using a set of control vectors for the following countdown:

$$x(k_i + Np \mid k_i) = A^{Np} x(k_i) + A^{Np-1} B\Delta u(k_i) + A^{Np-2} B\Delta u(k_i + 1) + \\ + \ldots + A^{Np-Nc} B\Delta u(k_i + Nc - 1) \quad (3.21)$$

Based on the system output calculated state variables [139] outpud defined as (3.22):

$$y(k_i + Np \mid k_i) = CA^{Np} x(k_i) + CA^{Np-1} B\Delta u(k_i) + CA^{Np-2} B\Delta u(k_i + 1) + \\ + \ldots + CA^{Np-Nc} B\Delta u(k_i + Nc - 1) \quad (3.22)$$

The system output derived from the current state $x(k_i)$ and future values where $\Delta u(k_i + j), j = 0, 1, \ldots N_c - 1$. Then the vector of system is as follows:

$$Y = [y(k_i + 1 \mid k_i); y(k_i + 2 \mid k_i); y(k_i + 3 \mid k_i); \ldots y(k_i + Np \mid k_i);]^T \quad (3.23)$$

$$\Delta U = [\Delta u(k_i); \Delta u(k_i + 1); \Delta u(k_i + 2); \ldots \Delta u(k_i + Nc - 1);]^T \quad (3.24)$$

$$Y = Fx(k_i) + \Phi\Delta U \tag{3.25}$$

$$F = \begin{bmatrix} CA \\ CA^2 \\ CA^3 \\ \vdots \\ CA^{N_p} \end{bmatrix}; \quad \mathrm{F} = \begin{bmatrix} CB & 0 & 0 & \dots & 0 \\ CAB & CB & 0 & \dots & 0 \\ CA^2B & CAB & CB & \dots & 0 \\ \vdots & \vdots & \vdots & \vdots & \vdots \\ CA^{N_p-1}B & CA^{N_p-2}B & CA^{N_p-3}B & \dots & CA^{N_p-N_e}B \end{bmatrix} \tag{3.26}$$

3.3.2 Determining the optimal control vector

For a given set point in time within the forecast horizon, the goal is to minimize system system deviation from defined within the forecast horizon setpoint $r(k_i)$. It is assumed that the vector setpoint remains constant during optimization. The goal of optimization is to find the control vector ΔU such that the error between the predicted value and setpoint output will be minimal.

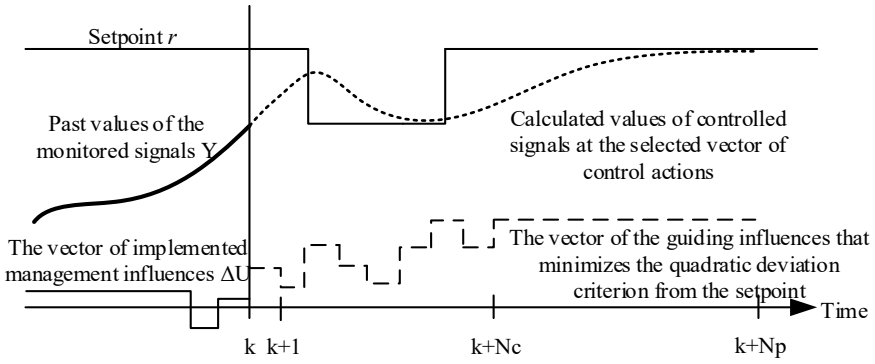

Fig.3.20. Diagram of the MPC optimal vector control

Vector set point is given in the form:

$$R_k^T = \overbrace{[1\,1 \dots\, 1]}^{N_p} r(k_i) = \overline{R_k} r(k_i) \tag{3.27}$$

The value of the quadratic criterion J that defines control quality is defined as:

$$J(U) = (R_k - Y)^T (R_k - Y) + \Delta U^T \bar{R} \Delta U \tag{3.28}$$

where the first term is responsible for minimizing the error between the predicted output and set point, while the second reflects control cost. R - diagonal matrix in a form $\bar{R} = I_{Nc \times Nc}$ $(r_w \geq 0)$ where r_w is used as a parameter settings of a closed control system. If r_w = 0 the value of vector control is not taken into account. With significant r_w, then J magnitude is considered to situations where ΔU has a

significant cost . When finding the optimal criterion minimized by using (3.28). In this case takes the form:

$$min\, J = \sum_{i=1}^{N_p} (R_k - Fx(k_i))^T \left(R_k - Fx(k_i)\right) - 2\Delta U^T \Phi^T \left(R_k - Fx(k_i)\right) + \\ + \Delta U^T (\Phi^T \Phi + \overline{R})\Delta U \quad (3.29)$$

On the first derivative:

$$\frac{\partial J}{\partial \Delta U} = \sum_{i=1}^{N_p} -2\Phi^T (R_k - Fx(k_i)) + 2(\Phi^T \Phi + \overline{R})\, \Delta U \quad (3.30)$$

It should be a minimum condition $\frac{\partial J}{\partial \Delta U} = 0$

The optimal solution can be obtained from the expression:

$$\Delta U = \sum_{i=1}^{N_p} (\Phi^T \Phi + \overline{R})^{-1} \Phi^T \left(R_k - Fx(k_i)\right) \quad (3.31)$$

If there is $(\Phi^T \Phi + \overline{R})^{-1}$ (matrix $(\Phi^T \Phi + \overline{R})^{-1}$- Hesse matrix), the optimal control signal considering setpoint $r(k_i)$ and state variables $x(k_i)$ can obtained in the form [139!!!]:

$$\Delta U = \sum_{i=1}^{N_p} (\Phi^T \Phi + \overline{R})^{-1} \Phi^T \left(\overline{R_k} r(k_i) - Fx(k_i)\right) \quad (3.32)$$

Given the existence of not determined perturbations only the first element (the next count) used from the resulting vector ΔU, after that the optimization process is repeated.

The study [93] showed that the MPC quality without restrictions similar to LQR control. The consequence of this property is the ability to assess the stability of the system with MPC (digital controller) using stability analysis of linear systems.

Optimality criterion for MPC given in a form where the setpoint output vector signals is zero, and the output signals are a deviation of normal form model state variables and frequencies of the CGG centers of inertia.

$$J(u_k) = \\ \left(\sum_{j=1}^{n_y} \sum_{i=1}^{p} \left[\frac{q_{i,j}^{y} (r_j^i - y_j^i)}{s_j^y} \right]^2 + \right.$$

$$\sum_{j=1}^{n_u}\sum_{i=0}^{p-1}\left[\frac{q_{i,j}^{u}(t_j^i-u_j^i)}{s_j^u}\right]^2+\sum_{j=1}^{n_u}\sum_{i=0}^{p-1}\left[\frac{q_{i,j}^{\Delta u}(u_j^i-u_j^{i-1})}{s_j^u}\right]^2\Bigg)=\min \tag{3.33}$$

where p, k - the forecast and control intervals, respectively; n_y, n_u- the number of inputs and outputs of the system, respectively; u - optimal control vector $[u^{k^T}\ u^{k+1^T}\ \ldots\ u^{k+p-2^T}\ u^{k+p-1^T}]$; y_j^i - prediction of j-th system output at i-th forecast horizon; u_j^i - prediction of j-th system output at i-th forecast horizon; r_j^i, t_j^i - setpoints of j-th output and i-th input at i-th forecast horizon, respectively; $q_{i,j}^{y}, q_{i,j}^{u}, q_{i,j}^{\Delta u}$ - weights of j-th output and input difference to neighboring forecast horizon steps, respectively; s_j^y, s_i^u - scale factors of j-th output and i-th input, respectively.

MPC important feature is possibility to calculate the constrained control vector. Constrained control problems on regime parameters (and their derivatives) solving on the basis of the initial, steady and pre-accident condition of the control object (EPS). In the proposed approach uses the limitations of the deviation from the specified default set points. Thus formed the range of parameter changes in transient conditions in terms of static and dynamic stability.

According to the basic control objectives, main process control limits are:

1) limitations on the size of available reserves:

$$u^{min} \le u_k \le u^{max} \tag{3.34}$$

2) limitations on the rate of change of power controls:

$$\Delta u^{min}/\Delta t \le \Delta u_k/\Delta t \le \Delta u^{max}/\Delta t \tag{3.35}$$

3) limitations on the relative angle between the CGG COI. This limitation can be used to prevent the abuse of static and dynamic stability between the two CGGs

$$\delta_{mn} \le \delta_{mn}^{max} \tag{3.36}$$

4) limitations on the size and the maximum rate of change of frequency:

$$y^{min} \le y_k \le y^{max} \tag{3.37}$$

$$\Delta y^{min}/\Delta t \le \Delta y_k/\Delta t \le \Delta y^{max}/\Delta t \quad (3.38)$$

Its important to consider technological limitations that can lead to conflicts in formalizing control problems. At a low "sensitivity" of the output signal with respect to control, restrictions on output require significant costs, which in turn also are limited. In this case, criterion (3.28) is not minimized, but the controls are fully loaded / exhausted. To solve such problems in setting limits advisable to introduce a "softening" s_v in the form:

$$y^{min} - s_v \le y_k \le y^{max} + s_v \quad (3.39)$$

The above method of forming restrictions can solve the problem of finding the optimal J considering the criterion vector control based on quadratic programming (QP).

The criterion of QP is given in the form

$$J(u_k) = \min_u \sum_{k=0}^{t_f} (z_k{}^T Q z_k + u_k{}^T R u_k + 2 z_k{}^T N u_k) + \varphi\left(x_{t_f}, t_f\right) = \min \quad (3.40)$$

where z - the vector of normal form model state variables; u - inputs vector;
Q, R, N - weighting matrix.

Restrictions are given in the form

$$M z_k \le \gamma(z_k) \quad (3.41)$$

where M - matrix that determines the shape of linear constraints.

If Q - positively defined matrix, and all constraints are linear, the optimization problem is reduced to convex (J - convex, restrictions - convex).

The investigations [94] proved that the principles of forming the MPC based control vector ΔU can effectively use nonlinear object model, which by its nature is electric power system. MPC efficiency was tested with algorithm (Fig.3.16). Simulation results of accident scenarios using Ukrainian EPS nonlinear model equivalent to three CGG Fig.3.21 are shown in Fig.3.22.

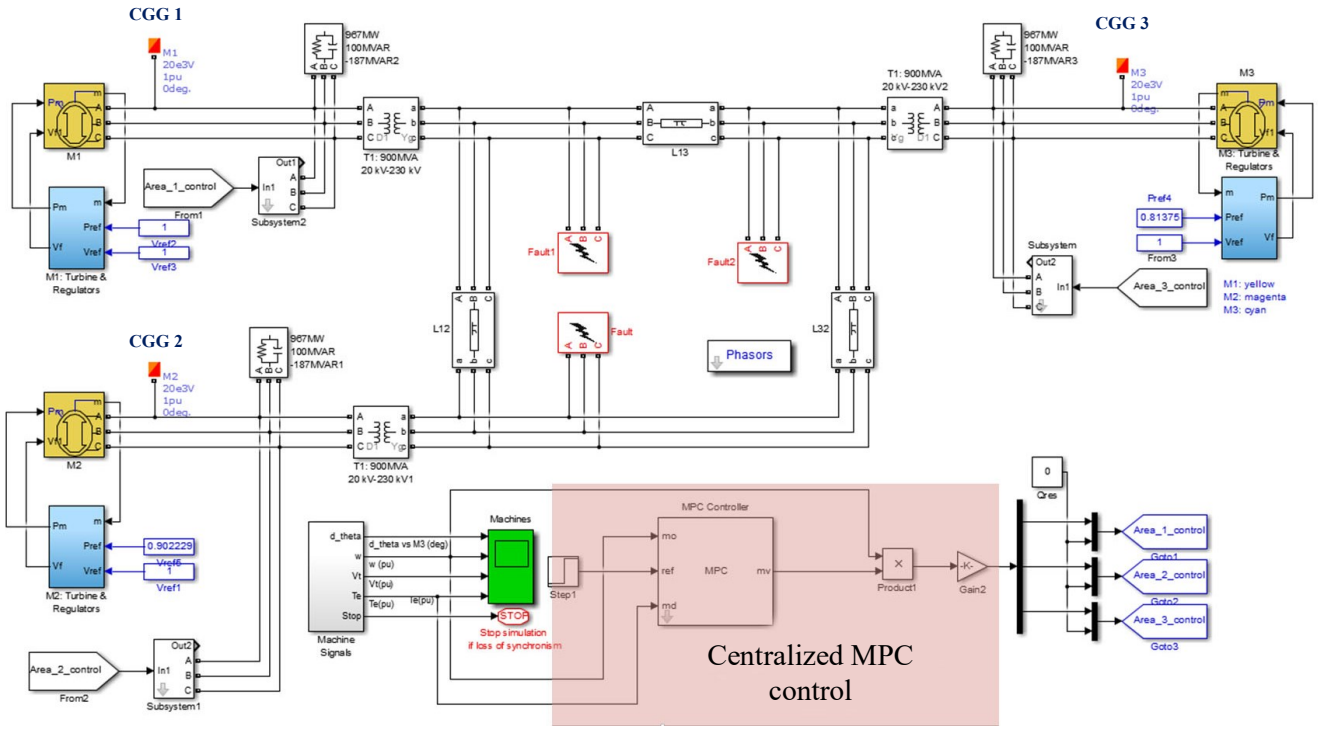

Fig.3.21. 3-machine EPS model with centralized MPC control

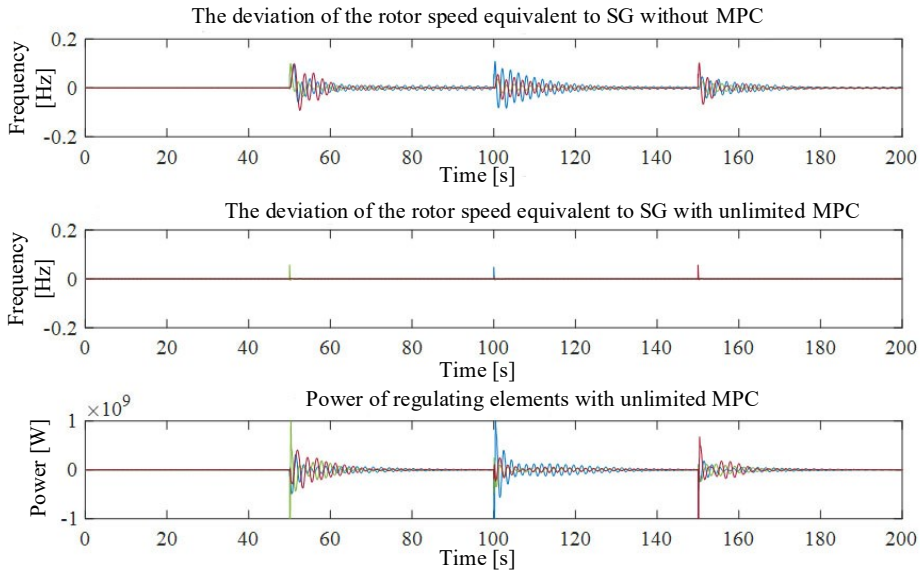

Fig.3.22. The results of calculation of transient frequency change during MPC control

Using MPC-based approach makes the imposition of restrictions on the registration time characteristics of disturbances, formation and implementation of executive decisions. In the process of EPS frequency control during transients subsystem communications and calculations must satisfy certain time criteria to work in real time.

Real-time mode defines the system, the efficiency of which depends not only on the logical correctness, but also on the time required to obtain results. Definition of the system in a hard real-time deterministic value provides response time, but does not impose limits on the absolute value - it can be a millisecond or weeks.

For the problem with 10 variables and 100 constraints execution convex optimization using the example code MatlabQPsolver (quadprog) on a PC with a frequency of 2GHz single-core processor takes about 10ms. Commercialization of quadratic programming perform the same task with a time less than 1 ms [95].

The actual problem is suboptimal efficiency of EPS frequency control during transients based on actual operational and technological constraints. Particular attention should be paid to the impact of delays in the channels of information transmission and reliability of synchronized WAMS measurements the stability and control quality.

3.3.3 Research of centralized frequency control with subject to the limitations

The main problem using linear-quadratic regulator is lack of possibility of consideration of physical and technological constraints that are inherent EPS. It should be noted limits of the ability to change over time. The main constraints which must MPC held are as follows:

- output values:

1) limitations on the size of available reserves of power (virtual power plants);

2) limitations on the rate of change of power;

- input values

1) limitations on the maximum frequency deviation;

2) restrictions on the maximum rate of change of frequency;

3) restrictions on the size of load mutual angle (δ_{ij}) between CGG.

Used subspace identification approach that forms the "black box" model prevents interpretation of the parameters of the model in the form of state variables as physical characteristics. The MPC restrictions can be formalized for incoming, outgoing and modal characteristics of the object of control. Because of this, operating parameters that are crucial should be reflected at the output of the identified system. If necessary to perform multi-criteria optimization or limit the range of variation of operational parameters during transient model of the system should allow the calculation of all operational parameters that are restricted and participating in the formation of process quality criteria.

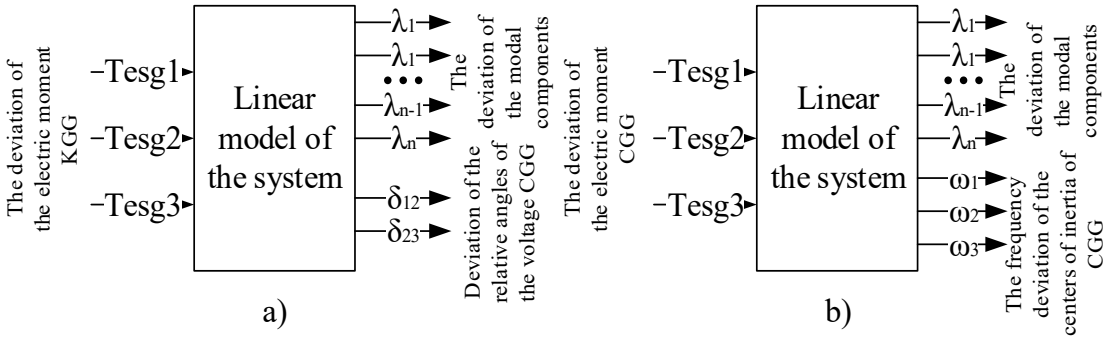

Fig.3.23. The structure of the EPS model with restrictions on mutual CGG angles (a) with restrictions on CGG center of mass frequency deviation (b)

In further research approach based on individual components compensation supplemented by modal characteristic of the EPS regime parameters whose values determines the quality of the system.

- limatations on the CGG frequency deviation

  Quality of EPS frequency is considered satisfactory if:

  - overnight [96] total duration frequency deviations from nominal ± 0,2Hz not exceed 5%, and the deviation ± 0,4 Hz absent;
- In one month, the standard deviation for 90 and 99% interval measurement should not exceed 0.04 and 0.06 Hz, respectively.

In particular, has ensured the maintenance of the current frequency between 50 Hz ± 0,05 (normal level) and within 50 ± 0,2 Hz (permissible level) to restore normal specified frequency levels and power flows of total external areas of regulation time; no more than 15 minutes to agree with the proposed frequency

deviations inventory capacity of the EPS transit network in normal conditions. Besides supporting frequencies within prescribed limits is due to the requirements to ensure static stability.

Using MPC to meet the requirements of GOST 13109 realized by imposing restrictions on the range of variation in the output system (frequency deviation from the nominal value). The results of calculation of system transient frequency change (Fig.3.24) showed the effectiveness of MPC frequency control during transient with constrains on the range of CGG frequency variation.

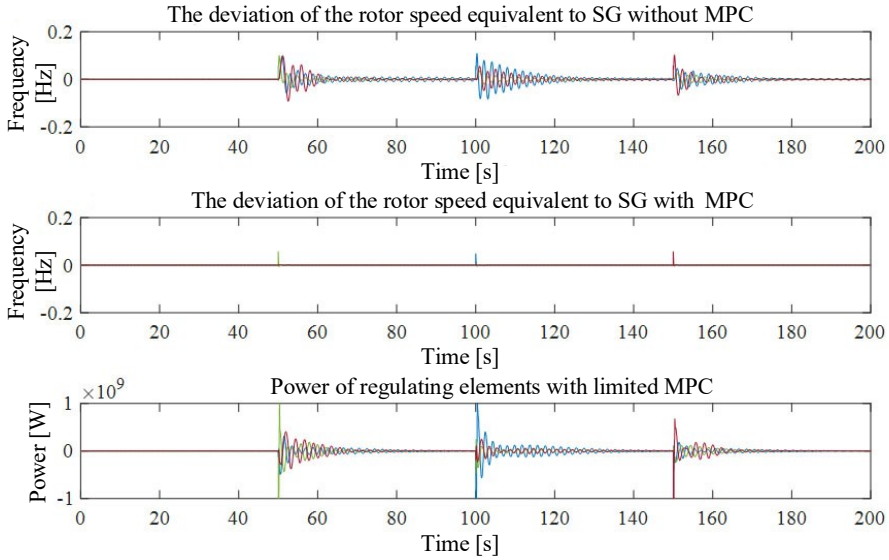

Fig. 3.24. The results of calculation of transient EPS frequency change (restrictions imposed on the CGG absolute frequency deviation)

- restrictions on mutual CGG loading angles deviation

The main parameters that determine the stability criteria are EPS static and dynamic stability margins. Past studies [97] have shown the need for additional control to maintain system stability. Moreover, the relevance of preserving the stability of the system with a significant share of renewables in the energy caused by the tendency to reduce rotating inertia of the EPS, which reduces the dynamic stability margins. Usage-based approach allows MPC to limit the range of variation of individual outputs of the system. One of the major operational parameters that determine the stability of EPS is mutual voltage angle between the EPS equivalent generators (CGG).

The results of calculation of system transient frequency change (Fig. 3.24) showed the effectiveness of MPC frequency control during transient states with limits on the range of variation of mutual CGG load angles. Along with dynamic stability control, static stability angle controlled on a similar principle limitations. The problem of controlling static stability voltage should be decided locally by regional regulator or a virtual power plant.

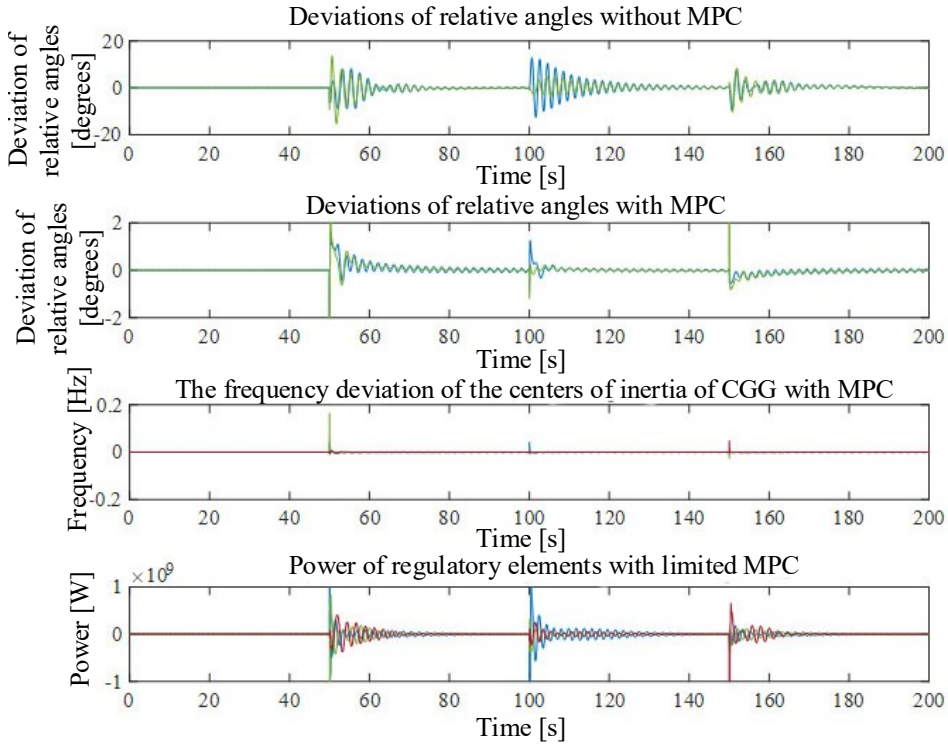

Fig.3.25. The results of calculation of CGG transient frequency change and control power means with limited MPC (restrictions imposed on the deviation of the relative voltage angle between CGG)

- restrictions on the size and speed of loading and unloading means

Renewable energy reserves provided by RES optimal functioning regime change or by limiting station generating. The decision on allocation of the power stations in the provision adopted by regional regulator by calculating scenarios of issuance of additional reserve capacity while preserving quality and stability of electric energy. Given the shortage of power reserves, especially fast RES reserves allocated for providing virtual inertia takes into account the limits on the size and speed of loading and unloading controls. Analysis of calculation of system

transient frequency change (Fig.3.26) showed MPC frequency control efficiency during transient states with restrictions on size of control actions. The results suggest the need to develop ways to ensure "fast" reserve capacity the use of which is essential for improving the efficiency of EPS frequency control. The basis for the provision of operational reserves that can be used in the regulatory process can be energy storages based on rotating masses, supercapacitors, batteries of electric vehicles, and others.

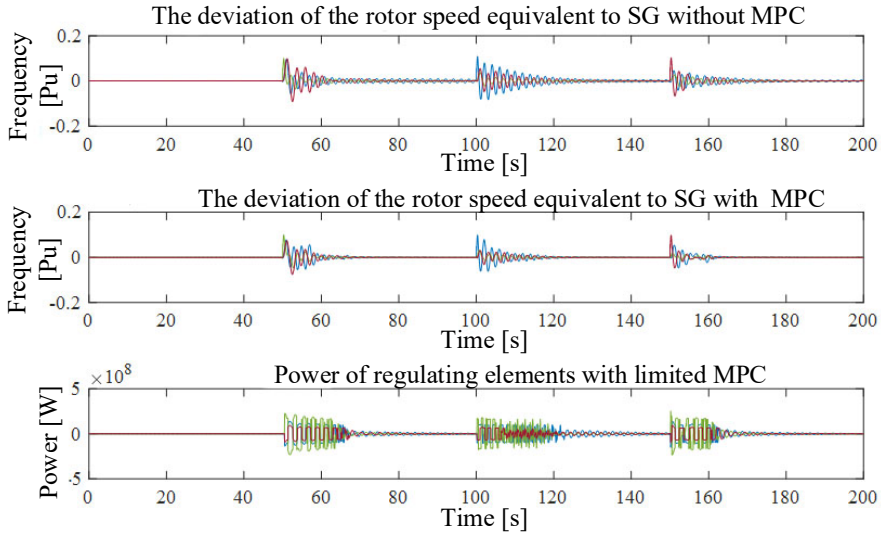

Fig. 3.26. The results of calculation of CGG transient frequency change and power regulators with MPC control (restrictions imposed by the amount of reserve power to exercise control)

One promising technology is the development of consumer-regulators that are able to address and quickly (usually discrete) apply power control in the direction of loading and unloading.

Analysis of EPS frequency control with limits on speed of power reserve change (Fig. 3.27-3.28) points to the importance of engaging fast governing actions in transient conditions.

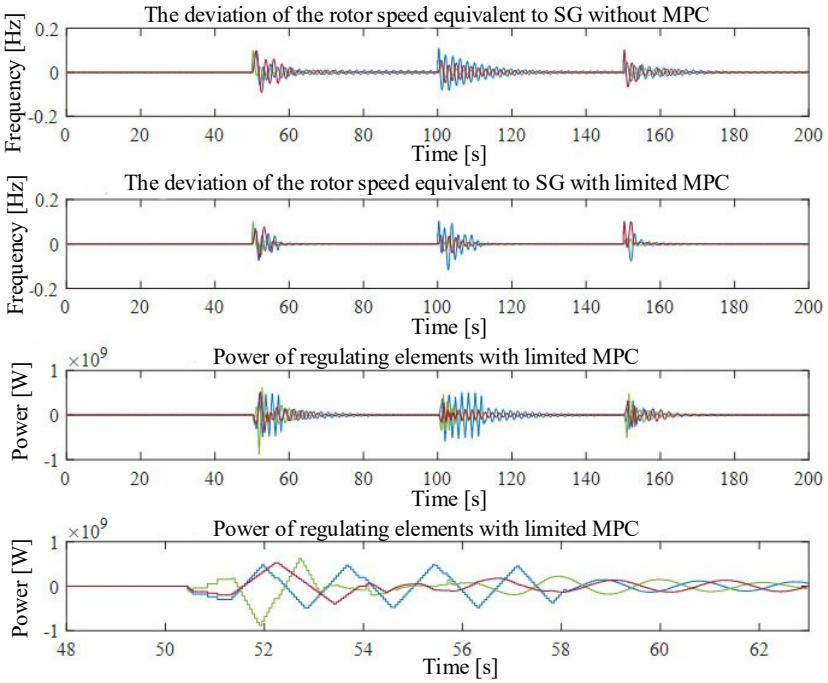

Fig.3.27. Calculation of EPS transient frequency change and power means with constrained MPC (restrictions imposed on the value of the rate of change of power reserves - 200MW / s)

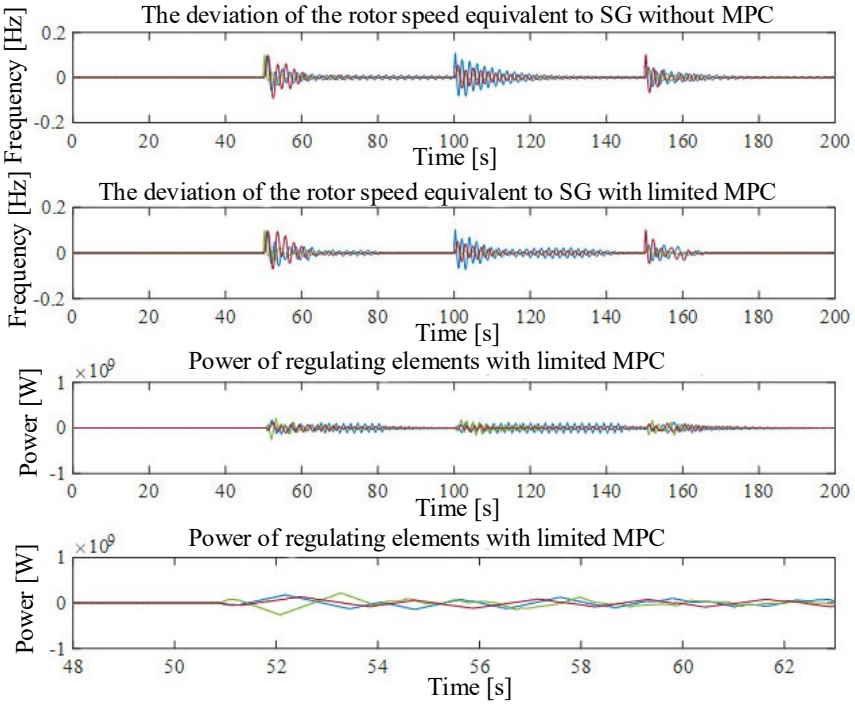

Fig.3.28. Calculation of EPS transient frequency change and power means with constrained MPC (restrictions imposed on the value of the rate of change of power reserves - 1MW/s)

With insufficient speed of power reserves regulator not activating slow reserves due to the inefficiencies in the use of transient modes. Set aside in reserve capacities is not used, which reduces the efficiency of the developed system as a whole. Thus the speed of loading and unloading of CGG reserves is one of the main factors that determine the efficiency of EPS frequency control during transients.

4. CREATING OF MICROGRIDS TO ENSURE THE RELIABILITY OF POWER SUPPLY OF ENTERPRISES

In the annual report on the performance of the National Commission for State Regulation in the Energy and Public Utilities Regulations for 2018 stated that the main indicators of reliability of electricity supply to electricity distribution companies: System Average Interruption Duration Index (SAIDI) - decreased by 4,4%, and the estimated Energy Not Suppliedy (ENS) decreased compared to 2017, as shown in Fig. 4.1, which provides statistics for recent years [98].

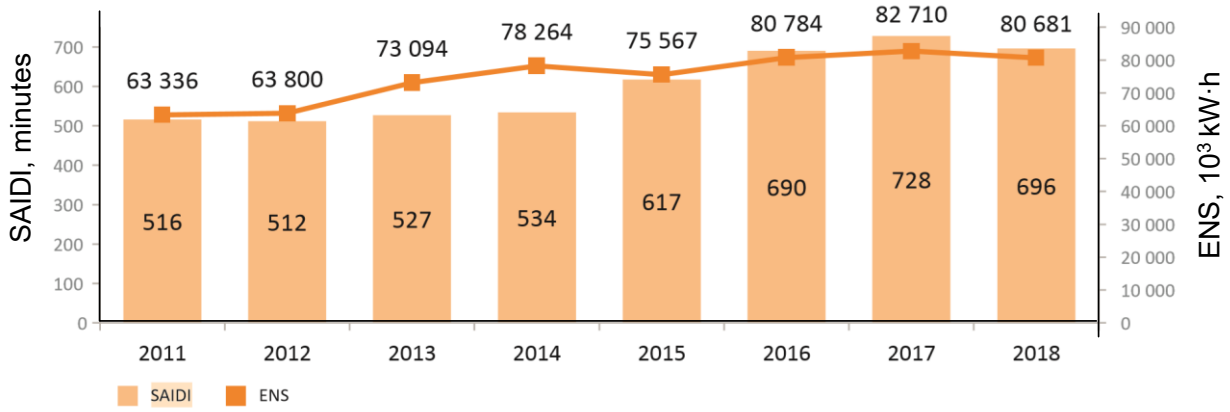

Fig. 4.1. Dynamics of SAIDI and ENS indicators for 2011-2018

SAIDI indicators in Ukraine are much higher than in EU countries. This is due also to the fact that the EU is not only monitoring the indicators of reliability of electricity, but also their regulation [98].

4.1 Development of promising means and methods for efficient control of microgrids based on distributed energy sources

Two methods of controlling the parameters of normal modes of microgrids with distributed energy sources are considered. The first method is based on the online monitoring of values of active and reactive power and the implementation

of control effects when deviating their values from the optimum, and the second method of control is based on the online monitoring of values of voltage and frequency and the implementation of control effects when deviating their values from the nominal. For the amplitude value of voltage and frequency, the magnitude of the deviation of the current value from the nominal influences the optimum value of the currents in the branches, therefore, the distribution energy source (DES) must have the appropriate operational characteristics and allow the operation of microgrid (MG) in both modes, by constantly monitoring this deviation [99-101].

In isolated operation, the problem of ensuring the nominal value of frequency and voltage and MG is solved with the help of DES, but taking into account the correction coefficients that depend on the power of DES and by which the value of deviation of frequency and voltage is adjusted. In the mode when the MG is connected to the centralized electrical distribution network, the deviation factor is set to zero to eliminate the effect of power losses and calculation error, as well as to provide the required load power.

MG can operate in the "island" mode, autonomously from the district's electrical distribution networks (EDN), or in the "connection" mode, ie some of the electricity is taken from the EDN, and the transient connection mode or disconnection from the EDN can be separated.

Over the last few years, distributed generation has become increasingly popular due to its benefits such as energy conservation, environmental protection and others. But the existing methods of optimal control of the parameters of the normal modes of power systems are difficult to adapt to networks with a large number of RES, so the technology of creating MG, is an effective way to solve this problem. MG is a low-voltage distribution network consisting of several RESs, energy accumulators and loads, and the micro-network can operate in two modes. In connection mode, MG is connected to a centralized electrical distribution network; in isolated mode - MG is disconnected from the centralized electrical

distribution network, and the mode of smooth transition of MG from one mode to another.

The optimal mode of operation of MG depends on a reliable control system, so it is necessary to improve the algorithms for controlling the parameters of the microwave mode.

Most RESs are connected to the MG through inverters, so optimal inverter control will ensure stable and efficient operation of the MG as a whole.

There are different operational requirements for RESs for the two MG modes. In the mode, when the microgrid is connected to the centralized electrical network (EN), the nominal voltage and frequency are provided by means of the centralized EN. If the RES is equivalent to a current source, in order to achieve the optimum value of active and reactive power flows in isolated mode, it is necessary to have a powerful EN that will be able to maintain the frequency and voltage values at the required level and guarantee power generation for consumers. If RES is equivalent to a voltage source, it is better not to control the power and frequency, but the frequency and voltage [102-105].

The scheme of RES in the microgrid is shown in Fig. 4.2.

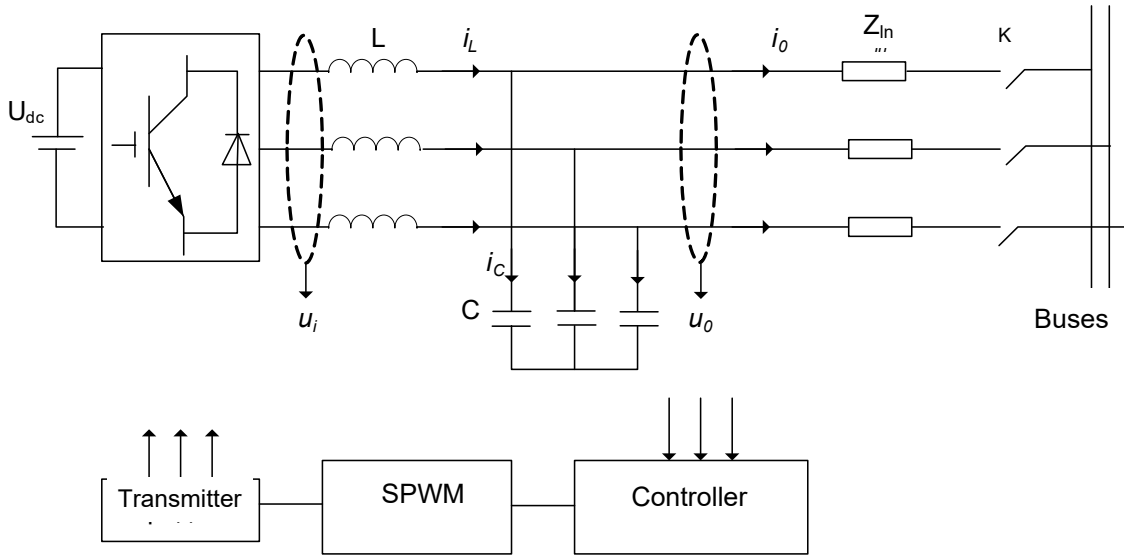

Fig. 4.2. The scheme of RES in the microgrid

The diagram uses the following notation: U_{dc} - DC voltage; L, C - filters; Z_{ln} - line resistance; u_i, u_0 are respectively the output voltage of the inverter bridge and the output voltage on the capacitor; I_L, I_C, i_0 are respectively the current of the inductor, the capacitive current and the output current of the RES. The controller is the core of the entire control system, defines the mode of operation of the RES.

A typical control unit, the scheme of which is shown in Fig. 4.3., is operated on an algorithm that implements a control method, which controls the values of active and reactive power and controls when deviating their values from the optimal ones, P*, Q* - values of active and reactive power, respectively; uref is the output voltage regulator after signal modulation; SPWM is a device for sinusoidal pulse width modulation. Only the inductance current enables effective control of the entire process. The main purpose of measuring the voltage at the output u0 is to obtain the values of the amplitude, frequency and phase of the voltage MG. This information is required for synchronization with the distribution network. RES, while adopting active and reactive power control mode, cannot be frequency and voltage based, but it can provide the required power value, which is why this control method is better proven when the microgrid is connected to a centralized power system circuit.

The controller circuit for the frequency and voltage deviation control mode is shown in Fig. 4.4. Unlike the previous method, this method does not require connection to the electrical distribution networks, and the output voltage and frequency is controlled directly by the controller itself and depends only on the RES. Low voltage power lines can be attributed to networks with predominantly active resistance. The difference between the phase (angle) of voltage on the RES and the bus bars is negligible, so the P and Q values are affected only by the difference in the amplitude values at the beginning and end of the line. The reactive power depends more on the phase (angle) change, so the equations underlying the control algorithm can be written as [105]:

$$\begin{cases} f^* = f_n + m(Q - Q_n) \\ U^* = U_n - n(P - P_n) \end{cases} \quad (4.1)$$

where f_n and U_n are the current frequency values and voltage amplitude; P_n and Q_n are the current values of active and reactive power (on buses) of RES; m and n are the coefficients of correspondence, frequency and voltage amplitude; f* and U* are calculated values of frequency and voltage that satisfy the steady state mode of the microgrid.

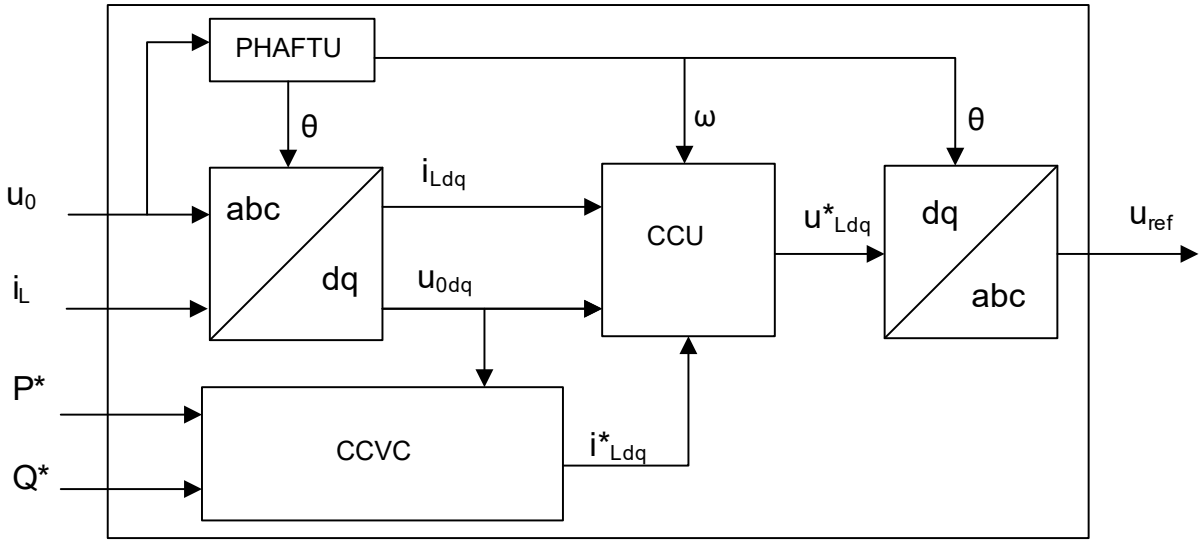

Fig. 4.3. P/Q controller block-scheme: PHAFTU - phase auto frequency tuning unit; CCVC - calculation of current value of current; CCU - current control unit.

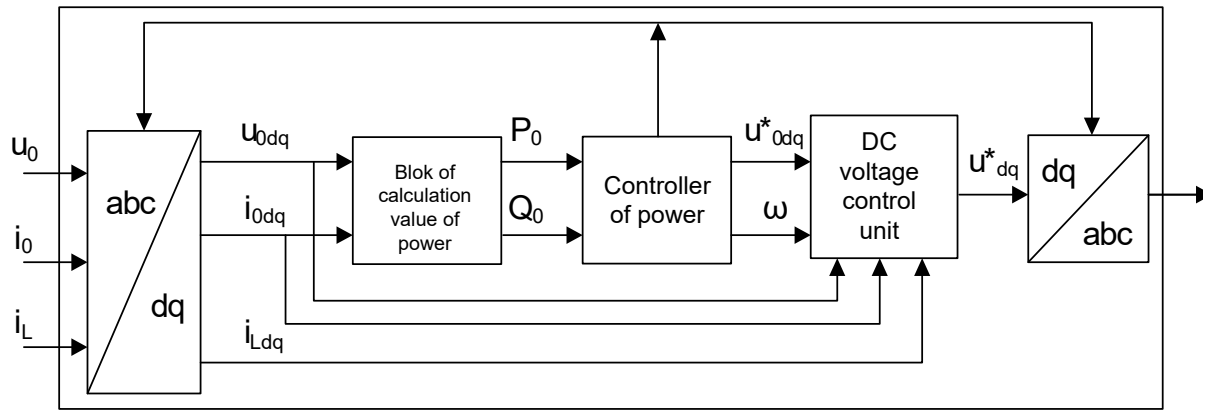

Fig. 4.4. Controller U/f block-scheme.

The advantage of controlling the frequency and amplitude of the voltage lies in the fact that the power of the RES changes in proportion to the change of *f* and *U* without switching to "island" mode. To this end, we introduce the coefficients *m* and n: in order to satisfy the following conditions: $m_1Sn_1 = m_2Sn_2 = \ldots = m_xSn_x$; $n_1Sn_1 = n_2Sn_2 = \ldots = n_xSn_x$, where Sn is the power of the RES;

The output power on the RES tires is determined by the formulas:

$$\begin{cases} Q = \dfrac{f - f_n}{m} + Q_n \\ P = \dfrac{U - U_n}{-n} + P_n \end{cases} \tag{4.2}$$

From equation (4.2), it can be concluded that the frequency and amplitude control method is more adapted to the mode in which the MG is connected to a centralized distribution EDN, since in order to use the RES as a frequency and voltage reference node, one must make sure that that on RES tires $f = f_{nom}$; $U = U_{nom}$, but now the value of voltage and frequency is set by the centralized distribution EDN and there are deviations and errors, which make it difficult to accurately control the output power of the RES.

It is possible to control the active and reactive power by changing the instantaneous value of the current, namely its transverse component, using the transformer.

The diagram of the microelectric network is shown in Fig. 4.5.

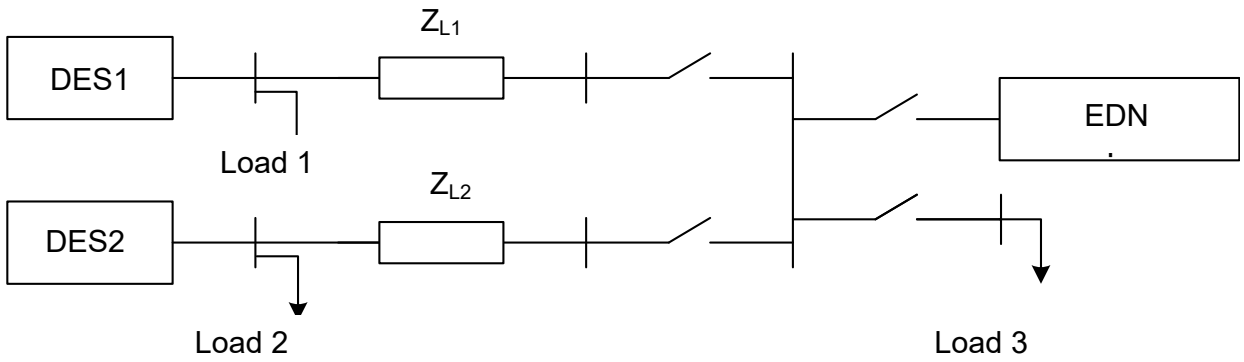

Fig. 4.5 Scheme MG

If the direction of the axis d (that is, the longitudinal component of the current) coincides with the voltage direction, then a simplified expression for determining P and Q between the current and voltage can be written as:

$$\begin{cases} P = u_d i_d \\ Q = -u_d i_q \end{cases} \tag{4.3}$$

where P is the active power; Q - reactive power; u_d - longitudinal component of voltage; i_q - transverse component of current; i_d - the longitudinal component of the current.

The output power on the RES tires is determined by the formulas:

$$\begin{cases} Q = \dfrac{f - f_n}{m} + Q_n \\ P = \dfrac{U - U_n}{-n} + P_n \end{cases} \tag{4.4}$$

Substituting expression (4.1) into expression (4.2) after transformations we obtain:

$$\begin{cases} i_{qn} + \dfrac{f_n - f}{mu_d} - i_q = 0 \\ i_{qn} + \dfrac{U_n - U}{mu_d} - i_d = 0 \end{cases} \tag{4.5}$$

Where f_n and U_n are the current values of voltage frequency and amplitude; P_n and Q_n are the current values of active and reactive power (on buses) of RES; m and n are the coefficients of conformity; f_i and U are nominal values of frequency and voltage amplitude; i_{qn} and i_{dn} - the current values of the transverse and longitudinal components of the current, respectively, they can be calculated through the current values of the active and reactive power; i_q and i_d - the value of the transverse and longitudinal components of the output current; u_d - is the value of the longitudinal component of the output voltage.

After entering the notation $K_m = \dfrac{1}{(mu_d)}$; $K_n = \dfrac{1}{(nu_d)}$; $\Delta f = f_n - f$; $\Delta U = U_n - U$, the system of equations (2.3) is written as:

$$\begin{cases} (i_{qn} + K_m \Delta f) - i_q = 0 \\ (i_{dn} + K_m \Delta U) - i_d = 0 \end{cases} \quad (2.6)$$

When the control of the parameters of the normal mode of operation of the microgrid is carried out by frequency and voltage deviation, then equation (2.4) should be applied in the control algorithms. If the active and reactive power control method is used, then equation (2.7) applies:

$$\begin{cases} i_{qn} - i_q = 0 \\ i_{dn} - i_d = 0 \end{cases} \quad (2.7)$$

The method of controlling the parameters of the normal mode of the microgrid on the deviation of frequency and voltage amplitude is equivalent to the method of "constant power control", in which there is a deviation of the frequency and amplitude from the nominal values at the passage of current ("Equivalent current"). The block diagram that implements this control method is shown in Fig. 4.6.

Based on the use of equation control algorithms [106-108]:

$$\begin{cases} f^* = (K_{p1} + \frac{K_{i1}}{S})[(i_{qn} + K_m \Delta f) - i_q] \\ U^* = (K_{p2} + \frac{K_{i2}}{S})[(i_{dn} + K_n \Delta f) - i_d] \end{cases} \quad (2.8)$$

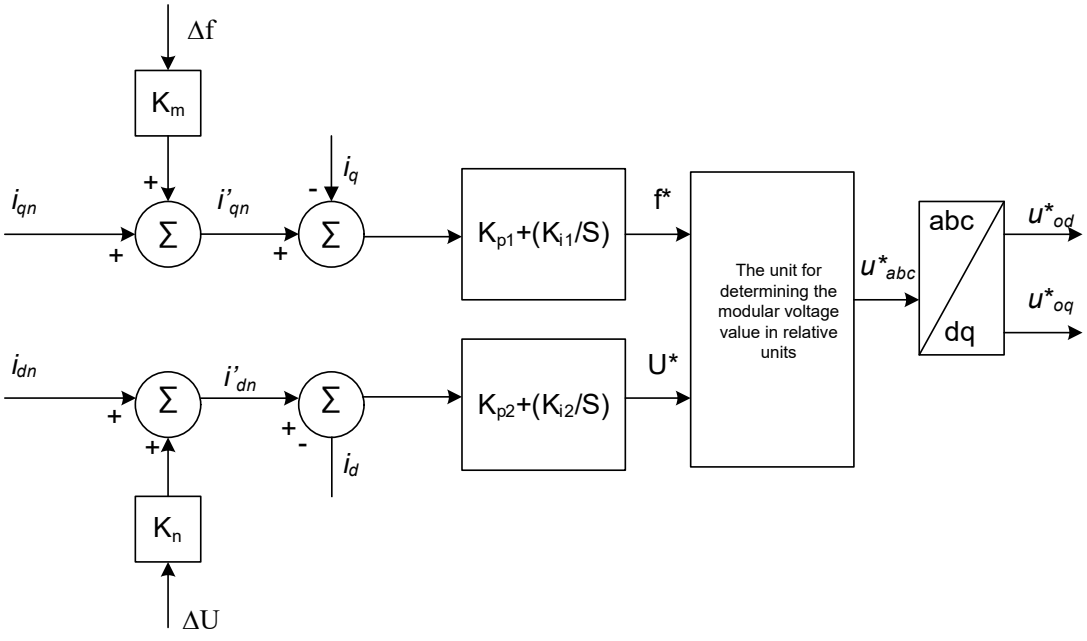

Fig. 4.6. Control unit diagram

The diagram of the control unit is shown in fig. 4.6, where: i_{dn} and i_{qn} are the values of the longitudinal and transverse current components, which are determined by the basic power value, and shownn and i_{qn} are the specified values of the longitudinal and transverse current components, taking into account the deviation of the amplitude value of voltage and frequency, respectively. Then the received signal is compared with the output current, as in the method of control for active and reactive power. As a result of comparison, the deviation of the values of the components of the current is determined, and the signal containing this information enters the PI controller, at the output of which there are calculated values of the frequency and voltage in the units f* and U*, which satisfy the established mode of operation of the microgrids.

4.2. Establishment of industrial microgrids using alternative energy sources

The experience of foreign countries and the possibility of its adaptation for Ukraine in the creation of the concept of microgrids are investigated. A unique feature of these networks is that they can use locally available resources, ie dispersed energy sources such as solar energy, wind, water flow and biomass to generate electricity. In order to evaluate the possibility of using microgrids, it is necessary to estimate the current electricity consumption and the future demand for it. Based on this you need to structure your power consumption within 24 hours. Such analysis can identify energy consumption and analyze available local energy resources. There is already a positive experience in the use of micro-networks in the Himalayas. A village has been selected to create a grid that has different resources for generating electricity, and looks at different configurations of the grid, so the information presented in this article will be useful for designing grids for remote locations in countries characterized by unstable power supply.

The use of dispersed energy sources for the creation of microgrids always faces the problems of energy storage and the seasonality of its generation. One of the ways to solve these problems is to use mini-thermal power plants.

In the future, on the basis of the gas-fired boiler, it is planned to implement a mini-CHP, the block diagram of which is presented in Fig. 4.9 [109].

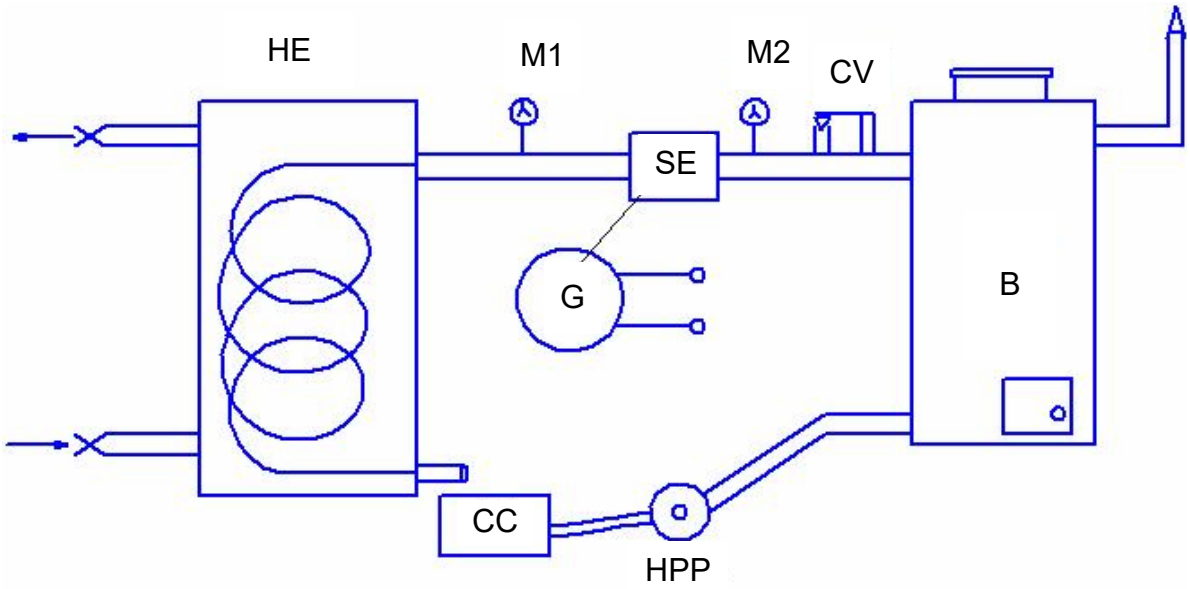

Fig. 4.9. Mini-CHP scheme: B - boiler; CV - check valve; M - manometer; SE - steam engine; G - generator; HE - heat exchanger; CC - condensate collection; HPP - the high pressure pump.

In order for the mini-CHP to pay for itself quickly, it is possible to use a gas-fired boiler of an improved structure.

According to the International Energy Agency (IEA): access to electricity is an integral part of the sustainable development of mankind, and according to the latest figures, by 2011, 1.6 billion people, or more than 20%, did not have access to electricity. Poor countries and even developing country regions may find themselves in a zone of poverty, social instability and low levels of development if they do not have access to modern commercial energy sources.

The Human Development Index is directly linked to the Electricity Development Index, which has been proven over a long period of time given the state of development of different countries in southern Asia and sub-Saharan

Africa. A similar case was found in remote areas of the Himalayas, although people have access to electricity, but this electricity has poor quality indicators and possible interruptions in its supply. Often renewables have an isolated and decentralized nature, forcing the offgrid control unit to be built and to meet local electricity needs in a decentralized manner. This decentralized system is called a distributed power generation system, that is, electricity is generated from local renewable energy and can be used to meet the needs of a particular type (cluster) of loads. The microgrid may include the generation of more than one type of distributed energy source, depending on the availability of various renewable resources to provide a stable and reliable energy supply to local loads. The micro-network can operate either in islanded mode or in parallel with the network. Installing renewable energy sources on a micro-grid in rural or small-scale industries will help reduce dependence on the quality and reliability of distribution networks, and also avoid the loss of electricity associated with transmission and distribution. It is possible to develop hybrid microgrids with locally available renewable energy sources that can be easily installed in these areas and to provide reliable power supply.

This will increase the standard of living and development of the agro-industrial complex, as electricity will be permanent, even in the absence of basic infrastructure such as roads, water, sewerage and communication. Many such studies have already been done and considered the energy potential of almost all countries in the world. The advantages of the proposed microgrids are the possibility of autonomous power supply and almost complete rejection of the centralized power supply. The concept of creating Vizaghapatnam (Vizag) microgrids has already been used in the Andhra Pradesh district to generate power from renewable sources [110].

A microgrid has been developed that contains several sources of generation, at least one of which is renewable and the other allows to accumulate energy for a certain time. The results of this study make it clear that the solar panel market is growing due to India's climatic conditions. Conducting research, it is possible to

predict an increase in the number of panels installed for the microgrids, but depending on the climatic conditions, it is proposed to use small hydropower plants, hydroelectric power plants, biogas plants and even diesel generators, and only a complex combination of them makes it possible to provide inaccessible regions of the country with electricity [110].

In Ukraine, the situation with power supply is not much better, the main problem is emergency shutdowns or poor quality of electricity, which are caused by low rates of renewal of electrical equipment of substations and transmission lines. Creating micro-networks can also be a solution to many problems. It may be financially advantageous to create microgrids for agro-industrial enterprises, whose capacities are generally more expedient to be located closer to the raw material bases, and therefore further away from high-quality power supply.

4.3 Improvement of the gas generator boiler structure

The essence of the proposed gas-fired boiler is explained in Fig. 4.10, which shows a diagram of a gas-fired solid fuel boiler [109].

The principle of operation and structure of the proposed gas-fired boiler is to burn the gas at once at the outlet of the gasification zone and to deliver thermal energy to the heat-transfer medium located directly in the housing of the gas-fired solid-fuel boiler consisting of a boiler, elongated tufts, annular manifold, tuyere directed upwards at an angle of 6… 8 ° to the horizontal, at the outlet of the gas-generating chamber a gas-air mixer nozzle with air is lined combustion measure, the tubular heat exchanger is immersed in a water jacket and connected to the chimney, the regulation of the combustion process is performed by the flaps in the primary and secondary air tubes, the air is inflated and the coolant temperature is maintained by adjusting the fan speed. The gas-fired solid fuel boiler works as follows. The fuel hopper 2 is loaded through the loading air-tight manhole 3 and closed. We burn the fuel through the ignition hatch 11, while opening the self-propeller valve 5, close the self-propeller valve 5 and the ignition hatch 11 after the fuel ignition, and turn on the fan 16.

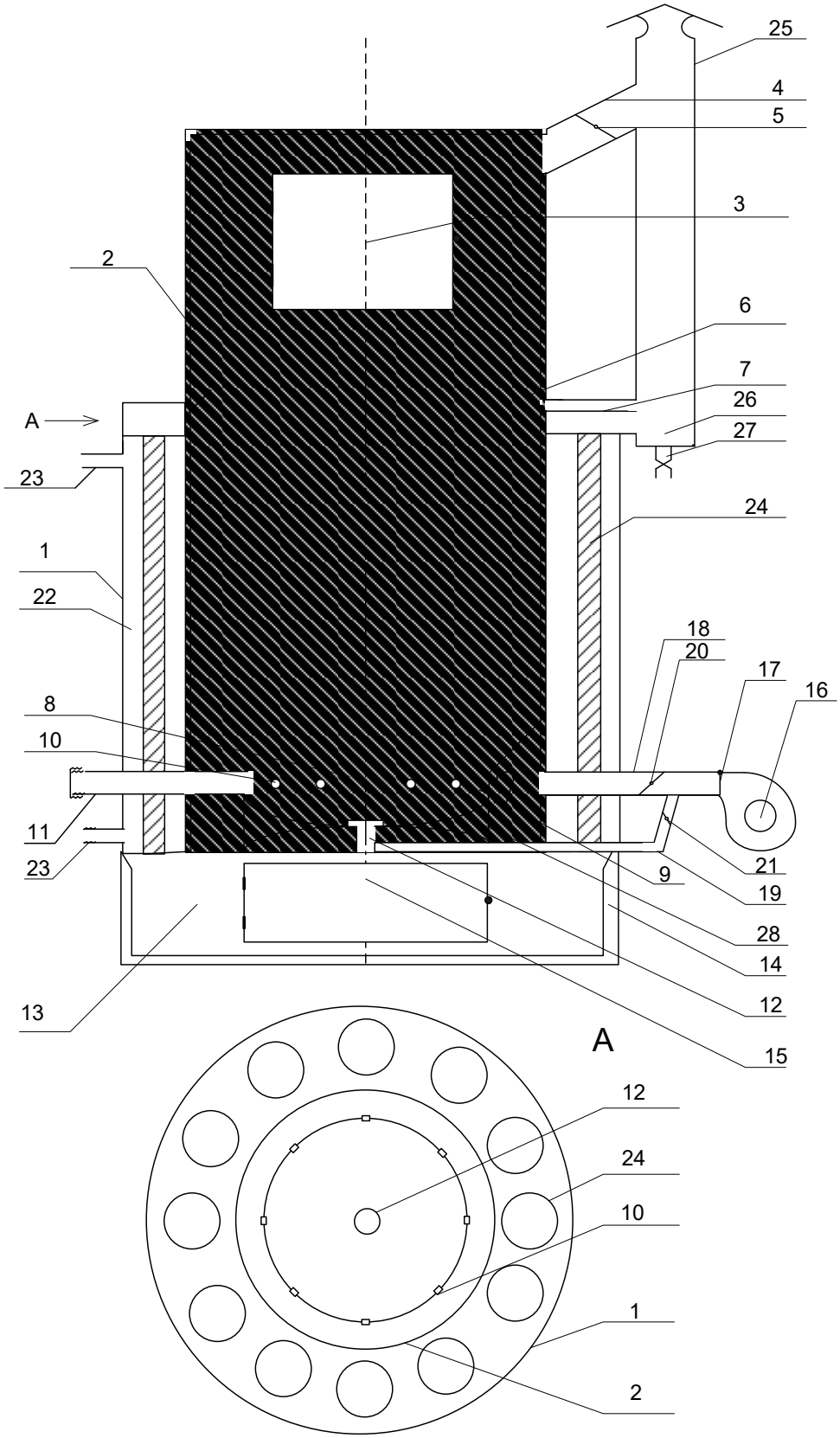

Fig. 4.10. The structure of the gas-fired boiler: 1 - the housing; 2 - the fuel hopper, 3 - the loading airtight hatch; 4 - the gravity pipe; 5 - the gravity damper; 6 - the condensate chute; 7 - the condensate discharge tube; 8 - the gasification chamber;

9 - air collector; 10 – tuyere; 11 - hatch of ignition; 12 - nozzles of the mixer; 13 - combustion chamber; 13, 14 - lining of walls; 15 - hatch of cleaning; 16 – fan; 17 - backpressure valve; 18 - primary air supply tubes and 19 - secondary air tubes; 20 and 21 - regulating flaps; 22 - coolant; 23 - hot water outlet pipes; 24 - heat exchanger tubes; 25 – chimney; 26 - condensate collection; 27 - drain tap; 28 - refractory bottom.

Through the cleaning hatch 15, we observe the normal operation of the boiler and regulate the primary and secondary air supply. complete combustion of gas, the indicator of which is the color of the flame in the combustion chamber 13. If the flame is red, then the gas burns in incomplete volume and this indicates that you need to reduce the supply of primary air other primary air supply 20 and increase the secondary air supply by the shutter 21 until a blueish flame is reached. Close the cleaning hatch 15 and heat the water. The fuel condensate chute 6 collects the evaporated fuel and condensed at the top of the moisture and through the condensate outlet 7, which makes the boiler more efficient and allows the use of wetter fuel.

The design solutions of the developed gas-fired solid fuel boiler allow to reduce the dimensions, metal consumption and make it possible to use not only dry fuel but also wet fuel.

Appearance and performance of the experimental sample.

In Fig. 4.11 In Fig. 4.12 shows a car gas generator, which is a prototype of the developed gas generator boiler. In Fig. 4.13 In Fig. 4.14 shows the appearance of an experimental gas-fired boiler, which was made according to an advanced scheme.

Fig. 4.11. Car gas generator

Fig. 4.12 Pilot of gas-fired boiler

In Fig. 4.13-4.14 presents some elements of gas-fired boiler:

Fig. 4.13. Appearance

Fig. 4.14. Fan and controls

Existing gas-fired industrial boilers are currently quite expensive for the average consumer (population and small business). Their cost exceeds 12 thousand UAH. for a boiler with a capacity of 10 kW. Therefore, the urgent task is to create an advanced gas-fired boiler with lower cost, which is possible on the basis of simplification of construction and reduction of the cost of its manufacture. Experimental studies have shown that burning 3-5 kg of solid wood allows to heat and bring to a boil 180 liters of water for 2 hours. In heating mode, this boiler burns from 40 kg to 60 kg of solid wood per day for space heating with an area of 200 m2. Fuel consumption depends on the ambient temperature. In the proposed boiler can be burned household waste: polymers, plastics, rubber, etc., with minimal pollution.

4.4. Analysis of electricity generation efficiency based on solar energy in Vinnitsa region

Therefore, research in the field of increasing the reliability of electricity supply to agribusiness enterprises by high-quality electricity from renewable energy sources is relevant. If in Ukraine now about 1% of electricity is produced by renewable sources, then in Podillya, and in particular in Vinnytsia region it is no longer produced 1%, but 8-9% of electricity is mainly solar plants. The integration of renewables into our electrical system and their application to the heat and power supply of powerful agricultural complexes is the subject of our research because existing electrical systems were designed at a time when renewable energy sources were unpopular. Therefore, there are a number of technical problems, namely the reconciliation of the operation of outdated electricity grids, which feed agricultural enterprises with the modes of operation of renewable energy sources. Nowadays, the adaptation of renewable energy sources to economic and market conditions, and purely technical ones, is urgent. Creating an enabling environment for solar power plant (SPP) development requires a number of technical and organizational challenges.

The parameters of the required solar installation with batteries for a one-room apartment with a total energy consumption of 115 W/h without the consumption of electricity for heating for the climatic conditions of Vinnytsia region were calculated in the work. Considering that the life of an autonomous solar power plant is 10-15 years, and the batteries included in its composition - up to 5 years, switching to an autonomous power system in the scale of one apartment or house is unjustified because the payback period was 10,5 years.

And if you add to this the cost of repair and operation, then these costs will increase. Generally, it is advisable to install SPP where centralized power supply is impossible or unreliable.

Authors of Stamatia Gkiala Fikari, Sara Ghaem Sigarchian, Harold R. Chamorro stated that autonomous hybrid power systems, combined with renewable

energy sources and energy storage, can have a significant impact on the quality of life in developing countries. Connecting to a mains power supply is not always appropriate and reliable, preventing locals from accessing services that affect their activities, health, well-being, education and financial development. The idea of creating a standalone hybrid remote energy system for a remote settlement of about 100 residents in Kenya is explored to explore its potential and evaluate the operating strategy chosen in terms of efficiency and reliability of customer service. An autonomous hybrid power system is believed to electrify a village near Garnish, Kenya. In Fig. 4.15 shows a diagram of a hybrid stand-alone grid with dispersed energy sources (wind farm, solar power plant and diesel generator).

There are also villages in Ukraine with an actual small population, such as the village. Doctors of Perechyn district (Transcarpathia), Buryany - a village in the Haysyn district of Vinnytsia region with a population of 105 people, Burdy - a village in the Tulchyn district of Vinnytsia region, with a population of 40, and others.

The introduction of proven models of electricity supply for this type of consumers with adjustments that take into account the climatic features of the terrain and load schedules of consumers, and reduce the cases of damage or inefficient operation of the SPP, will yield a positive result.

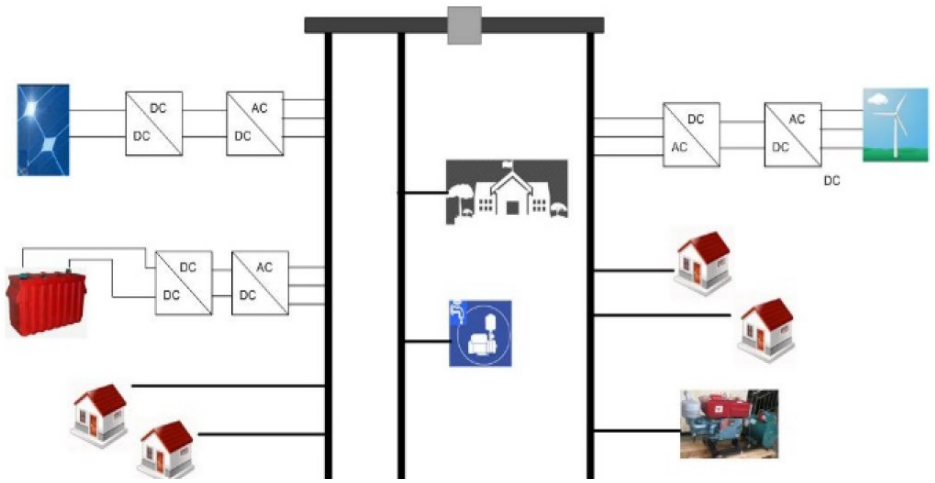

Fig. 4.15. Diagram of a hybrid autonomous grid with dispersed energy sources (wind farm, solar power plant and biofuel diesel generator) and consumers in the form of domestic sector, water treatment plant and school.

Therefore, the study of solar power plants in the Vinnitsa region is relevant. Already installed solar panels in the Vinnytsia region are generally privately owned, so not every landlord will allow them to do research.

All this is possible in the presence of a solar panel in the laboratory. Currently, the capacity of the solar panel is sufficient to provide LED illumination of the corridor 2 floors 3 of the educational building of Vinnitsa National Agrarian University, and plans to connect the information board. Type of solar panel TALESUN TP-660P-260.

The appearance of the solar panel and the location of the installation and connection of the measuring equipment is shown in Fig. 4.16. The design dimensions and structure of the TALESUN TP-660P-260 solar panel are shown in fig. 4.16.

Fig. 4.16. The appearance of the solar panel and the location of installation and connection of measuring equipment

Generation schedules for SPP in Vinnitsa region (Fig. 4.17 and Fig. 4.18). Measurements of July 3 and July 4 were analyzed. The ordinates in the relative units show the generation of the relative abscissa of the hour in the axis from 8:00 to 17:00.

Analysis of graphs in Fig. 4.17 and Fig. 4.18 indicates that even on a cloudy day the solar panel works quite effectively. The system of monitoring the parameters of the mode of operation of the solar panel.

It is important to measure the voltage in a solar panel monitoring system in real time, as it allows the performance of the modules that make up the solar panel

to be monitored and is the most accurate way of detecting system malfunctions. The DC voltage is measured by a simple voltage distribution circuit, which results in a voltage drop to the measured range.

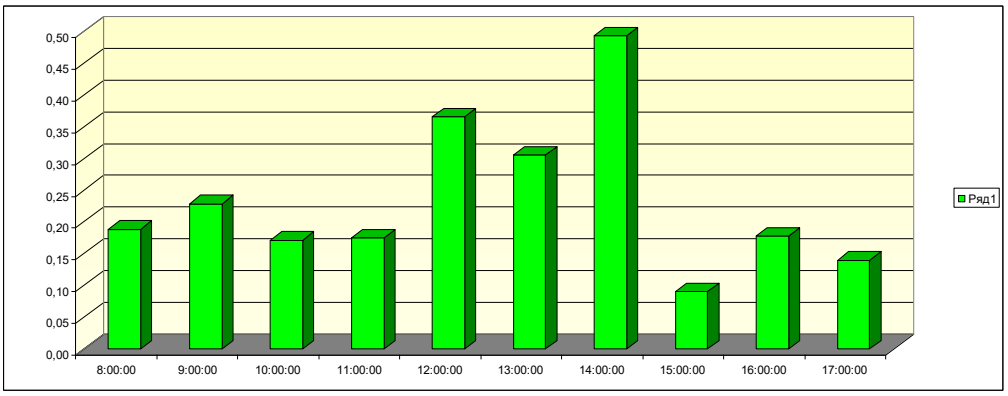

Fig. 4.17. Estimated Generation in Relative Units from 8:00 am to 5:00 pm on a cloudy day (July 3)

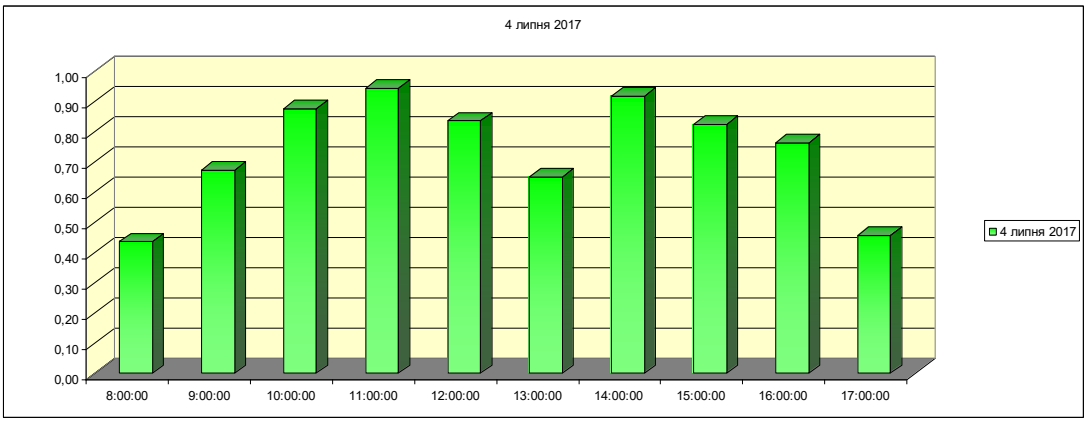

Fig. 4.18. Estimated Generation in Relative Units from 8:00 AM to 5:00 PM on a Clear Day (July 4)

Much of the solar radiation absorbed by the solar panel module does not convert to electrical energy, but instead increases the temperature of the module, resulting in a short-circuit current increase of approximately 0.1% by 1° C and a decrease in voltage of approximately 2 mV at 1° C. Therefore, the temperature parameter is an important parameter to measure in order to predict the performance of a solar panel system. Data is collected by a controller used to collect data from different sensors before sending them to a central computer. The sensor data

consists of analog signals, which the controller then converts to digital data for storage, analysis and presentation.

There are many databases available for use on an Android smartphone: SQLite Database, Sybase SQL Anywhere Database, OracleDBLite Database, IBM DB2 Everyplace Database. There are three main types of servers that can be run on Android-based smartphones (Fig. 4.19). To run as a server, your Android device must know the protocols for sharing information. Each protocol is a set of connection rules that are enforced by all computers or programs to connect to the server. There are three types - web server, file server, media server.

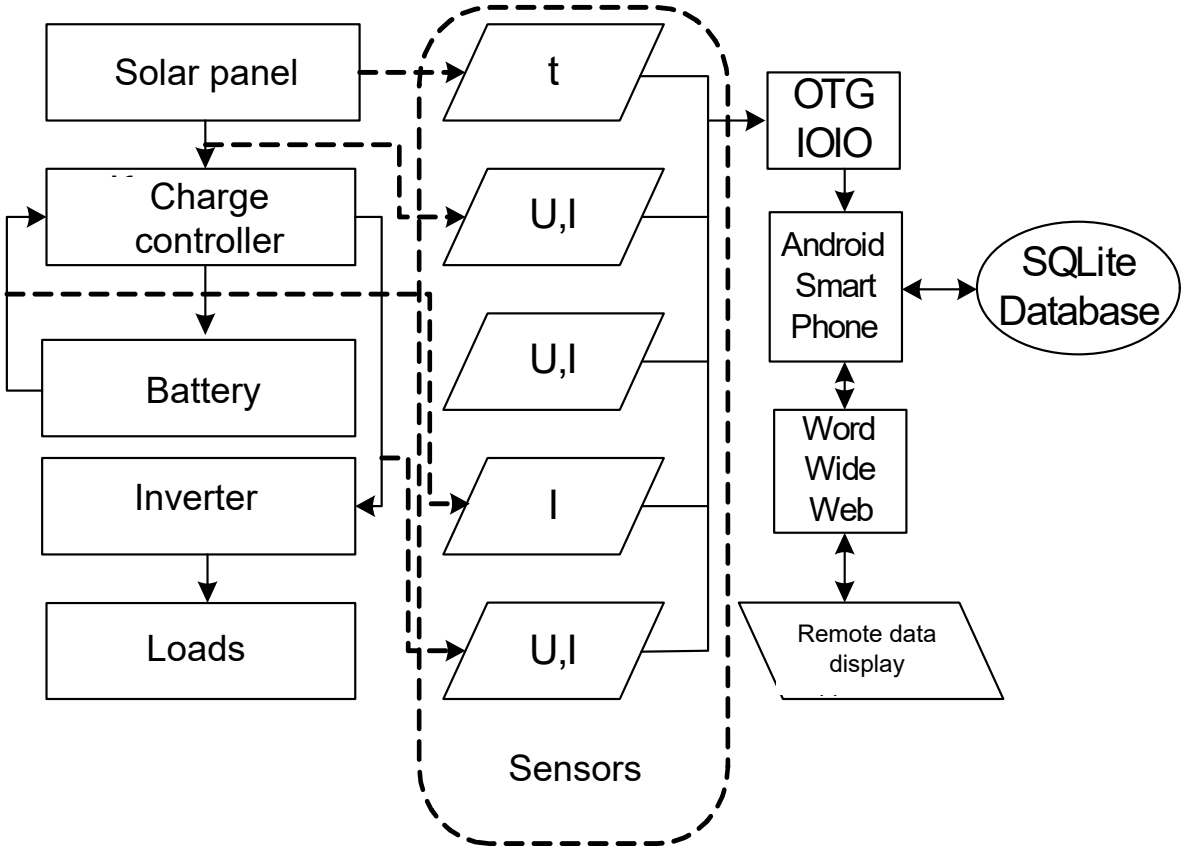

Fig. 4.19. Scheme of the system monitoring the parameters of the solar panel

Voltage and current sensors between the solar panel module and the charge controller measure the power generated by the solar panel. Voltage and current sensors between the charge controller (charge function) and the battery measure power and accumulate. The current sensor between the battery and the charge controller (charge function) in combination with the voltage sensor between the

battery and the charge controller (charge function) will measure the power output from the battery. Voltage and current sensors between the charge controller (boot function) and the power inverter measure the power generated by the battery through a power inverter. The analogue data collected will be processed and digitized by the IOIO OTG controller. The digital data will be transferred to a smartphone (Android) where it will be stored in a SQLite database. The smartphone (Android) will also work as a server and the stored data will be accessible via the Internet.

CONCLUSIONS

1. Asymmetry and non-sinusoidal voltage leads to a decrease in the efficiency of the electrical receivers and reduce their service life. With a load close to the nominal additional power loss in the T-1 transformer, 10,000 kVA 35/6 kV DSS 35 may exceed the nominal, and in a 1000 kVA 6 / 0.4 kV transformer, powered by the substation M 6, reach 50% of their nominal value. With a constant impact of asymmetry and non-sinusoidality, which correspond to their average values over the measurement period, a reduction in the service life of a transformer of 10,000 kVA 35/6 kV can be 8–10%, and a transformer of 1000 kVA 6 / 0.4 kV of about 3%. With a constant action of asymmetry and harmonics equal to normally acceptable values according to GOST 13109-97, these values will be 25-40% and 1.9-2.4 times, respectively.

2. When the transformer T-1 DSS 35 is loaded by 80%, the service life decreases only at the maximum recorded values of harmonics and asymmetry. Transformers 1000 kVA 6 / 0.4 kV, powered by p / st M 6, decrease service life when loading 80% and fixed values of harmonics and asymmetry does not occur. Power losses in the BC-5 with a capacity of 8430 kVAr of the DSS 35 substation increase slightly. Reducing its service life in modes that are close to the measured, will be 1.5 - 2%.

3. Thus disconnecting phases groups of shunt reactors are effective measures to prevent overvoltages and it can be recommended as one of the main measures to incomplete mode of group shunt reactors and power lines EHV. Note that if the line has two groups, the disconnecting similar phase one group during single phase auto-reclosure lead to the fact that the voltage will increase in line with one group. In case of three groups, switching from phase of one group will transit line mode with two groups. In case of disconnecting the same name phase, in the installation on line one group, led to absence of resonance increasing of voltage. It should be noted that the transition to a lower unit groups of shunt reactor in line is purely arbitrary, performed to analyze the occurrence of

overvoltages at SPAR. In fact, the operation of line with groups shunt reactors will work only incomplete phase of group.

4. When applying express-method to analyze resonance overvoltages the influence of mutual inductance is not so critical due to relatively negligible shifting maximum value of overvoltages. But due to the fact that determination of resonance length of the line is approximation method without considering distributed parameters of line, additional inaccuracy may lead to incorrect conclusion about existence of overvoltages as in the case of imitation model application.

5. Thus disconnecting phases groups of shunt reactors are effective measures to prevent overvoltages and it can be recommended as one of the main measures to incomplete mode of group shunt reactors and power lines EHV. Note that if tne has two groups, the disconnecting of similar phase of one group during single phase auto-reclosure leads to the fact that the voltage will increase in line with one group. In case of three groups, switching from phase of one group will transit line mode with two groups. In case of disconnecting the same name phase during the installation of line one group leads to absence of resonance increase of voltage. It should be noted that the transition to a lower unit groups of shunt reactor in line is purely arbitrary, was performed to analyze the occurrence of overvoltages at single phase auto-reclosure. In fact, the operation of line with groups shunt reactors will work only incomplete phase of group.

6. The classification of abnormal overvoltages for nonsinusoidal and asymmetric sources of distortion of main electrical networks has been created. It is established that the particular type of overvoltage differs from the traditional internal ones: the duration and values that significantly exceed the maximum permissible values given in the international and domestic standards for the correlation of 750 kV power equipment. Each of the sources of distortion are considered a non-sinusoidal, asymmetric or combined phenomenon characterized by a resonant circuit in which at the fulfillment of the necessary and sufficient

conditions there is a currents resonance, which will lead to abnormal resonant voltage increase.

7. It is established that one of the characteristic and widespread examples of an asymmetric source of distortion is the single-phase automatic re-closer, in which abnormal resonant overvoltages occur in a linear resonant circle. In such an abnormal incomplete phase mode, abnormal resonance overvoltages are characterized by duration of approximately 0.4 seconds and values exceeding the maximum permissible 2-3 times, the shape of the voltage curve is sinusoidal. A typical example of a non-sinusoidal abnormal regime is the connection of a EHV line on an unloaded autotransformer, in which an abnormal resonant voltage rise occurs due to oscillatory processes in a nonlinear resonant circuit. With such a nonsinusoidal source of distortion, the curve of the sinusoid voltage is distorted by the pair harmonics. The duration of the existence of abnormal resonant overvoltages in this mode reaches a second or even a minute, and values exceed the maximum permissible by 1.5 times.

8. An abnormal resonant overvoltage in accordance with the developed classification due to sources of distortion and significant characteristics of existence constitute a real danger to the reliable functioning of the combined power system of Ukraine and is a significant obstacle to the implementation of the conditions for integration with the European energy association system operators of ENTSO-E.

9. Subsequent studies will be aimed at the development of mathematical models and methods for analyzing ARO in asymmetric and nonsinusoidal modes of extra high voltage transmission lines. With the help of the developed ensemble of the means, the analysis of the factors that most influence the conditions of the occurrence of this class of internal overvoltage will be performed. According to the analysis, effective measures will be developed to prevent ARO. It is also considered appropriate to carried out a study of the effects of ARO with values that exceeding the maximum permissible values several times for such traditional measures as arrests, varistors and nonlinear overvoltages limiters.

10. Thus, as the importance of the problem itself, as well as the peculiarities of its emergence, the course and the presence of a whole series of unspecified interrelated factors were among the main circumstances that determined the scientific and practical significance of research aimed at increasing the energy efficiency of the power system from under conditions of abnormal resonance overvoltage.

11. Thus disconnecting phases groups of shunt reactors are effective measures to prevent overvoltages and it can be recommended as one of the main measures to incomplete mode of group shunt reactors and power lines EHV. Note that if line has two groups, the disconnecting of similar phase of one group during single phase auto-reclosure leads to the fact that the voltage will increase in line with one group. In case of three groups, switching from phase of one group will transit line mode with two groups. In case of disconnecting the same name phase during the installation of line one group leads to absence of resonance increase of voltage. It should be noted that the transition to a lower unit groups of shunt reactor in line is purely arbitrary, was performed to analyze the occurrence of overvoltages at single phase auto-reclosure. In fact, the operation of line with groups shunt reactors will work only incomplete phase of group.

12. Taking into account influence of mutual inductance is a necessary requirement for adequate analysis of resonance overvoltages. The neglecting of influence of mutual inductance leads to incorrect conclusion about existence of overvoltages, which may cause accident in bulk energy system. This especially concerns modeling imitation model of real extra high voltage lines, due to alignment sensitivity of resonance circuit to initial data such as values of inductance shunt reactors.

13. When applying express-method to analyze resonance overvoltages the influence of mutual inductance is not so critical due to relatively negligible shifting maximum value of overvoltages. But due to the fact that determination of resonance length of the line is approximation method without considering distributed parameters of line, additional inaccuracy may lead to incorrect

conclusion about existence of overvoltages as in the case of imitation model application.

14. In the normal operating conditions of a LES with a SES norms of quality of electric energy are not violated, and in transitional modes of work, the LES is violated by the parameter of the coefficient of harmonic components of the voltage.

15. Consistent or with little difference in time, the inconsistency between switching on and off the PV and powerful consumers, especially with a large number of LES inverters, leads to an increase in the number and amplitudes of the harmonics in the stress phase of the LES and in the prolonged transients.

16. Harmonious components in the stress of LES have a negative effect on the technical condition of the high-voltage equipment of the LES (especially the one that worked out the passport resource), and can lead to its damage.

17. It is necessary to develop methodological, hardware and software for coordinated switching on and off of PV in the LES, which corresponds to the implementation of the principles of the Smart Grid concept - the creation of active intelligent LES.

18. There are many different aspects to managing MG AC. The choice of control method for power inverters depends on the role that the inverter plays in the microgrid. Research into the creation of MG in Ukraine is an urgent task, the solution of which will provide powerful agricultural enterprises with high quality electricity in the required volume. Two modes of MG operation are considered in the work and the optimal control method for each mode is selected: "connection" - that is, MG is connected to the centralized distibuted electrical network (DEN) - the method of control over frequency and amplitude; in isolated mode - MG is disconnected from the centralized distribution DEN - method of control over active and reactive power. In the future, it is planned to develop a control method, which is to control the deviation of the current mode parameters from the nominal during the transition from isolated mode to the mode of connection to the DEN, in order to provide a smooth transition for changing the modes of operation, as well as can

effectively improve the dynamic characteristics of voltage regulation and frequencies in isolation, and to achieve direct control of the power delivered to the network.

19. Creating microgrids, taking into account the experience of other countries, such as India, is a promising area of providing quality electricity to consumers in remote areas. Depending on the type and schedule of load of a typical village located in a remote area, an autonomous electricity generation system based on local renewable energy sources may have different configurations, but based on geographical location and availability of different energy sources. For Ukraine, it may be relevant to use a mini-CHP as a solution to the problems of electrification and district heating in rural areas where there are no networks or significant problems with their operation. Improvement of the structure of gas-fired solid fuel boiler made it possible to reduce dimensions, metal consumption and made it possible to use not only dry fuel but also wet. Experiments are currently underway with a gas-fired boiler to switch it to steam generation to generate electricity by means of a steam turbine and a steam engine. Due to the fact that the steam turbine creates a lot of noise and causes discomfort in the farm, it is planned to use steam engines based on the industrial combustion engine by replacing the gas distribution mechanism and modernization of the lubrication system.

20. Analyzing the dynamics of changes in the use of renewable energy sources in Ukraine and Vinnitsa region, we can conclude that their percentage increases every year, so the development of monitoring systems for micro or mini-power plants running on renewable resources is extremely relevant. The annual generation value will be about 30% of the installed capacity only in the light of day, plus the fact that the solar panel does not work at night. On an auspicious day, the solar panel will generate about 24% of the installed capacity, in the days of the year with the lowest generation rates, as a rule, in the winter, the daily generation level can drop to 5-10% of the installed power. year and throughout the day. Changes can be made using solar trackers or manually. The more accurate the location of the sun in the sky is, the greater the amount of electricity the panels will

be able to generate in a year. When stationary installation of solar panels that do not monitor the position of the sun, it is necessary to install the solar panels so that they are perpendicular to the fall of the sun's rays when it is in a position of 179 ° in azimuth for the Vinnytsia region, but you still need to take into account the change in the height of the position of the sun above the mountain during the year. If the angle of change relative to the height of the sun above the horizon is also not carried out for some reason, it is necessary to determine the highest height of the position of the sun during the year and set the angle of inclination of the solar panel relative to it; will be able to generate the most electricity. Electricity production by solar power plants has a high potential for development both in Vinnytsia region and in other regions of Ukraine, according to the analysis of statistical data. At the same time, it should be noted that the capacity of solar plants in the overall grid is very small and the task of the state is to develop and implement an effective strategy to support the development of alternative sources of electricity in general and solar energy separately on the example of other states. If Ukraine had the same development of solar energy as in Germany, then 22% of Ukraine's energy needs could be covered by solar energy and 5 million tonnes of coal or 3.2 million m3 of natural gas would be saved every year.

REFERENSES

1. Souza J. R. M. S., Pereira Filho C. S., De Conti A., Evaluation of the Effect of Parameters of Three-Phase Transformer Core Models on the Harmonic Content of Inrush Currents: Implications on the Setting of Inrush Detection Functions,– IPST'15, Cavtat, Croatia, June, 2015.

2. Bratslavsky S. Kh., A.I. Gershengorn., S.B. Losev. Special calculations of extra-high voltage power transmission lines, M.: Energoatomizdat, 1985. 312 p. (Rus)

3. Chiesa N., Mork B. A., Høidalen H. K., Transformer Model for Inrush Current Calculations: Simulations, Measurements and Sensitivity Analysis, IEEE Transactions on Power Delivery – Vol. 25, No. 4 – October 2010.

4. Bojić S., Electromagnetic Transients Caused by Switching Small Inductive and Capacitive Currents in High Voltage Switchyards, Ph.D. dissertation, Faculty of electrical engineering and computing, University of Zagreb, Zagreb, Croatia, 2015. 154 p.

5. Resonance and Ferroresonance in Power Networks, CIGRE WG C4.307, TB 567,2014.

6. Kuchanskyi V.V. The application of controlled switching device for prevention resonance overvoltages in nonsinusoidal modes. Proc. 37th IEEE International Conference on *Electronics and Nanotechnology* (ELNANO 2017), Ukraine, Kiev, 17-19 April 2017. Pp. 394-399.

7. Girgis R. S., teNyenhius E. G., Characteristic of Inrush Current of Present Designs of Power Transformers", Proc. IEEE Power and Energy Society General Meeting, Tampa, USA, June, 2007.

8. Kuchanskyi V.V. Controlled switching of circuit breakers in main power electrical networks. Proceedings of the Institute of Electrodynamics of the National Academy of Sciences of Ukraine 2017. № 48 P.38–43.

9. Libkind M.S. Higher harmonics generated by transformers. M.: Publishing house of the academy of sciences of the USSR, 1962. – P. 104.

10. Tugay Y.I. The resonance overvoltages in EHV network. IEEE International Conference on Electrical Power Quality and Utilization. 2009. Lodz. - Iss. 1. PP. 14–18.

11. I.Sadeghkhani, A. Ketabi, R. Feuillet, “New approach to harmonic overvoltagess reduction during transformer energization via controlled switching,” Proceedings of in Proc. 15th International Conference on Intelligent System Applications to Power Systems, Curitiba, Brazil, 2009. – pp. 1589–1595.

12. V. Kuznetsov, Y. Tugay, V. Kuchanskyy, O. Shpolyansky. The use of controlled switching to improve the reliability of the transmission line EHV. Proceedings of the Institute of Electrodynamics of NAS of Ukraine, 2012. vol. 32, pp. 123–129.

13. T. H.Krasyl'nykova Comparative Analysis of Ways of Transient Single Line to Ground Fault Removal on EHV and UHV Transmission Untransposed Lines / T. H. Krasyl'nykova, S. H. Dzhononaev // Elektrychestvo. - 2017. – № 11. – P. 22-29

14. V. Kuznetsov, Y. Tugay, V. Kuchanskyy Investigation of transposition EHV transmission lines on abnormal overvoltages. Technical electrodynamics, 2013, Vol.6, pp.51–56.

15. V. Kulik, S. Wisniewski. Combined electric model normal mode systems with regard to extra-long power lines. Scientific works of Vinnitsa National Technical University, 2012, vol 1, pp. 1–10.

16. A. Ravluk, V. Stetsyk. Modeling of switching processes of high voltage lines 750 kV. Journal of Lviv Polytechnic National University. Electrical power engineering and electromechanical systems, 2016, vol. 840, pp. 102-107.

17. V. Sobchuk, , N. Sobchuk, V. Kondakov Mathematical model of injury (electric breakdown) of epoxy bushing 750 kV circuit breakers. Journal of Vinnitsa Polytechnic Institute, 2007, vol. 2, pp. 41–45.

18. I. Naumkin, M. Balabin, N. Lavrushenko, R. Naumkin. Simulation of the 500 kV SF6 circuit breaker cutoff process during the unsuccessful three-phase autoreclosing. ”Proceedings of International Conference on power systems Transients, Kyoto, Japan, June 14-17, 2011 – pp. 5–11.

19. I. Naumkin, Crash when switching of gas insulated circuit breakers 500-1150 kV overhead line compensated. Electricity, 2012, vol. 10, pp. 22–32.

20. L. M. N. de Mattos, A. M. P. Mendes, J. F. de Lima Filho, M. C. Tavares, Enhanced Analysis of Oscillatory Undamped Overvoltages in Transformer Energization // Proceedings of International Conference on power systems Transients IPST 2013 in Vancouver. Canada, July 18-19. – 2013. – P. 55–61.

21. J. F. Piñeros, J. A. Vélez, J. M. Salas, O. Monroy, M. T. Gutiérrez, F. Montaño,Undesired Trip of a 230 kV Transmission Line due to 500 kV/450 MVA Autotransformer Energization // Proceedings of International Conference on power systems Transients IPST 2013 in Vancouver. Canada, July 18-19. – 2013. – P. 45–50.

22. V. Kuznetsov, Y. Tugay, V. Kuchanskyy, O. Shpolyansky. The use of controlled switching to improve the reliability of the transmission line EHV. Proceedings of the Institute of Electrodynamics of NAS of Ukraine, 2012. vol. 32, pp. 123–129.

23. V. Kuznetsov, Y. Tugay, V. Kuchanskyy. Abnormal overvoltages in the modes of transmission lines EHV. Technical electrodynamics, 2012, vol. 2, pp. 40–41.

24. Stohnii B. S. Intelektualni elektrychni merezhi elektroenerhetychnykh system ta yikhnie tekhnolohichne zabezpechennia [Tekst] / B. S. Stohnii, O. V. Kyrylenko, S. P. Denysiuk // Tekhnichna elektrodynamika. – 2010. – № 6. – S. 44–50. – ISSN 1607-7970.

25. Stohnii B.S. Evoliutsiia intelektualnykh elektrychnykh merezh ta yikhni perspektyvy v Ukraini [Tekst] / B. S. Stohnii, O. V. Kyrylenko, A. V. Prakhovnyk, S. P. Denysiuk // Tekhnichna elektrodynamika.– 2011. – № 5 – S. 52–67. - ISSN 1607-7970.

26. Kuznetsov V. H. Optymyzatsyia rezhymov эlektrycheskykh setei [Tekst] / V. H. Kuznetsov, Yu. Y. Tuhai, V. A. Bazhenov. – K. : Naukova dumka, 1992. – 216 s. – ISBN 512-002-958-4.

27. Kuznietsov M. P. Harantovani rivni uchasti VES u pokrytti potuzhnosti enerhosystemy [Tekst] // Vidnovliuvana enerhetyka. – 2015. – № 1 (40). – S. 43-47. - ISSN 1919 - 8058.

28. Vasko P. F. Aktualnыe voprosы razvytyia maloi hydroэnerhetyky v Ukrayne na sovremennom эtape [Tekst] / P. F. Vasko, Yu. A. Vykhorev // Vidnovliuvana enerhetyka. – 2012. – № 3 (30). – S. 60 - 65. - ISSN 1919 - 8058.

29. Yandulskyi O. S. Optymalne rehuliuvannia napruhy v rozpodilnii elektrychnii merezhi z dzherelom rozoseredzhenoho heneruvannia z urakhuvanniam yikh nalezhnosti odnomu vlasnyku pry vykorystanni rezervu aktyvnoi potuzhnosti [Tekst] / O. S. Yandulskyi, H. O. Trunina, A. B. Nesterko //

Visnyk Kremenchutskoho natsionalnoho universytetu imeni Mykhaila Ostrohradskoho. - 2015. - № 2/91. – S.50 – 54. - ISSN 1995-0519.

30. Bazhenov V. A. Vykorystannia metodiv liniinoho prohramuvannia dlia optymizatsii rozvytku elektrychnykh merezh suchasnykh enerhosystem/ V. A. Bazhenov [Tekst] // Visnyk Vinnytskoho politekhnichnoho instytutu. – 2016. – № 2 – S. 93-96. - ISSN 1997-9266.

31. Denysiuk S. P. Osobennosty analyza vlyianyia pomekh ot raznorodnыkh typov ystochnykov raspredelennoi heneratsyy na protsessы v nahruzkakh [Tekst]/ S. P. Denysiuk, D. H. Derevianko, K. Yu. Shcherban // Zhurnal ynzhenernыkh nauk. – 2014. – № 2. – S. 1–7. - ISSN 2312-2498.

32. Lezhniuk P.D. Vidnovliuvani dzherela enerhii v rozpodilnykh elektrychnykh merezhakh : monohrafiia [Tekst] / P. D. Lezhniuk, O. A. Kovalchuk, O. V. Nikitorovych, V. V. Kulyk. – Vinnytsia : VNTU, 2014. – 204 s. – ISBN 978-966-641-577-9.

33. Kudria S. O. Netradytsiini ta vidnovliuvani dzherela enerhii [Tekst] / S. O. Kudria . – K. : NTUU «KPI», 2012. – 492 s. - ISBN 978-966-622-521-7.

34. Kyrylenko O. V. Tekhnichni osoblyvosti funktsionuvannia enerhosystem pry intehratsii dzherel rozpodilenoi heneratsii [Tekst] / O. V. Kyrylenko, I. V. Trach // Pratsi Instytutu elektrodynamiky Natsionalnoi akademii nauk Ukrainy. - 2009. - Vyp. 24. - S. 3-7. – ISSN 1727

35. Tuhai Yu. I. Intehratsiia ponovliuvanykh dzherel enerhii v rozpodilni elektrychni merezhi silskykh rehioniv [Tekst] / Yu. I. Tuhai, V. V. Kozyrskyi, O. V. Hai, V. M. Bodunov // Tekhnichna elektrodynamika. - 2011. - № 5. - S. 63-67. – ISSN 1607

36. Poliakov V. S. Ferrorezonans v setiakh s yzolyrovannoi neitraliu [Elektronnyi resurs] / V. S. Poliakov // Эlektrycheskye systemы y sety. Ynformatsyonno-spravochnыi эlektrotekhnycheskyi. Rezhym dostupu: http://esistems.ru.

37. Saenko Yu. L. Yssledovanye prychyn povrezhdenyia transformatorov napriazhenyia kontrolia yzoliatsyy [Tekst] / Yu. L. Saenko , A. S. Popov // Эnerhosberezhenye. Эnerhetyka. Эnerhoaudyt – 2011. - №7 (89). - S.59-66. – ISSN 2218-1849

38. Lezhniuk P.D. Doslidzhennia stanu obladnannia lokalnykh elektrychnykh system [Tekst] / P. D. Lezhniuk, I. O. Hunko // Kontrol i upravlinnia v skladnykh

systemakh (KUSS-2014): KhII Mizhnarod. nauk.-tekhn. konf.: tezy dopovidi. – Vinnytsia, 2014. – S. 137.

39. Lezhniuk P.D. Vplyv invertoriv SES na pokaznyky yakosti elektrychnoi enerhii v LES [Tekst] / P. D. Lezhniuk, O. Ye. Rubanenko, I.O. Hunko // Visnyk Khmelnytskoho natsionalnoho universytetu. Seriia: Tekhnichni nauky. - 2015. - № 2. – S. 134-145. - ISSN 2307-5732.

40. Lezhniuk, P. D. Optymizatsiia sektsionuvannia v lokalnykh elektrychnykh systemakh za kryteriiem vtrat elektrychnoi potuzhnosti z urakhuvanniam vidmov [Tekst] / P. D. Lezhniuk, I. O. Hunko, O.Ie. Rubanenko // Tekhnika, enerhetyka, transport APK. – 2016. – № 2 (94). – S. 90 -98.

41. Pat. №76464 Ukraina, MPK N02J23/00. Sposib optymalnoho keruvannia rezhymamy roboty elektroenerhetychnoi systemy. / P. D Lezhniuk., V. O. Lesko, O. O. Rubanenko, I. O. Rubanenko; zaiavnyk ta patentovlasnyk Vinnytskyi natsionalnyi tekhnichnyi universytet. - №2012 058664; zaiavl. 14.05.2012; opubl. 10.01.2013, Biul. №1.

42. Vynohradov A.V. Analyz povrezhdaemosty эlektrooborudovanyia эlektrotekhnycheskykh setei y obosnovanyia meropryiatyi po povыshenyiu nadёzhnosty эlektrosnabzhenyia potrebytelei [Эlektronnыi resurs]/ A. V. Vynohradov, R. A. Perkov // Vestnyk Nyzhehorodskoho hosudarstvennыi ynzhenerno-эkonomycheskyi ynstytut. - 2015 - №12 (55).- S.12-21. – ISSN 2227-9407. – Rezhym dostupu: http://cyberleninka.ru/article/n/analiz.

43. Enslin J. Harmonic Interaction Between a Large Number of Distributed Power Inverters and the Distribution Network [Текст] / J. Enslin, P. Heskes // IEEE Transaction on power electronics. – 2004. – № 6. – C.1586-1593. - DOI: 10.1109/PESC.2003.1217719.

44. Kuznetsov V. H. Vykorystannia shtuchnoi neironnoi merezhi dlia vyznachennia kharakterystyk anormalnykh perenapruh [Tekst] / V. H. Kuznetsov, V. V. Kuchanskyi, Yu. I. Tuhai // Pratsi Instytutu elektrodynamiky Natsionalnoi akademii nauk Ukrainy. Zbirnyk naukovykh prats.– 2012. — vyp. 31. — S. 5-11. – ISSN 1727-9895.

45. Tuhai Yu. I. Analiz umov vynyknennia ferorezonansnykh protsesiv v elektrychnykh merezhakh [Tekst] / Yu. I. Tuhai // Visnyk Natsionalnoho universytetu «Lvivska politekhnika» - 2007. - vyp. 596 - S.132-136.

46. Tuhai Yu. I. Modeliuvannia ferorezonansnu v transformatorakh napruhy z urakhuvanniam efektu starinnia stali [Tekst] / Yu. I. Tuhai, O. B. Besarab // Tekhnichna elektrodynamika. – 2014. – №5. – S. 62–64. – ISSN 1607-7970.

47. Tuhai Yu. I. Ferorezonansni protsesy za paralelnoi roboty transformatoriv napruhy elektromahnitnoho typu [Tekst] / Yu.I. Tuhai, O. B. Besarab, V. A. Melnychuk // Visnyk Kharkivskoho natsionalnoho tekhnichnoho universytetu im. P.Vasylenka. – 2014. – № 153. – S. 57-59. – ISBN 5-7987-0176X.

48. Tuhai Yu. I. Model elektromahnitnoho transformatora napruhy dlia doslidzhennia ferorezonansnykh protsesiv [Elektronnyi resurs] / Yu. I. Tuhai, O. B. Besarab // Naukovi pratsi Vinnytskoho natsionalnoho tekhnichnoho universytetu – 2014. – № 4. ISSN 2307-5376. Rezhym dostupu: http://nbuv.gov.ua/jpdf/VNTUV_2014_4_11.pdf.

49. Zhurakhivskyi A. V. Rezhymy roboty transformatoriv napruhy v elektromerezhakh z izolovanoiu neitralliu [Tekst] / A. V. Zhurakhivskyi, A. Ya. Yatseiko, R. Ya. Masliak // Elektroinform. – 2009. – № 1. – S. 8–11. – ISSN 1684-2243.

50. Makarenko V. Prohramnaia sreda modelyrovanyia эnerhosystem PScad [Tekst] / V. Makarenko // Modelyrovanye radyoэlektronnыkh ustroistv. – 2013. – № 11. – S. 44–48. ISSN 1817-2369.

51. Melnikov. N. A. Matrix method of electric grids analysis / N. A. Melnikov. – M. : «Energiya». 1996. – 120 p.

52. System reliability theory: models, statistical methods, and applications / Marvin Rausand, Arnljot Hoyland a john wiley & sons, inc., publication. – 2004. – 644 p. – ISBN 0-471-47133-X (acid-free paper)

53. Lezhnyuk P. D. Optimization of electric grids with small hydropower plants modes in conditions of address energy supply [Text] / P. D. Lezhnyuk. V. V. Kulik. O. B. Burikin. O. A. Kovalchuk // Technical electrodynamics. Special issue: Problems of modern electric engineering. Part. 3. – 2010. – p. 31–34. – ISSN 0204–3599.

54. Lezhniuk. P.D. Influence of distributed power sources on active power loss in electric grid // Petro Lezhniuk, Iryna Hunko, Sergiy Kravchuk, Paweł Komada, Konrad Gromaszek, Assel Mussabekova, Nursanat Askarova, Abenar Arman/ PRZEGLĄD ELEKTROTECHNICZNY. – R. 93. – NR 3/2017. – P. 107–112.

55. Lezhnyuk P.D. Analysis of optimal solutions sensitivity in complex systems by criterial method: monograph. [Text] / P. D. Lezhnyuk. – Vinnitsya: Universum – Vinnitsya. 2003. – 131 p. – ISBN 966-641-059-1.

56. Impact of distributed generation on the quality of distributed electric grids operation _. Technical electrodynamics.– 2012. – №2. – p. 34-35. Komar V.O. Kovalchuk O.A. Kuzmyk O.V.

57. Andrew Keane, Luis (Nando) F. Ochoa, Eknath Vittal, Chris J. Dent, Gareth P. Harrison“Enhanced Utilization of Voltage Control Resources With Distributed Generation” IEEE Transactions on Power Systems, vol. 26, no. 1, pp. 252-260, February 2011.

58. Nikhil K. Ardeshna, Badrul H. Chowdhury, “Supporting Islanded Microgrid Operations in the Presence of Intermittent Wind Generation”, IEEE Transactions on Power Systems, pp. 1-8, 2010.

59. Seyed Mohammad Hossein Nabavi, Somayeh Hajforoosh, Mohammad A.S. Masoum, "Placement and Sizing of Distributed Generation Units for Congestion Management and Improvement of Voltage Profile using Particle Swarm Optimization", IEEE, 2011.

60. Andrew Keane, Luis (Nando) F. Ochoa, Eknath Vittal, Chris J. Dent, Gareth P. Harrison "Enhanced Utilization of Voltage Control Resources With Distributed Generation" IEEE Transactions on Power Systems, vol. 26, no. 1, pp. 252-260, February 2011.

61. R. Medeiros, X. Xu, E. Makram, "Assessment of Operating Condition Dependent Reliability Indices in Microgrids", Journal of Power and Energy Engineering. – 2016. – No. 4. – P. 56-66. – doi: 10.4236 jpee.2016.44006 7

62. Rozenvasser E. N. Sensitivity of control systems [Text] / E. N. Rozenvasser. R. M. Yusupov – M: Nauka. 1981. – 464 p

63. Kyrylenko O.V. Problems of ensuring the reliable operation of the UES of Ukraine in the conditions of energy reformation / O.V. Kyrylenko // Bulletin of the Mikhail Ostrogradsky KSPU. – 2009. – Vol. 1, Pp. 135–141

64. SOE - NO EE 04.157: 2009. Regulatory document of the Ministry of Fuel and Energy of Ukraine. Methods and recommendations for the organization of primary and secondary frequency and power regulation at TPPs.

65. Current state, problems and prospects of development of hydropower in Ukraine. Analytical Report // National Institute for Strategic Studies. - 2014 - 54p.

66. Definition of a set of requirements for generating units // Union for the Coordination of Transmission of Electricity. - 2008. - pp. 206.

67. Guerrero J.M. Hierarchical Control of Droop - Controlled AC and DC Microgrids - A General Approach Towards Standardization / J.M. Guerrero, J.C. Vasquez, J. Matas, L.G. de Vicuna, M. Castilla // IEEE Transactions on Industrial Electronics. - 2011. - 58. P. 158–172.

68. Katiraei F. Power Management Strategies for aMicrogrid With Multiple Distributed Generation Units / F. Katiraei, M.R. Iravani // IEEE Transactions on Power Systems. - 2006. - Vol. 21 No. 4. P. 1821–1831.

69. Yandulsky OS Peculiarities of voltage regulation in distribution electric networks with sources of distributed generation / O.C. Yandulsky, A.B. Nesterko // Modern problems of electrical engineering and automation. 2012. - C. 22–25.

70. McDONALD, J. R. The Dynamics of Distributed Generation in Distribution Systems / McDONALD, J. R., DUDGEON, G. J. W., EDWARDS, F. E., LEITHEAD, W. E. // Proceedings of the IEEE PES. - 2000. - №1. P. 45-51.

71. Requirements for wind and solar photovoltaic power plants for connection to external power grids [Electronic resource]. - Access Mode: http://www.uself.com/fileadmin/documents/Wind_and_Solar_PV_Tech_Req__Final__Version_Ukrainian.pdf

72. Connection of wind power facilities to the electricity grids. Procedure and Requirements [Electronic resource]. - Access mode: http://normativ.org.ua/types/tdoc18738.php

73. Kirilenko OV Technical Aspects of Implementation of Distribution Generation Sources in Electric Networks / O.V. Kirilenko, VV Pavlovsky, LM Lukyanenko // Technical electrodynamics. - 2011. - №1. - C. 46-53.

74. Yandulsky O.S. Peculiarities of the analysis of modes of electric power systems with wind power stations / O.C. Yandulsky, P.L. Denisyuk, S.O. Yandulsky. // Scientific papers of Donetsk National University. - 2011. - №11 (186). - C. 464-465.

75. Kovalev O.P. Renewable energy sources and energy supply of autonomous consumers [Text] / O.P. Kovalev // Proceedings of DVTU. - No. 134. - Thermal power. - Vladivostok: Publishing house of DVSTU, 2003. - P. 16-20.

76. Donnelly M. Impacts of distributed utility on transmission system stability / M. Donnelly, J. Dagle, D. Trudnowski, G. Rogers // IEEE Transactions on Power Systems. - 1996 - Vol. 11, No. 2. P. 741-746.

77. Ruttledge L. System-wide contribution to the frequency response from variable speed wind turbines / L. Ruttledge, F. Damian // IEEE Power and Energy Society General Meeting. - 2012. - №1. P. 1-8.

78. Antonis G.T. Centralized Control for Optimizing Micro-grids Operation / G.T. Antonis, D.H. Nikos // IEEE Trans. Energy Conversion. - 2008. - vol. 23, No. 7. P. 241–248.

79. Sharma S. System inertial frequency response estimation and impact of renewable resources in ERCOT interconnection / S. Sharma, S. H. Huang, N. D. R. Sarma // IEEE Power and Energy Society General Meeting. - 2011. - № 1. - P. 1-6.

80. Chaly VV Alternative energy sources as reserves of energy resources of Ukraine / Chaly VV // Management of development. - 2014. - № 5. - P. 152–153.

81. Hydro-Quebec Trans Energy Transmission Provider Technical Requirements for the connection of Power Plants to the Hydro-Quebec Transmission System. – 2009. [Online] available at: http://www.hydroquebec.com/ transenergie / fr / commerce / pdf / exigence_raccordement_fev_09_en. pdf

82. Briseboisand J. Wind farm inertia emulation to fulfill Hdyro – Quebec specific need / J. Briseboisand // Proceedings of the IEEE Power and Energy Society General Meeting. - 2011. - № 1. - P. 1–7.

83. Hansen L. Generators and power electronics technology for wind turbines / L. Hansen, P. Madsen, F. Blaabjerg, H. Christensen, U. Lindhard, K. Eskildsen // IEEE Industrial Electronics Society (IECON). - 2001. - vol. 3, No. 20. - P. 2000 – 2005.

84. Baroudi J. A review of power converter topologies for wind generators / J. Baroudi, V. Dinavahi, A. Knight // IEEE International Conference on Electric Machines and Drives. - 2005. - № 1. - P. 458 –465.

85. Muljadi E. Validation of wind power plant models / E. Muljadi, A. Ellis // IEEE Power and Energy Society General Meeting – Conversion and Delivery of Electrical Energy in the 21st Century. - 2008. - № 1. - P. 1–7.

86. Behnke M. Development and validation of WECC variable speed wind turbine dynamic models for grid integration studies / M. Behnke, A. Ellis, Y. Kazachkov, T. McCoy, E. Muljadi, W. Price, J. Sanchez-Gasca // AWEA WindPower Conference. - 2007. - № 1. - P. 24–28.

87. Teninge A. Contribution to frequency control through wind turbines inertial energy storage / A. Teninge // IET Renewable Power Generation. - 2009. - № 3. - P. 358–370.

88. Rawn B.G. A Static Analysis Method to Determine the Availability of Kinetic Energy from Wind Turbines / B.G. Rawn, M. Gibsecu, W.L. Kling // PES General Meeting. - 2010. - № 1. - P. 1-8.

89. Voitov ON , Voropai NI, Gamm A.Z. Analysis of the inhomogeneities of power systems - NBSS: Nauka, 1999. - 256 p.

90. Butkevich OF Real-time identification of low-frequency oscillations of power system mode parameters / О.Ф. Butkevich, V.V. Chizhevsky // Technical Electrodynamics, 2014, № 4. - P. 35–37.

91. Yandulsky O.S., Marchenko A.A., Nesterko A.B. Local control of dispersed energy sources in transient modes // Bulletin of the Vinnitsa Polytechnic Institute. - 2014. - № 1– P. 82–85

92. L. Wang An improved structure for a predictive control model using non-minimal state space realization / L. Wang, C. Young. / / Journal of Process Control. - 2006. - 16. - P. 355–371.

93. Scokaert R. Constrained linear quadratic regulation / R. Scokaert, J. B. Rawlings. // IEEE Transactions on Automatic Control. - 1998. № 43. P. 1163–1169.

94. Zong Y. Application of a predictive control model for active load management in a distributed power system with high wind penetration / Y. Zong // IEEE Transactions On Smart Grid. - 2012. - № 3. - P. 1055–1062.

95. Mayne Q. Constrained model predictive control: Stability and optimality / D. Q. Mayne // Automatica. - 2000. - № 36. - P. 789–814.

96. I.I. Kartashev, Electricity Quality Management / II Kartashev, VN Tulsky, RG Shamonov et al .; ed. Yu. V. Sharov. - M.: Publishing House of MEI, 2006. - 320 p.: Ill.

97. Butkevich O.F., Levkonyuk A.V., Zorin E.V., Bulanaya V.S. On the Use of Synchronized Measurements of Voltage Angles from the Objects of the UES of Ukraine in Determining the Admissibility of Its Current Regimes for Static Stability Stocks // Techn. electrodynamics. – 2010, No. 6. – P. 51-58.

98. Report on the results of the activities of the National Commission for State Regulation in Energy and Utilities in 2018. NERCEP Resolution No. 440 of 29.03.2019.- K.: NERCEP, 2018. 304 p. [Online] available at: https://www.nerc.gov.ua/data/filearch/Catalog3/Richnyi_zvit_NKREKP_2018.pdf

99. Dong Y. Control strategy of low voltage microgrid based on equivalent reference current control / Yuanxiao Dong, Chen Bing, Li Qun, Liu Jianhua // Materials of China International Conference on Electricity Distribution (CICED 2014) Shenzhen. – 23-26 Sep. 2014. – P.70-76.

100. K. D. Brabandere. Voltage and frequency droop control in low voltagegrids by distributed generatros with inverter front-end: Ph.D. dissertation, Dept. Elektrotechniek, Katholieke Univ. Lueven, Leuven Belgi / K. D. Brabandere. - 2006.

101. A. Engler. Applicability of droops in low voltage grids / A. Engler // Int. J. Distrib. Energy Resources, Technology and Science Publisher, Germany, Kassel. - 2005. - vol. 1, no. 1.6.

102. H. Laaksonen. Voltage and frequency control of inverter based weak LV network microgrid / P. Saari, and R. Komulainen // Int. Conf. Future Power Syst., - 2005, – P. 1-6.

103. Matviychuk V. Analysis of modes of microgrids and control methods / V. Matviychuk, O. Rubanenko, V. Yavduk // Series of machinery, energy, transport of agroindustrial complex – 2017. – № 1(96). – P. 162-165.

104. Rubanenko O. Investigation of monitoring system of parameters of sun-panel operation mode / O. Rubanenko, O. Rubanenko, I. Gunko // Series of machinery, energy, transport of agroindustrial complex – 2018. – № 1(100). – P. 91-98.

105. Che Yanbo, Ren Jingding, Liu Kun. Construction of multi-energy micro-grid laboratory // 4th IEEE International Conference Power Electronics Systems and Applications (PESA).– 8-10 June 2011. – P. 1- 5.

106. Parimita Mohanty, G. Bhuvaneswari, Balasubramaniam D. Optimal Planning and design of Distributed Generation based micro-grid // 2012 7th IEEE International Conference on Industrial and Information Systems (ICIIS). – 6-9 Aug. 2012. – P.– 1-6.

107. Wen-Chih Yang, San-Yi Lee. Development of Operation Procedures of Distributed Generation Sources in a Micro-Grid. // Fourth International Conference on Genetic and Evolutionary Computing (ICGEC). – 13-15 Dec. 2010. – P.185 - 188.

108. Cameron L. Smallwood. Distributed Generation in Autonomous and Non-Autonomous Micro Grids // Rural Electric Power Conference.IEEE, Colorado Springs. - 05 May 2002-07 May 2002. – P. D1-D1-6.

109. Patent of Ukraine for invention No. 117142 Ukraine, IPC8 G10J3 / 20. Gas-fired solid fuel boiler / Rubanenko O.E., Rubanenko O.O., Dmitrishen O.M., Hunko I.O.; applicant and patent holder of Vinnitsa National Technical University. - stated. 10.05.16; publ. 25.06.18. Bul. # 19, 2018 [Online] available at: http://base.uipv.org/searchINV/getdocument.php?claimnumber=a201605098&doctype=ou

110. G. Sree Lakshmi, Rubanenko Olena, Hunko Iryna. Analysis of Three-level Diode Clamped Inverter for Grid-connected Renewable Energy Sources (2019). *Proceedings* IEEE International conference Computational Problems of Electrical Engineering, 15-18th September, 2019, Lviv, Ukraine